University of São Paulo
"Luiz de Queiroz" College of Agriculture

Ontogenetic development of *Pennisetum purpureum* cv. Napier: consequences for grazing management

Guilherme Portes Silva

Thesis presented to obtain the degree of Doctor in Science. Area: Animal Science and Pastures

Piracicaba
2017

Guilherme Portes Silva
Agronomist

Ontogenetic development of *Pennisetum purpureum* cv. Napier: consequences for grazing management

Advisor:
Prof. Dr. **SILA CARNEIRO DA SILVA**

Thesis presented to obtain the degree of Doctor in Science. Area: Animal Science and Pastures

Piracicaba
2017

Dados Internacionais de Catalogação na Publicação
DIVISÃO DE BIBLIOTECA – DIBD/ESALQ/USP

Silva, Guilherme Portes

Ontogenetic development of *Pennisetum purpureum* cv. Napier: consequences for grazing management / Guilherme Portes Silva. - - Piracicaba, 2017.

127 p.

Tese (Doutorado) - - USP / Escola Superior de Agricultura “Luiz de Queiroz”.

1. Morfogênese 2. Gramínea tropical 3. Perfilhos axilares 4. Alongamento do entrenó 5. Meristema apical I. Título

To my wife Leila Furtado, for her love and support.

To my parents José Nelson da Silva and Eliane Sanglard Portes, for their support and education.

To my brother Tiago Portes Silva, for being part of my life.

To all my relatives.

ACKNOWLEDGMENTS

I would like to thank Prof. Dr. Sila Carneiro da Silva for beeing an example of professor and researcher, with professionalism, dedication, and commitment. Thank you for trusting in my work and for all exchanges since my master degree. I am very grateful for the opportunity of being part of his graduate team since 2012.

I would like to express my sincere gratitude to Dr. Gilles Lemaire for all the support given to me during my doctorate, and all experience shared in France, receiving me as a visiting student. I am very grateful for all the discussions and advices that allowed me to see science in a truer and more pleasurable way, which helped me to develop a broader perspective view of science. I also would like to express my gratitude to Drs. Gaëtan Louarn and Abraham J. Escobar-Gutiérrez who generously gave their time to offer me valuable teaching and comments towards improving my knowledge and providing constructive criticism. Thanks also to my colleagues from INRA for the good moments and motivation day after day.

All comments and discussion during the planning of the experiments were essential for the improvements of the project. For that, I would like to thank Dr. Carlos Guilherme Silveira Pedreira, Dr. André Sbrissia and Dr. Lilian Elgalise Techio Pereira for their valuable explanation and discussion in the qualifying exame and throughout my doctorate programme.

The experiment would be not carried out without the contribution of very dedicated people who who helped me with all the field and laboratory work. Special thanks to Marcela (Çofrida) for helping me during the entire experimental period. Thanks also to my colleagues who helped me during some steps of the project, Diogo Olímpio, Henrique Bauab e Steben Crestani. Thanks also to Zezinho for all the support given during the experimental period regarding instalation and maintainance of irrigation system and transplantation.

I would like to express my special thanks to Dr. Marília Chiavegato Barbosa for the good time together during my doctorate and for the valuable contributions in reviewing the thesis and suggestions for improving it.

Thanks are also due to USP/ESALQ and the Department of Animal Science for the opportunity of completing my doctorate programme, and to the faculty and staff of the Department of Animal Science for all training and support.

Thanks to the friends from the research group “GEPF” with whom I have shared important moments. These include Cleunice Fialho, Eliana Geremia, Lucas Carvalho,

Guilhermo Congio, Larissa Garcia, Caio Macret. I would like to thank the colleagues in the laboratory: Patricia , Solange, Otávio, Valdson, Junior, Gabriel, Sara and Henrique.

Thanks to the São Paulo State Research Foundation (FAPESP) for funding of the project. I also would like to thank CAPES for the scholarship provided during the doctorate programme and for the scholarship of International Research Internship, which allowed me to spend six months at INRA-France. I also would like to thank CNPq for granting a scholarship at the beginning of my doctorate programme.

"The highest reward for man's toil is not what he gets for it, but what he becomes by it"

-John Ruskin

"People don't care how much you know until they know how much you care"

-Theodore Roosevelt

CONTENTS

RESUMO

Desenvolvimento ontogênico do *Pennisetum purpureum* cv. Napier: consequências para o manejo do pastejo

A caracterização do desenvolvimento ontogênico é de fundamental importância para inferir sobre estratégias de adaptação das plantas. Frequentemente, a morfogênese de gramíneas tropicais é reportada como análoga à de gramíneas de clima temperado. No entanto, gramíneas tropicais apresentam colmo ainda na fase vegetativa e com elevada disponibilidade de luz. O alongamento de colmo potencialmente altera a dinâmica do desenvolvimento, com implicações sobre o manejo do pastejo. Em condições tropicais, o capim-elefante cv. Napier é considerado uma das gramíneas mais produtivas sob condições de pastejo. Objetivou-se com esse estudo caracterizar o desenvolvimento ontogênico do capim-elefante, a coordenação entre fitômeros, o alongamento de colmo e a coordenação entre folha e entrenó em perfilhos principais e axilares, em condições de plantas isoladas. O experimento foi conduzido em Piracicaba-SP, durante a Primavera (2015), Verão (2016) e Outono (2016), utilizando um delineamento em blocos completos casualizados, com 4 repetições. Foram instalados 80 tanques de fibrocimento (0,343 m^3). Cada bloco era composto por 20 tanques, sendo que 10 foram utilizados para avaliar as características morfogênicas e de desenvolvimento e os outros 10 para as avaliações destrutivas. Medições do alongamento da lâmina foliar e do colmo foram realizadas a cada dois dias, para determinação das variáveis: taxa de aparecimento de folhas (TAF), taxa de alongamento de folhas (TAlF), duração do alongamento de folhas (DAF) e comprimento final da folha (CFF). A partir do dia 10 do período de avaliação no Verão e no Outono e do dia 25 na Primavera, foram feitos 10 cortes para avaliações destrutivas, a cada 5 dias. Por ocasião das avaliações destrutivas, as seguintes variáveis foram medidas: altura do meristema apical (AMA); comprimento do tubo de bainha (CTB); número de folhas em expansão (NFE); número de folhas expandidas (NFEX). Medições da bainha foliar (BF) e do comprimento do entreno (CE) foram realizadas apenas para o eixo principal (perfilho basal). No eixo principal, a TAF (0,02 folhas graus-dias^{-1}) e a TAlF (0,26 cm graus-dias^{-1}) foram constantes, enquanto que a DAF e o CFF aumentou com nível de inserção da folha no perfilho. A DAF variou de 150 a 280 graus-dias do fitômero 10 ao 20. No Outono, em função do florescimento, a DAF diminuiu com o nível de inserção da folha. O comprimento da BF foi crescente até atingir um valor máximo de aproximadamente 10-12 cm do fitômero 12-13 em diante. Quando avaliado em unidades filocrônicas, padrão semelhante foi observado entre épocas do ano para um grupo comum de níveis de inserção de folhas. No entanto, em todas as estações, níveis de inserção de folhas superiores apresentaram maiores DAF. Maiores TAF foram reportadas para eixos primários (perfilhos axilares) localizados acima do nível do solo e a TAlF foi crescente com o nível de inserção da folha até atingir um nível máximo, apartir do qual foi constante. A DAF foi crescente com o nível de inserção da folha em todos os eixos. O alongamento do colmo ocorreu a partir do fitômero 8 no eixo principal em todas as estações do ano, e em fitômeros anteriores para os demais eixos primários. No eixo principal, o CE variou de 0,5-2,0 cm no fitômero 8 até atingir valores máximos de 8-10 cm do fitômero 12-13 em diante, na Primavera e Verão. No Outono, valores máximos de entrenó foram de aproximadamente 20 cm. O alongamento do entrenó inicia-se concomitantemente ao término do alogamento da folha, e a um tempo de 5 filocronos do aparecimento da folha. Em todos os eixos, o CTB aumentou até atingir um valor máximo de aproximadamente 12-13 cm no verão e 11-12 cm na primavera, momento que coincidiu com o início do alongamento do colmo. O desenvolvimento ontogênico descrito para capim-elefante diverge daquele descrito para gramíneas de clima temperado. Houve efeito de sazonalidade. O desenvolvimento dos eixos apresenta organização hierárquica e sincronizada. No entanto, para os eixos superiores e fitômeros acima do nível do solo, o comportamento é diferente. O alongamento do colmo pode ser descrito pelo número de folhas produzidas. Este estudo fornece um elemento-chave para a compreensão da plasticidade fenotítipa e informações úteis para identificar o início do alongamento do colmo no campo. Este resultado pode ser utilizado potencialmente para modelagem de processos estrutura-função da planta.

Palavras-chave: Morfogênese; Gramínea tropical; Perfilhos axilares; Alongamenteo de entrenó; Meristema apical

ABSTRACT

Ontogenetic development of *Pennisetum purpureum* cv. Napier: consequences for grazing management

Characterization of the ontogenic program is essential to infer about palnts adaptation strategies. Frequently, morphogenesis of tropical forage grasses is reported to be analogous to that of temperate forage grasses. However, tropical grasses show stem development still during the vegetative phase of growth and under high light availability conditions. Stem elongation potentially impacts plants growth, with implications for grazing management. In tropical conditions, elephantgrass cv. Napier is considered one of the most productive grass species under grazing. The objective of this study was to characterize the ontogenic development of elephantgrass, coordination between phytomers, stem elongation and leaf and internode coordination in main and primary axes, using an isolated plant protocol. The experiment was conducted in Piracicaba, SP, during the Spring (2015), Summer (2016) and Autumn (2016), using a complete randomized block design, with 4 replicates. Eighty fiber cement tanks (0.343 m^3) were used. Each block was composed of 20 tanks, 10 used to evaluate the morphogenic and developmental characteristics and 10 for the destructive evaluations. Measurements of leaf and stem elongation were performed every two days to determine the following variables: leaf appearance rate (LAR), leaf elongation rate (LER), leaf elongation duration (LED) and final leaf length (FLL). From day 10 of the evaluation period in Summer and Autumn and day 25 in Spring, 10 cuts were performed for destructive assessments every 5 days. At the time of the destructive evaluations, the following variables were measured: apical meristem heigth (AMH); sheath tube length (STL); number of expanding leaves (NEL); number of expanded leaves (NEXL). Measurements of sheath length (SL) and internode length (IL) were performed only on the main axis. On the main axis LAR (0.02 leaves degree-$days^{-1}$) and LER (0.26 cm degree-$days^{-1}$) were constant, whereas LED and FLL increased with leaf rank on the axis. LED ranged from 150 to 280 degree-days from phytomer 10 to 20. In Autumn, due to flowering, LED decreased with leaf rank. SL increased until reaching a maximum value of approximately 10-12 cm from the phytomer 12-13 onwards. When evaluated in phyllochronic units, similar pattern was observed across seasons of the year for a common leaf rank group. However, in all seasons, higher leaf ranks presented greater LED. Higher LAR were reported for topmost primary axes and LER increased with leaf rank until reaching a maximum, remaining constant afterwards. The LED increased with leaf rank in main and primary axes. The stem elongation began from phytomer 8 on the main axis in all seasons of the year, and in earlier phytomers for the other primary axes. In the main axis, internode length ranged from 0.5-2.0 cm for phytomer 8 until reaching a maximum value of 8-10 cm for phytomers 12-13 onwards, in Spring and Summer. During Autumn, maximum values of internode length were approximately 20 cm. Internode elongation begins concomitantly with the cessation of leaf elongation, and after 5 phyllochronic units from leaf appearance. In all axes, STL increased until reaching a maximum value of approximately 12-13 cm in Summer and 11-12 cm in Spring, coinciding with the beginning of stem elongation. The ontogenic development described for elephantgrass differs from that reported for temperate forage grasses. There was a seasonality effect. Axes development presents a hierarchical and synchronized organization. However, for the upper axes and topmost phytomers behavior is different and needs to be investigated. The stem elongation process can be described by the number of produced leaves. This study provides a key element for understanding phenotypic plasticity and corresponds to an useful information to identify the onset of stem elongation in field conditons. This result can potentially be used for functional-structural plant modelling.

Keywords: Morphogenesis; Tropical grass; Axillary axis; Internode elongation; Apical meristem

1. INTRODUCTION

Livestock production in Brazil is essentially pasture-based, and represents the largest commercial herd in the world with over 215 million animals (IBGE, 2016). Over the past 15 years there was an increase of 37% in animal production with a decrease in 6% in the grassland area used (ABIEC, 2016), which suggest that recommendations from the science have been, at some point, applied by farmers to obtain higher grazing efficiency. In Brazil, the climate varies from subtropical conditions, located mainly on the south, to tropical climate, comprising larger area of Brazil. In the central region of the country, the average temperature ranges from 15 to 28°C with approximately 1100 to 1600 mm of pluvial precipitation. In comparison with temperate climate areas, the tropical climate favors the optimization of livestock production for a longer period of the year. This particular condition instigates managers to use their grazing lands more efficiently and in a sustainable manner. Thus, contrary to livestock systems in temperate regions where significant amount of forage resources has to be stored (hay or silage) for winter feeding, in Brazil grasslands are grazed throughout the year with adjustments in stocking density according to variations in herbage growth across seasons.

Grassland areas in the central region of Brazil are mainly cultivated with monoculture of perennial grasses of a limited number of species from genera *Urochloa*, *Panicum* and *Cynodon* (Da Silva et al., 2015; Sbrissia et al., 2017), comprised mostly of C4 species with a large variety of morphogenetic traits (Rodrigues et al., 2011). In fact, C4 species are more efficient in forage production under tropical conditions due to their photosynthetic pathway that allows higher water use efficiency and also higher nitrogen use efficiency under high temperatures (Lambers et al., 2008). Among several studies presented in the literature, there is practically a consensus that the most productive grass in tropical conditions belongs to the species *Pennissetum purpureum* (elephant grass), specially the cultivars Cameroon and Napier (Pereira et al., 2010), the latest being the object of this study.

Elephant grass is a perennial C4 grass native to Sub-Saharan Africa, but given its wide agro-ecological adaptation, it has adapted in several areas of Central and South America, tropical parts of Asia, Australia, the Middle East and Pacific Islands (Negawo et al., 2017). Historically, elephant grass has been primarily used as animal feed, however, it has also been used as a source of bio-fuel (Woodart and Sollenberger, 2015), windbreak, phytoremediation purposes (Ishii et al., 2013) and others (Rusdy, 2016). This multiple purpose found in elephant grass is due to its many desirable agronomical characteristics, including high

biomass per unit area, deep root system, that aid to tolerate intermittent drought, and an ability to withstand repeated cutting with rapid regeneration (Lowe et al., 2003).

Elephant grass was introduced in Brazil in the early 1920's, and initially used for livestock feeding through cutting, and later through direct grazing. The importance of elephant grass for livestock production in Brazil can be demonstrated by a number of studies published in the 1990's and 2000's, which were the main subject of several books and events held in Brazil (Carvalho et al., 1994; Carvalho et al., 1997; Cóser, 2000; Lira et al., 2010; Mello et al., 2008; Passos, 1999; Peixoto et al., 1994). The progress made by research is evident, especially with regards to the philosophy behind grazing management. Much of the studies developed at the early years were concerned with technical and practical aspects, mainly the need for simplifying processes involved in grassland ecosystems. However, these studies were conducted without integrating plant responses to environmental cues. The objectives at the time were to determine empirical rules for managing grazing systems. One example is the use of fixed occupation periods on rotational grazing management strategies, which resulted in large inconsistencies in the results obtained and explains the low adoption of elephant grass as a forage plant for grazing (Pereira, 2013). Variations of plant growth dynamics and plant morphogenetic composition according to season of the year and environmental conditions led to large difficulties in determining grazing strategies. Innapropriate grazing management resulted in low efficiency due the use of fixed empirical grazing intervals of elephant grass. In fact, much progress was made since the studies started to integrate aspects of plant ecophysiology to understand plant responses to management strategies in a more complex and integrative manner.

Plant ecophysiology can be defined as the study of the interactions between plants with their own environment: how individuals perceive and react to any constraint and change on their environment, and how the functioning of plants as a population can modify their own environment (Lemaire, 2001). For a grazed plant population, the environment perceived by plants is determined by sward structure. Sward structure itself is determined by both (i) growth and development of all neighboughing plants; and (ii) animal grazing behaviour that determines the defoliation pattern of these plants. In that sense, an indivudual plant perceives the sward structure around it through the modification of its own light microclimate. Then the plant adapts to this environment through morphological plasticity. Therefore, much progress in sward management for tropical pastures has been made by integrating the light enviroment impacts on plant responses to understand plant plasticity and modifications in structural characteristics to determine the grazing strategy and identify management targets. Important

results have been obtained for elephant grass using the criteria of 95% canopy light interception as a target for interrupting the regrowth process by defoliation. The criteria generated an adequate balance between leaf and stem proportion and resulted in higher quality/quantity of herbage produced, nutritive value, herbage intake and animal performance and productivity (Chaves et al., 2013; Gomide et al., 2011; Gomide et al., 2015; Pereira et al., 2014a; Pereira et al., 2014b; Sousa et al., 2012; Voltolini et al., 2010). Important results have been obtained mainly in regards to stem production and its effects on different grazing strategies concerning light environment.

The identification of grazing targets in tropical grasslands mainly focus on the control of stem production and in the proportion between leaf and stem in sward herbage mass. Most studies developed with perennial tropical grasses describing the process of stem elongation were performed on pasture, considering the implication of light relations within the plant comunity, the main agent known to impact stem production (Ballare et al., 1991) and tillering (Baldissera et al., 2014, Deregibus et al., 1983; Verdenal et al., 2008). However, stem elongation may occur even with relatively high light availability during the vegetative growth phase. The potential reasons for it and how stem development impacts on leaf production are still unknown. Therefore, to analyse the effect of plant competition in such enviroment, it is necessary to first understand the model of resource acquisition and use by individual plants in the absence of competition (Lemaire and Millard, 1999). These studies are usually performed by assessing the dynamics of plant growth using an isolated plant protocol. This protocol allows to elucidate intrinsic morphological changes in plant development without competition, i.e. ontogenetic development (Poethig, 1990; Wiltshire et al., 1994).

In this sense, this study aimed to characterize the ontogenic program of development of elephant grass cv. Napier using an isolated plant protocol in the absence of retro-action of sward structure on plant morphogenesis, in order to: i) define the ontogenetic plant development; and ii) identify the coordination of development of internode elongation and leaf development of the phytomers in main and primary axes. The determination of the ontogenetic development of the plant is a prerequisite for analysing plant morphogenetic adaptation to both sward structure (competition for light) and defoliation pattern (plant-animal interactions). Otherwise, in absence of this basic information of ontogenetic plant development, it will be very difficult to clearly understand how plants adapt to sward structure and how plants respond to defoliation and other biotic and abiotic environmental factors. Further, this study intended to analyse the determinism of stem elongation in elephant grass in order to provide a reference framework to improve grazing management.

2. LITERATURE REVIEW – "STATE OF THE ART"

2.1. General principles of grazing management

Efficient management of grassland ecosystems consists in optimizing the functionality of its components (i.e. soil, water, atmosphere, flora and fauna, etc) to ensure a continuous output to human needs while maintaining or enhancing the quality of the environment (Bohlool et al.,1992 apud TAC, CGIAR, 1978). Under this scenario, the intensification of livestock production should be achieved through management strategies that allow efficient use of the available resources (such as water and nutrients) and optimize the use of light by the plant community.

The crucial point in grazing management is to understand the principles of herbage production and utilization in order to achieve the optimal trade off between leaves harvesting and leaves remaining to allow fast regrowth. In grasslands, herbage growth follows a sigmoid pattern divided in three phases (Brougham, 1955). In the first phase, sward leaf area index (LAI) is low and growth rate increases progressively as LAI increases. The main reason is that initially the expansion of new leaf area depends on the re-mobilization of carbohydrate and protein reserves from the stubble. In the second phase, growth rate is maximum and nearly constant, and LAI is large enough to maximize light interception. Growth rate and herbage mass increase until leaves begin to overlap and shade each other, leading to the third phase. In the third phase, growth rate declines as a consequence of a proportionally larger increase in leaf senescence relative to leaf growth. Brougham (1955) demonstrated the importance of LAI and sward canopy light interception (LI) to herbage accumulation for mixed perennial ryegrass (*Lolium perenne* L.), white clover (*Trifolium repens* L.) and red clover (*Trifolium pratense* L.) swards. The relationship between LAI and carbon fluxes (photosynthesis, respiration and senescence) were also presented by Parsons et al. (1988), demonstranting in a clear manner the importance of controlling LAI to balance the process of leaf growth and senescence according to strategies of grazing management. It was plausibly showed that to maximize harvesting, pasture should be harvested when the average growth rate is maximum; corresponding to the optimum balance between leaf growth and senescence regardless of what grazing method is used to distribute defoliations in space and time (Figure 2.1).

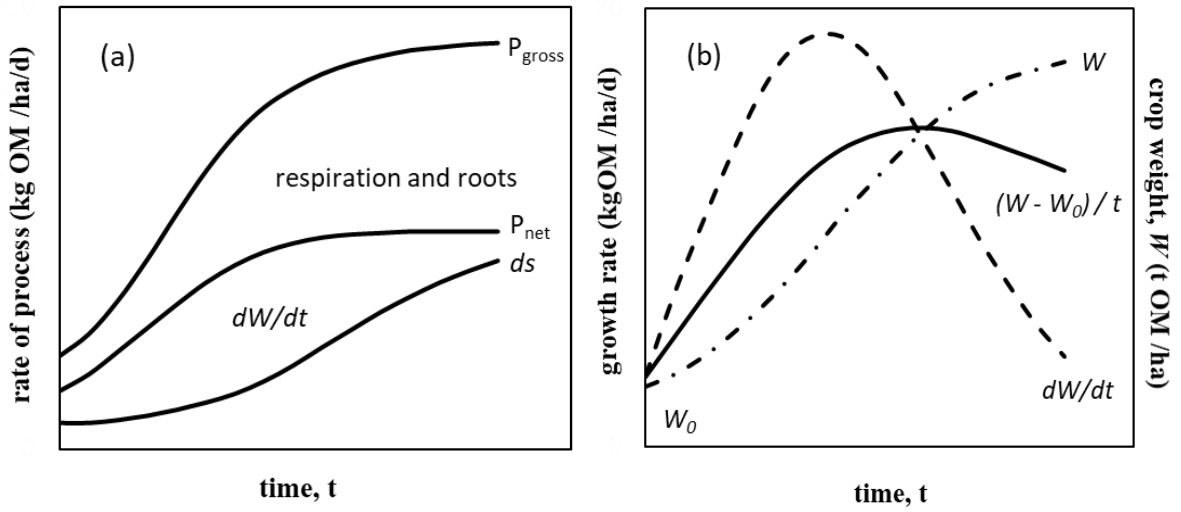

Figure 2.1. (a) Effect of the duration of regrowth on the major processes involved in net herbage accumulation: gross photosynthesis (P_{gross}), gross (shoot) tissue production (P_{net}) and death (*ds*); and (b) the corresponding changes in the instantaneous growth rate (d*W*/d*t*), the crop weight (*W*) and average growth rate (*W*- W_0)/*t*). Adapted from Parsons and Penning (1988).

The central role of LAI in grazing management was further corroborated by understanding the response of plants and animals by manipulating sward structural characteristics (Hodgson, 1985). The convergence of plant and animal responses means that grazing management strategies should be based on LAI through control of sward structure (sward height and herbage mass).

Those studies provided the basis for developing efficient grazing management strategies based on the concepts of LAI and balance between growth and senescence. However, due to difficulty of measuring aspects of light interception and LAI in field conditions, the challenge for scientists in grassland ecophysiology is to translate the ecophysiological principles into sward characteristics that should be as efficient as LAI and ease to apply, so farmers could monitor the grazing process and make the "complex seem simple" (Chapman, 2016). In this context, several grazing management guidelines have been developed, with the definition of sward height targets (Carvalho et al., 2016; Da Silva, 2011; Hodgson, 1990) and leaf stage indicator (Fulkerson and Slack, 1995; Gomide and Gomide, 1999; Solomon et al., 2017) being some of the most used. Independently of the sward structural characteristics used, the idea is to maintain the optimum balance between leaf growth and senescence favoring high herbage accumulation and utilization efficiency, ensuring pasture persistence and herbage consumption by animals.

The key for understanding the principles of growth and utilization of grass is recognizing the harvestable components as the photosynthetic organs – predominantly leaves (Parsons et al., 2011). High proportion of leaves in the sward is directly related to forage quality, since it favours the intake by grazing animals, as leaves require less strength to be harvested, and also because they have higher nutritive value than stems. In this sense, the development of efficient pasture-based systems with perennial tropical C4 grasses generally focuses on the control of stem production by management and optimization of the leaf/stem proportion balance (Da Silva and Carvalho, 2005). In studies with elephant grass, the use of canopy light interception to interrupt regrowth was tested under rotational grazing conditions. The pre-grazing target of 95% canopy light interception ($LI_{95\%}$), as compared to maximum canopy light interception (LI_{Max}), increased leaf production and, therefore, nutritive value, ensuring high herbage intake and daily milk production per animal and per hectare (Carareto, 2007; Geremia, 2013; Pereira et al., 2014a; Voltolini et al., 2010; Voltolini, 2006). When associated with moderate defoliation severity (50% of the pre-grazing height), $LI_{95\%}$ resulted in high proportion of leaves at both pre- and post-grazing, allowing for shorter grazing intervals (Voltolini et al., 2010) and greater milk production per hectare (Carareto, 2007; Voltolini, 2006). In addition, the lower stem production favored the branching of tillers close to the soil surface, allowing better occupation and soil cover due to better tussocks distribution (Pereira et al., 2014b). The optimization of canopy light interception can also be evidenced by the high leaf accumulation rate in detriment of stem and dead material (Pereira et al., 2014a), consequence of the higher tiller population density and lower stem elongation (Pereira et al., 2013).

Although the use of canopy light interception has proved to be efficient for monitoring grazing on elephant grass, the authors always face the condition that is mandatory not to have scarcity of other abiotic factors, such as nutrient availability, that impacts growth rate and perenization of plants. Under unfavorable conditions, sward canopy may not reach high levels of light interception and still have high proportion of stems and dead material in the herbage mass. This indicates that intrinsic factors related to the ontogenetic development of plants, other than competition for light, could be related to stem production. In this sense, knowledge regarding plants' ontogenetic program for producing stems is essential to understand the development of sward canopy at the individual or community level, and potentially useful as a complement with other structural charateristics for determining grazing strategies.

2.2. General framework of grass morphogenesis

Herbage production in the sward is a result of the sum of processes occuring at plant individual level. Therefore, it is possible to integrate responses of individual plant growth to infer upon the community level. The accumulation of herbage is regulated by environmental factors and by morphogenetic plant growth. In this context, grasses are essentially modularly organized structures (Oborny, 2004). The elementary unit is the phytomer (leaf (sheath and blade), node, internode and axillary bud; Moore and Moser, 1995) differentiated by a common apical meristem (Langer, 1979). Each phytomer potentially generate branches, and branches construct branching systems in a hierarchical manner (Oborny, 2004).

Shoot development follows a stepwise well-defined sequence of events, beginning with leaf initiation. Leaf growth begins with the production of cells that encircle the apical dome in the outer layers of the shoot apical meristem. Cells, then, grow further through cell expansion, so that duration and rate of cell expansion affect the final leaf area. Once a leaf primordium is initiated at the apical meristem, it grows following a sigmoid pattern, described in four phases (Fournier et al., 2005). The first phase follows an exponential pattern, where the entire primordium is a homogeneous division zone and cell length remains constant. In the second phase, there is an abruptly acceleration in relative elongation rate since cells stop dividing and form the “elongation only” zone. Third, cells stop elongating, enter the mature zone, giving a relative stability of the leaf elongation rate, and ultimately, the growth zone regresses and gives rise to the fade-out phase of elongation. Phytomer differentiation continues as long as the apical meristem remains in a vegetative status giving rise to a series of leaf primordia at progressive stages of development (Hull, 1999) (Figure 2.2).

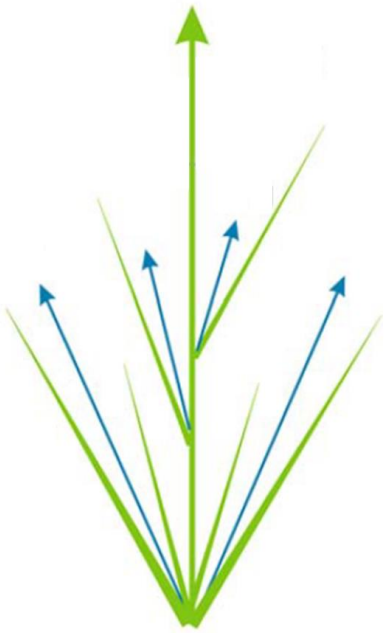

Figure 2.2. Schematic representation of a generalised grass: Green lines represent primary axes; blue lines represent axillary branches; arrows represent active indeterminate meristems. Adapted from Bennett and Leyser (2006).

Plant morphogenesis can be defined as the dynamics of generation and expansion of plant form in space (Chapman and Lemaire, 1993) and is expressed as the rate of appearance and expansion of plant organs, as well as their disappearance rate by senescence. Conceptually, morphogenesis is a continuum of differentiation processes, growth, senescence and death, leading to the acquisition of its form by an organ or organism. The sward LAI is the product of leaf area per tiller (composed by number of leaves per tiller and individual leaf area) and tiller population density. These characteristics, however, are determinated by morphogenetic variables (Lemaire and Chapman, 1996), which integrate plant morphogenetic and structural characteristics as a determinant of LAI, demonstrating its importance and relationship in a given environment (Figure 2.3).

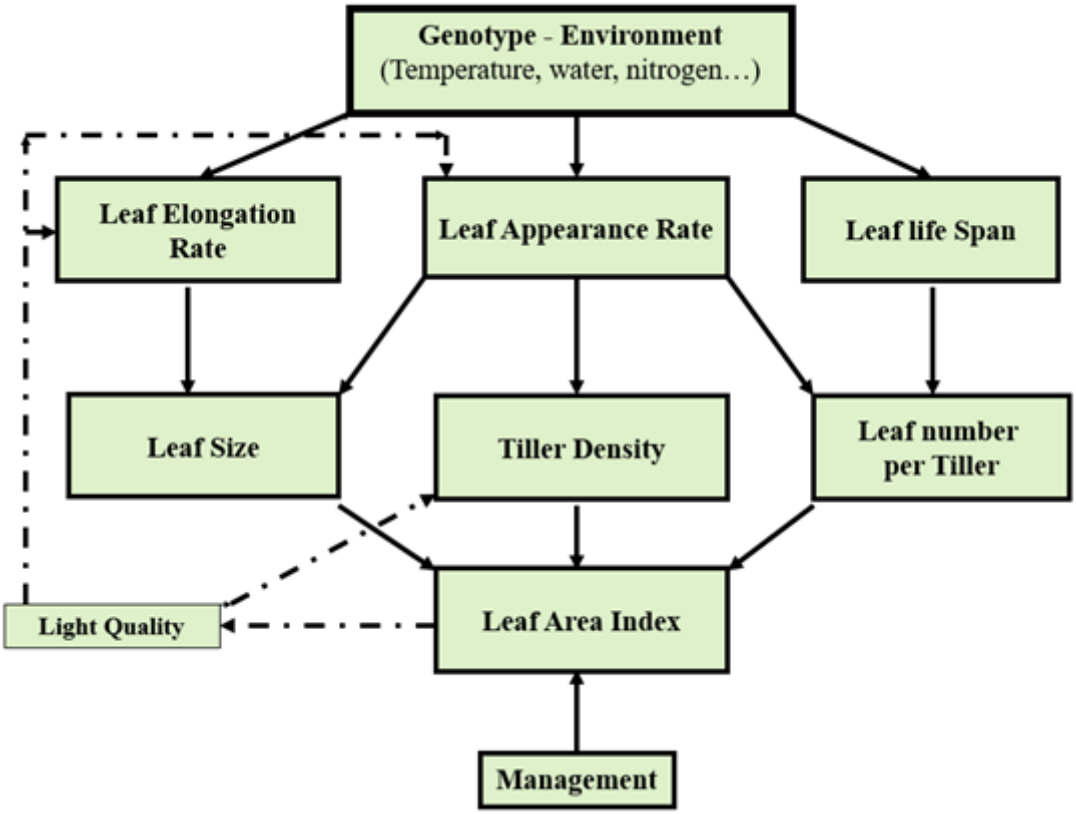

Figure 2.3. Relationship between morphogenetic variables and sward structural characteristics (after Lemaire and Chapman, 1996)

The three structural variables presented in Figure 2.3 (final leaf length, tiller population density, leaf number per tiller) are determinants of sward LAI. Considering that leaf length is proportional to leaf area, and consequently determines the LAI that intercepts light, as LAI increases it impacts the light micro-climate (red/far-red ratio and blue light) within the sward, which is perceived by individual plants. As consequence, leaf elongation rate (LER) and leaf appearance rate (LAR) are deeply affected by changes in light quality occurring as LAI develops. As LAI increases, LER and phyllochron (Ph) tends to increase, leading also to increased leaf elongation duration (LED) and then to increased tiller size while tiller population density decreases. The impacts of the light environment on leaf growth and tiller appearance were also descrided by Bahamani et al. (2000). Self-shading within a dense canopy at the tiller base is associated with an increase of leaf length through increased LER and LED, and inhibits branching, resulting in compensation for the lower light interception. Consequently, the effect of high sward LAI inhibiting tillering is an important mechanism related to leaf length, which in turn is a major component of sward LAI. Accordingly, control

and restoration of growth dynamics in a given environment is achieved by adjusting the light enviroment within the sward canopy through defoliation (i.e. grazing management).

In a given environment, the morphogenesis of tufted grass species can be decomposed in three main variables: i) Leaf elongation rate – the rate at which a leaf increases in length; ii) Leaf appearance rate or its reciprocal, the Phyllochron - the time interval between the appearance of successive leaves on a tiller; and iii) Leaf life span - the time between leaf tip appearance and the beginning of leaf tissue senescence. In grasses, the leaf appearance rate is a key variable, since it influences the other plant structural characteristics. Under favorable climatic conditions and adequate fertilization, the leaf appearance rate is directly influenced by temperature and depends on the sheath length of the previous leaf (Cruz and Boval, 2000). In grasses, the apical meristem is folded by the sheath tube, which is determinant of leaf dimensions (Casey et al., 1999; Wilson and Laidlaw, 1985) (Figure 2.4). The sheath tube impacts in the way that the cessation of cell division in the lamina is determinated by the appearance of the leaf tip above the whorl of older leaf sheaths and this supports the relation of the dimensions of leaf blade and sheath of the oldest leaf (Wilson and Laidlaw, 1985).

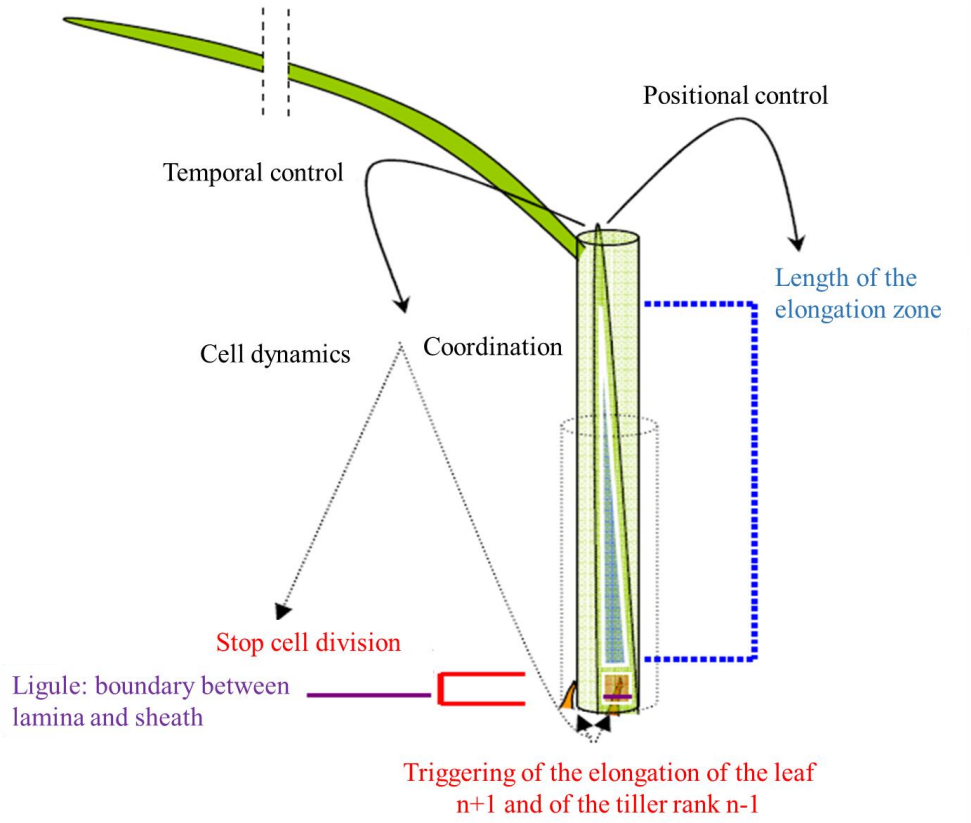

Figure 2.4. Diagram summarizing the influences of the sheath tube on the shoot morphogenesis of ryegrass. The length of the sheath tube can affect the length of the leaf elongation zone by a positional control. Simoultaneously, by temporal control, sheath tube affects tip leaf appearance period: i) ceasses cell division at the leaf base and consequently determines the total number of cells produced; ii) partitions cell stock created between sheath and blade; ii) triggers growth of the next leaf and of preceding node tiller (Verdenal, 2009).

The combination of the morphogenetic variables allows for the determination of sward structural characteristics, such as: (i) Final leaf length (FLL), which is directly dependant of LER and LED; (ii) Maximum number of leaves per tiller, which depends on both LAR and leaf life span (LLS); and (iii) Tiller population density, which depends directly on LAR, as tiller branchs arise from the nodes present in each phytomer. In temperate forage grasses during the vegetative phase these morphogenetic variables can be integrated as demonstrated in the following diagram (Figure 2.5).

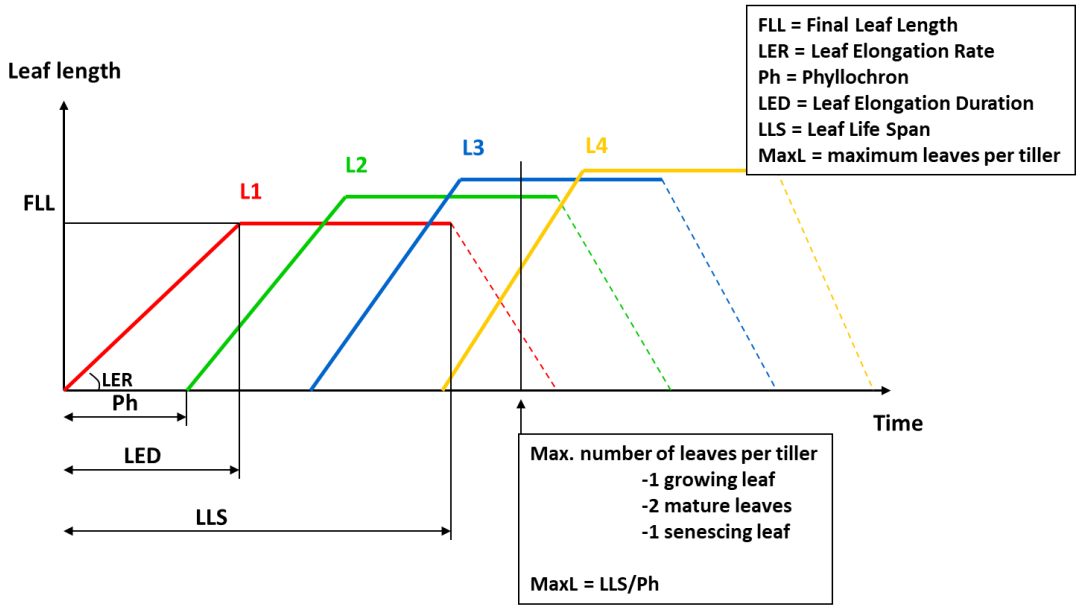

Figure 2.5. Relationship among the morphogenetic variables of temperate grasses (After Lemaire, unpublished).

The FLL of expanded leaves can be directly derived from the individual leaf elongation rate and the duration of the elongation period:

- $FLL = LER \times LED$ (1)

Considering that leaves elongate at a constant rate during some period, the LED is proportional to Ph multiplied by the number of leaves expanding simultaneously (a):

- $LED = a \times Ph$ (2)

Therefore, it is possible to relate the final leaf length to both the Ph and the LER:

- $FLL = a \times LER \times Ph$ (3)

The LLS determines the maximum number of live leaves per tiller (NLL), and can be calculated as follow:

- $NLL = LLS / Ph$ (4)

In temperate grasses during the vegetative phase, as plant grows, leaf appearance rate decreases and the duration of leaf elongation (growth) and leaf length increase. Such changes occur concomitantly with the increase in sheath length at a rate that depends on environmental growth conditions, such as temperature (Duru and Ducroq, 2000b). An important feature is that the number of expanding leaves per tiller remains stable across different sward states

reported for temperate grasses, so final leaf length can be directly estimated by equation 3. This relation holds for several species and seasons of the year as well as for the whole range of sward heights investigated (Gastal and Lemaire, 2015; Lemaire and Agnusdei, 2000).

These ecophysiological processes described above related to the dynamics of growth are well applied for temperate forage grasses and useful to study coordination of plant development. The synchronization of growth between phytomers and parts of the phytomers presents conservative traits in their morphology, making it possible to follow the dynamics of plant growth using stable features of the developmental process as a basis to relate the coordination of plant development. The iterative stability of growth implies that the plasticity of plants can be mediated by a self-regulatory process, which encompasses a coordinated self-organization of growth of its components (Verdenal et al., 2008). In tall fescue (*Festuca arundinacea* Schreber), the ontogenetic events occur simultaneously on three adjacent nodes (Skinner and Nelson, 1994). When the leaf tip of phytomer *n* is exposed to light, the formation of the ligula is trigered, and concomitantly blade elongation begins on phytomer *n* + 1 and tiller elongation on phytomer *n* – 1 (Andrieu et al., 2006; Skinner and Nelson, 1994). These events could be triggered by the direct exposure to light of the tip of leaf *n* (Skinner and Nelson, 1994) (Figure 2.4). On other hand, for the perennial C4 grass species *Cleistogenes squarrosa* (Trin. ex Ledeb.), there are approximately 4 phytomers expanding simultaneously per main tiller and an indicative of an increase in number of visible phytomers expanding simultaneously on a developing tiller (Yang et al., 2016). Although that study was performed during the development of only two phytomers (number 13 and 14), at the time of the final sampling, five phytomers were expanding simultaneously on an individual tiller, indicating that more leaves were expanding simultaneously as oberserved in the dissection of the plants. The phytomers presented a conservative gradual transition in stages of development, demonstrating that they are tightly coordinated during its development (Yang et al., 2016). The stability of this coordination was held within a range of nitrogen availability and vapour pressure deficit, making it possible to relate phytomer development to regularity of triggering events between phytomers growth.

For temperate forage grasses, the dynamics of growth is well estabilished during the vegetative developmental phase (Lemaire and Chapman, 1996; Skinner and Nelson, 1994) and present a strong coordination of development between tillers and its components. Usually, studies with tropical forage grasses adopt the conceptual framework established for temperate forage species, but there is no conceptual model developed for tropical forage grasses

illustrating the coordination and growth dynamics during the vegetative and reproductive developmental phases. An important difference between temperate C3 and tropical C4 perennial grasses relies on the stem elongation process, an event that occurs also during the vegetative phase of development, in absence of any flower initiation, on the latest. This needs to be considered as an additional morphogenetic characteristic determining plant responses and coordination of development in tropical forage grasses (Da Silva et al., 2015; Hodgson and Da Silva, 2002).

Knowledge regarding growth characteristics of plants is essential for their effective management and genetic improvement. Further, basic processes need to be understood in order to allow evaluation of growth potential of forage plants within a given environment and how they adapt morphologically to grow and persist in such environment (Nelson, 2000). Nelson (2000) mentioned that except for some range grasses, very little information exists on C4 forage grasses and some questions need to be answered, such as: (i) How many leaves on C4 grasses are expanding at one time? What is the plasticity for this trait? (ii) Do shoot apices of C4 grasses function like those of C3 grasses? Other questions also essential in the understanding about the developmental framework of perennial C4 tropical grasses are the ones presented on this thesis: How is the coordination of development operated at the phytomer level for successive leaf ranks? How can this information be applied into a functional-structural plant modelling?

2.3. Regulation of stem elongation in individual plants

The peculiarity of studies about morphogenesis on temperate plants during the vegetative phase lies on considering a phytomer essentially for studying aspects of leaf growth. In these plants, internode growth can be ignored (Verdenal et al., 2008), since it is especially related to the transition from vegetative to the flowering stage. However, in tropical plants stem elongation occurs still during the vegetative growth stage, and needs to be considered as part plant the growth dynamics. The important characteristics reported in the literature about stem elongation are: i) elevation of the photosynthetic organs (leaves) for interception of photosynthetically active radiation; ii) elevation of reproductive organs to assure successful pollination, and; iii) change in plant architecture to improve the vertical distribution of leaf area and optimizing the leaf area index for augmenting light interception

(Birch et al., 2008; Morrison et al., 1994). Even though such characteristics ensure a greater competitive ability for plants that elongate stems, especially in grasslands, the objective and challenge rely in controlling excessive stem elongation and accumulation, since it impacts negatively on the nutritive value of the herbage produced, its utilization efficiency and herbage intake by the grazers.

In wheat, during the stem elongation period, the partition of assimilates changes because internode elongation is a powerful sink for exported carbon (Patrick et al., 1972). In maize, Robertson (1994) reported the relationship between the onset and cessation of internode and sheath elongation with leaf appearance. As elongation activity in one internode decelerates, the elongation of the internodes above accelerates, and yet an additional internode above them begins to elongate. In his study, about 4 internodes where elongating at any time and the duration of growth from node 9 to node 16 varied from 4.5 to 5.0 phyllochrons. The author suggested that plant height could be modelled based on the relationship between plant height and final leaf number, assuming an average stem elongation rate per phyllochron.

A series of experiments with different grasses has revelead synchronization between the beginning of fast internode elongation with the cessation of sheath elongation of the same phytomer (Fournier and Andrieu, 2000a; Fournier and Andrieu, 2000b; Gallagher, 1979; Kirby et al., 1994; Lafarge, 1998; Robertson, 1994; Sharman, 1942). Fournier and Andrieu (2000a) reported a stable synchrony of sheath emergence with the end of the exponential phase of internode growth for phytomers 11 to 15 in maize. The authors described that the transition from sheath length to internode length was a striking event coordinating the beginning of the linear internode growth phase, suggesting that sheath tube length indirectly controls internode length. Recently, Zhu et al. (2014) presented a framework for the structural development of a maize plant integrating the internode component in the synchrony of growth events. The authors presented the dynamics of phytomer extension based on three coordination rules, in sequence of succession of leaf emergence events: i) tip emergence of leaf *n* is coordinated with initiation of sheath *n* and stabilization of the elongation zone length of blade *n* (Andrieu et al., 2006); ii) collar emergence of leaf *n*–1 is coordinated with the beginning of linear elongation of sheath *n*; and iii) collar emergence of leaf *n* is coordinated with the decline in elongation rate of sheath *n* and the rapid increase in the elongation rate of internode *n* (Fournier and Andrieu, 2000a) (Figure 2.6).

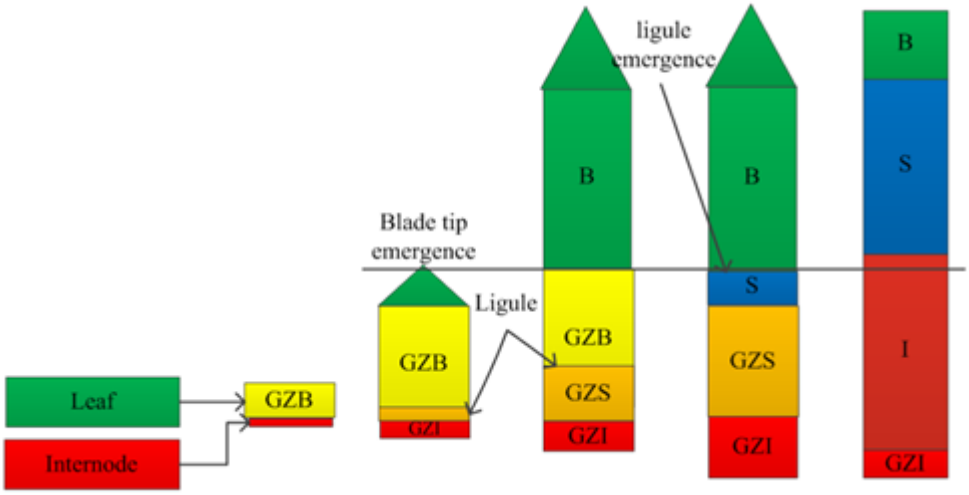

Figure 2.6. Growth scheme of one phytomer of maize. GZ is growing zone where cells divide and elongate. B, S and I represent blade, sheath and internode, respectively. Internode initiation occurs half a plastochron after blade initiation. Before tassel initiation, the ligule appears at the bottom of the growing zone, synchronized with the time of blade tip emergence. After tassel initiation, ligule appears in GZB with a regular thermal time interval (Andrieu et al., 2006). The length of the GZB is linked with time when ligule appears on it, and growth activity gradually shifts from blade to sheath after this. Ligule emergence triggers the growth activity transition between sheath and internode. (Zhu et al., 2013).

The available studies in the literature that integrate internode elongation were carried out with annual grasses during their transition from vegetative to flowering stage, such as maize (Birch et al., 2002; Birch et al., 2008; Fournier and Andrieu, 2000a; Fournier and Andrieu, 2000b; Morrison et al., 1994; Moulia et al., 1999; Robertson, 1994; Zhu et al., 2014), wheat (Barillot et al., 2016; Chen et al., 2009; Gonzales et al., 2005; Kronenberg et al., 2017; Zhu et al. 2009;), sorghum (Nakamura et al., 2011) and rice (Jaffuel and Dauzat, 2005). For annual crops, the dynamics of internode growth is related to the transition to flowering and to associated hormonal balances, in order that little is known about the dynamics of internode growth and ontogeny of perennial C4 tropical forage grasses during their vegetative developmental stage. The information regarding coordination of successive tillers growth and the impacts of internode growth on the dynamics of phytomers and plant growth is still scarce and needs to be clarified since it impacts the growth dynamics of successive phytomers. There are no models describing how stem elongation is regulated during the ontogenic pattern of plant development for perennial C4 tropical grasses. In this sense, this study aimed at characterizing the ontogenic program of development of elephant grass cv. Napier using an isolated plant protocol under free growth condition, identifying the coordination of development including the internode elongation and leaf development on the main and the

primary axes. This information for tropical C4 grasses is crucial for understanding plant functioning and necessary for modelling tropical plant growth. Further, it is necessary to allow adequate planning of management strategies for controlling stem development and accumulation in pasture-based systems.

3. OBJECTIVES OF THE THESIS AND EXPERIMENTAL HYPOTHESIS

The general objective of this study is to elucidate the morphogenesis of the perennial tropical C4 grass *Pennisetum purpureum* cv. Napier (elephant grass) integrating the internode component. This information will be used to discuss aspects of ontogenetic development during the vegetative and reproductive growth phases, and in a broader view, to infer upon consequences for grazing management. The specific objectives are:

- To characterize the ontogenic development of elephant grass and the coordination between phytomers and primary axes arising during the development of the main axis;
- To describe the seasonality effects on the ontogenetic development of elephant grass;
- To characterize the process of stem elongation during the ontogenetic development and the coordination of internode and leaf development.

According to these objectives, two questions represent the main experimental hypotheses structuring the research work:

- Is the coordination of development observed in temperate forage grasses valid for tropical forage grasses?
- Is internode elongation coordinated with leaf development ontogeny? If so, how is this coordination operated?

4. MATERIAL AND METHODS

4.1. Experimental site

The experiment was conducted at the Experimental Unit of Forage Plants (UEPF), in the Department of Animal Science of the Luiz de Queiroz College of Agriculture (ESALQ), University of São Paulo, SP, Brazil (22°42'S, 47°37'W, 552 m a.s.l.). The climate is subtropical with dry winters. Average annual rainfall is 1328 mm (CEPAGRI, 2017). Eighty fiber cement tanks, measuring 0.70 × 0.70 × 0.70 m (0.343 m^3) were installed 2 meters from each other (Figure 4.1). The tanks were arranged according to a randomized complete block design with four replications. Each block was composed of 20 tanks, 10 of which were used to evaluate the morphogenic and developmental characteristics of the plants and the other 10 were used for destructive evaluations (Figure 4.2).

Figure 4.1. Aerial view of the experimental area.

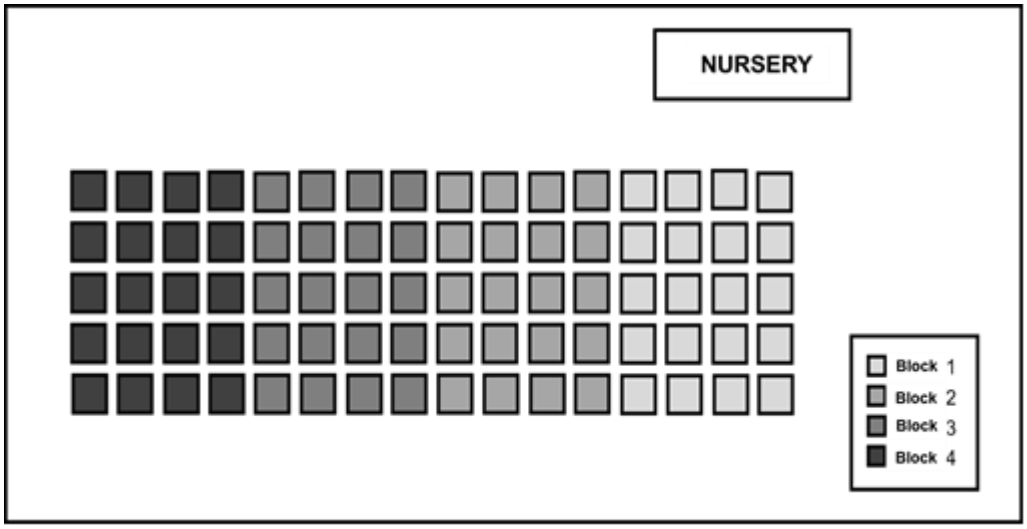

Figure 4.2. Layout of the experimental area

In each tank a bottom layer of approximately 10 cm of gravel and a drainage blanket were added to facilitate water drainage. Subsequently, the tanks were filled with high fertility soil. Average soil characteristics were: pH $CaCl_2$ = 5.7; organic matter = 77.0 g dm^{-3}; P (ion-exchange resin extraction method) = 393.0 mg dm^{-3}; Ca = 96.0 mmol dm^{-3}; Mg = 26.0 mmole dm^{-3}; K = 19.5 mmol, dm^{-3}; H+Al = 34.0 mmol dm^{-3}; sum of bases = 141.5 mmolc dm^{-3}; cation exchange capacity = 175.5 mmolc dm^{-3}; base saturation = 81%.

Throughout the evaluation period, soil moisture in the tanks was monitored. Soil was maintained with water potential close to field capacity using a drip irrigation system. Irrigation was determined through three tensiometers per tank positioned at 15, 30 and 45 cm depth (Figure 4.3). The field capacity was determined by the direct gravimetric method (Embrapa, 1997; Souza et al., 2000), through soil sampling of 20 tanks before the beginning of the experiment. The soil samples, approximately 100 g, were deformed, moistened until saturation, and drained to total cessation of free drainage. Soil surface was covered to avoid evaporation. In order to avoid water stress, every three days, readings of the tensiometer were taken and irrigation was adjusted to field capacity. In the nursery for propagation of seedlings, the irrigation system used was microsprinkler.

Figure 4.3. Alocation of the three tensiometers positioned at 15, 30 and 45 cm depth (1); arrangement of the tensiometers in the tank (2); Monitoring of the soil humidity using tensimeters (3)

Seedlings were produced via stems collection in a well-established *Pennisetum purpureum* cv. Napier pasture. During each season of the year, elephant grass stems were cut in stakes containing only one node and planted in 210 cm^3 tubes containing expanded vermiculite (Figure 4.4). The stems were collected on July 27, 2015, November 28, 2015, March 11, 2016, for the Spring, Summer and Autumn plantings, respectively.

Figure 4.4. Nursery to produce seedlings. Details of the design and irrigation system (1); Allocation of the node within the tubes (2); Seedling emergence (3)

After rooting, seedlings were selected containing five leaves and three seedlings were transplanted per tank. Once plants were established, thinning was performed in order to leave only one plant per tank prior to the beginning of the experimental evaluations. When plants presented the tenth visible leaf, nitrogen fertilization with ammonium nitrate was carried out in an amount equivalent to 70 kg ha^{-1} N. The fertilizer was weighed individually for each tank and diluted in 500 ml of water for application in the tank. This day was considered as the first day of the evaluation period, which consisted of 70 days for Spring and 55 days for the other seasons of the year: Spring (21 September to 30 November, 2015); Summer (January 4 to February 27, 2016); and Autumn (April 10 to June 4, 2016).

The meteorological data for the experimental period were collected at a meteorological station of the Department of Biosystems Engineering of ESALQ - USP, located about 200 m from the experimental site. Temperature, precipitation, global radiation and daylength varied according to season of the year (Figure 4.5 and 4.6). Average daily temperatures and global radiation were higher in Summer relative to Spring and Autumn. During Summer, the average daily temperature was constantly around 25-27°C, while in Spring the temperature ranged from 15 °C at the time of node collection to approximately 23-

25°C after the beginning of the morphogenetic evaluations. During Autumn the average daily temperature ranged from around 25°C in the beginning of the experimental period but decreased to 15°C between April 15th and the end of the experiment. During Spring, the global radiation was lower (around 15 MJ m^{-2} day^{-1}), increasing after September 20th (approximately), with sharp variations. During Autumn, global radiaton was close to 15 MJ m^{-2} day^{-1} at the time of node collection and decreased abruptly to around 5-7 MJ m^{-2} day^{-1} after the beginning of the morphogenetic evaluations.

The amount of pluvial precipitation was greater during Summer (total of 680 mm) relative to Spring (total of 510 mm) and Autumn (total of 250 mm). During Summer, precipitation was well distributed, while during Spring precipitation started after the beginning of the morphogenetic evaluations (September 21). Daylength ranged from 10.6 h (lowest value observed in Autumn) to 13.4 h (highest value observed in Summer) (Figure 4.6). During Summer, values of daylength were less variable, with average of 13.13 h (ranging from 12.5 to 13.4 h), while in Spring the daylength varied from 10.9 to 13.3 h (average of 12.16 h) and in Autumn ranged from 10.6 to 12.2 h (average of 11.3 h).

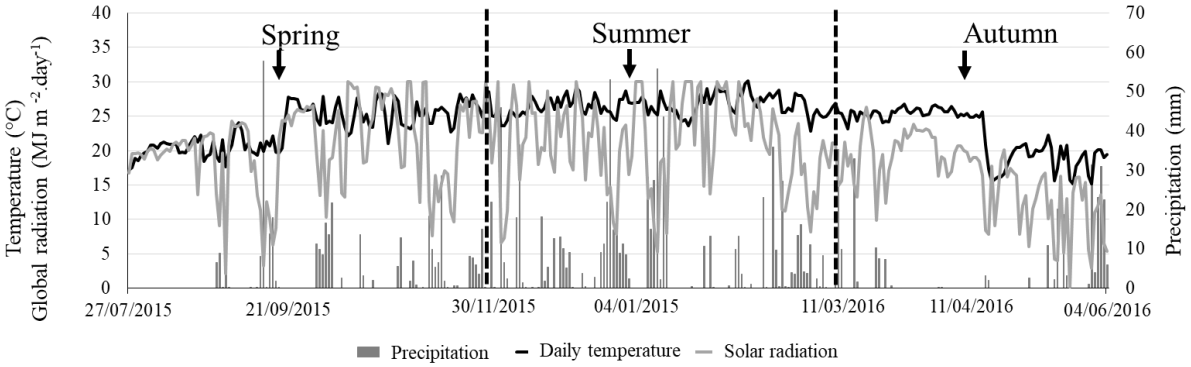

Figure 4.5. Mean daily temperature (ºC), solar radiation (MJ m^{-2}), and precipitation (mm) during seasons of the year from the node sowing of the Spring until the last day of evaluation in Autumn. Vertical arrows indicate the starting date of evaluation for each season and vertical dashed lines indicates the date of the node sowing for Summer and Autumn.

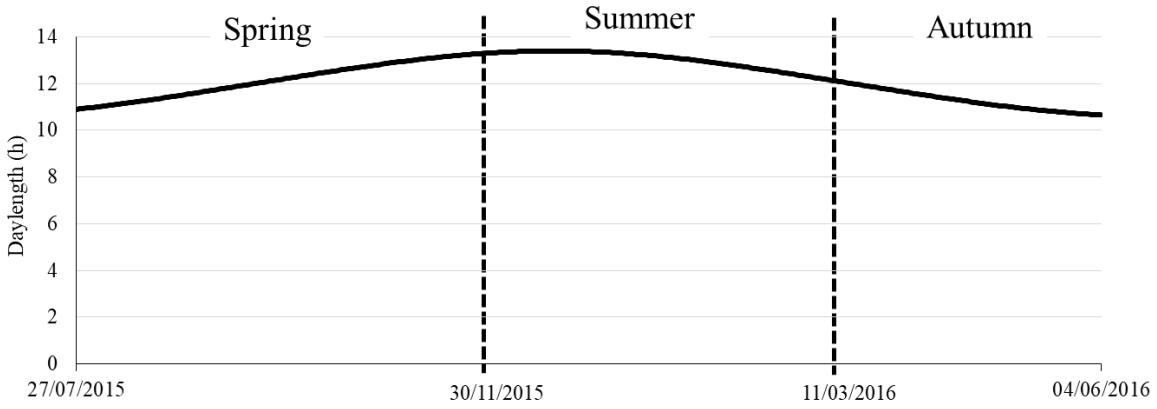

Figure 4.6. Mean daily daylength (h) during seasons of the year from the node sowing of the Spring until the last day of evaluation in Autumn. Vertical dashed lines indicate the date of the node sowing for Summer and Autumn.

4.2. Non-Destructive analysis

For evaluations regarding plant morphogenesis and characterization of plant development, 40 tanks were separated in 10 tanks per block. Measurements of leaf lamina growth and stem elongation dynamics where carried out every two days (Figure 4.8). Leaves were classified as: (1) in expansion, when the ligule was not exposed and their reference for length measurement was the ligule of the last fully expanded leaf; (2) expanded, when the ligule was visible; (3) senescencing, when part of the leaf blade showed signs of senescence (yellowing). At the time of morphogenesis evaluations, leaves were numbered according to their order of appearance, on both main and primary axes. It is customary to refer to the first shoot as the parent shoot and subsequent shoots developed from axillary branchs are termed tillers (Bell, 1991). By convention, the terminology used to refer to the different shoot axes was summarized according to the following diagram.

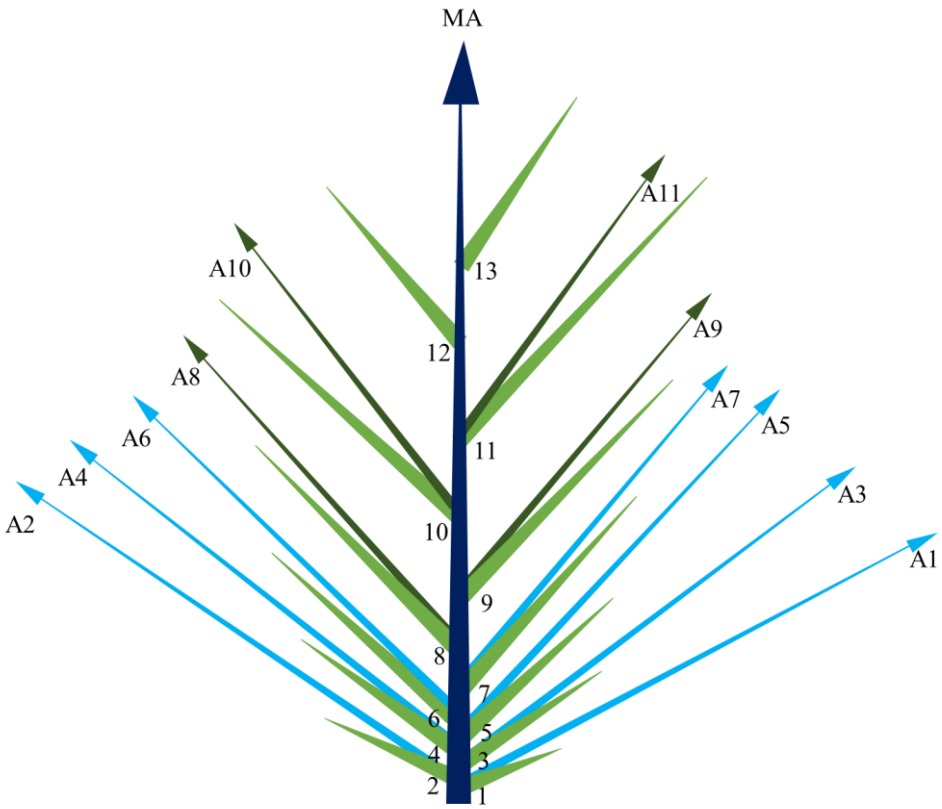

Figure 4.7. Diagrammatic representation of the classification of shoot axes. Dark blue represents the main axis (MA). Green represents the leaves arising from the main axis. Leaves were numbered following their sequence of appearance and each number represents its respective rank (number 1 to 13 represents leaf ranks 1 to 13 on the main axis). Light blue represents primary axes branching close to soil surface. Dark green represents primary axes branching above soil surface. Primary axes were numbered according to their position on the main stem (axes from A1 to A11 represent primary axes ranks). Leaf ranks were also assessed for primary axes, but are not presented in this scheme.

Figure 4.8. Evaluation of leaf blade growth

4.3. Destructive analysis

For the destructive evaluations 40 tanks were used, separated in 10 tanks per block (corresponding to 4 replicates, total of 10 destructive samples per block). At the time of sampling, the main axis and all the associate axillary axes were collected by cutting close to the soil surface. Phytomers were identified according to their sequence of appearance and the corresponding primary axes were listed according to the rank in which they arised from the main axis, as presented above (Figure 4.7). The components of the phytomer were classified according to Figure 4.9.

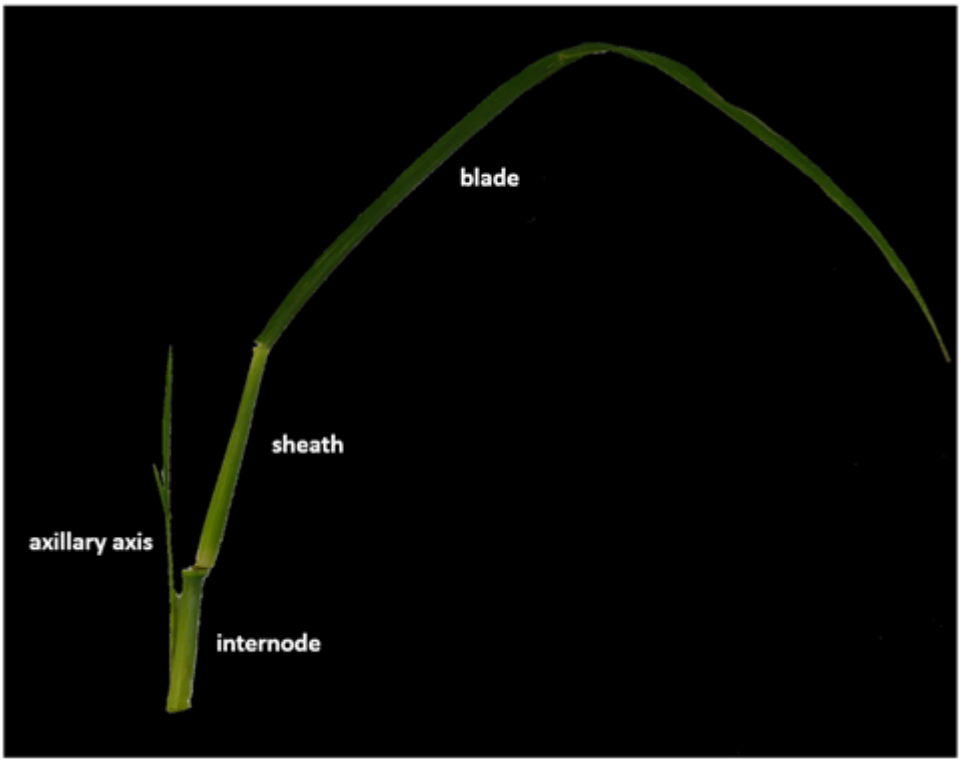

Figure 4.9. Components of a mature phytomer of *Pennisetum purpureum* cv. Napier

The following variables were measured on main and primary axes: apical meristem height; sheath tube length; leaf blade length; number of expanding leaves; number of expanded leaves. Measurements of leaf sheath and internode length were performed only for the main axis. The position of the apical meristems was determined by longitudinal dissection, based on the distance of the apical meristem relative to the soil (stem length) (Figure 4.10). Sheath tube length was measured as the distance from the apical meristem to the ligule of the last fully expanded leaf.

Figure 4.10. Longitudinal section of the axis to identify the position of the apical meristem in main and primary axes in *Pennisetum purpureum* cv Napier.

In Spring 2015, the first evaluation season, destructive assessments began on the 25th day after day 1 of morphogenesis measurements. Thus, considering a total of 10 destructive samples collected at 5-day intervals, the evaluation period lasted 70 days. However, for the other two seasons, Summer and Autumn, destructive samples collection started earlier, due to the increased plant growth rate and accelerated stem elongation. During Summer and Autumn of 2016, destructive evaluations began on the 10th day after the beginning of morphogenesis measurements, and the evaluation period lasted 55 days.

4.4. Coordination of leaf growth

The analysis of coordination between phytomers and coordination between leaf blade and internode growth on successive phytomers was perfomed on the main axis. The analysis was made by transformation of a series of measurements since data collection on the field according to the following diagram.

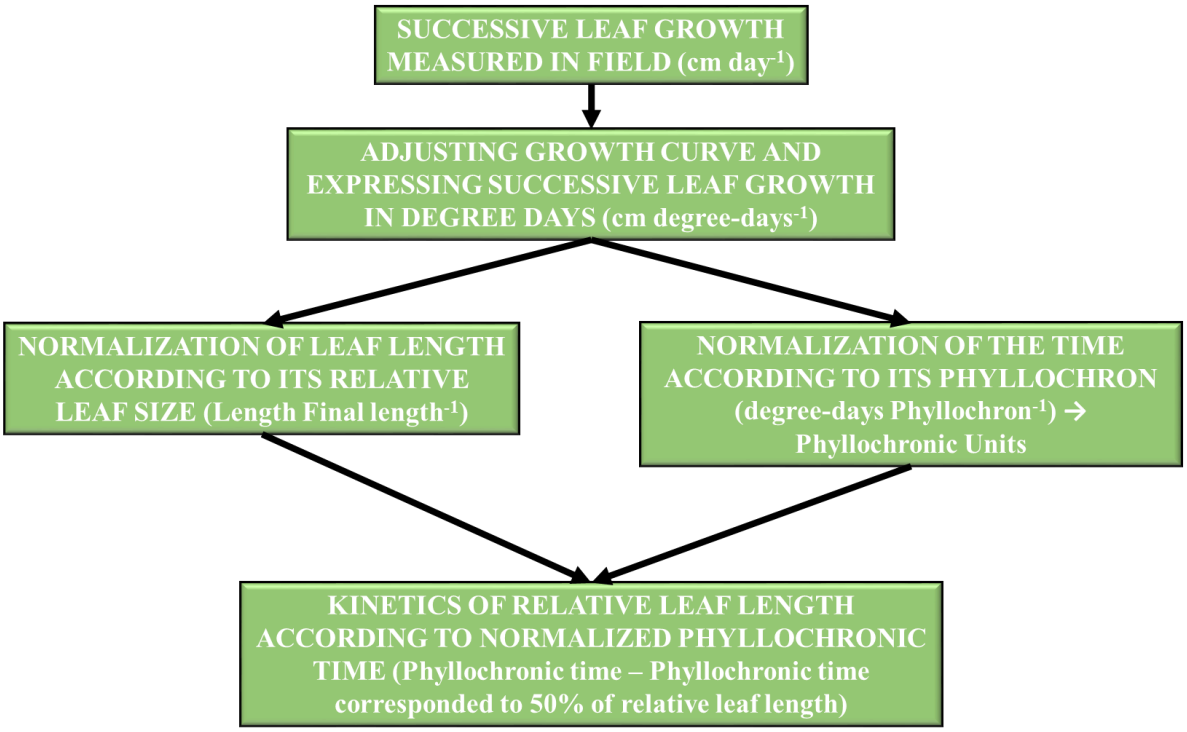

Figure 4.11. Diagram representing the successive steps of transformation of the data to represent the coordination of growth between phytomers on main axis.

The schematic representation of the successive procedures is presented below (Figure 4.12). The data collected on the field was first adjusted with a hyperbolic curve, expressing the time in degree-days (°C) (Figure 4.12-I). Then, the dynamics of leaf gowth was standardized by normalizing leaf length relative to its final leaf length (Figure 4.12-II). Subsequently, the time, expressed in degree-days (°C), was normalized for the phytomers considering that the time 0 (zero) corresponded to 50% of the final leaf length (Figure 4.12-III). Lastly, time was converted to phyllochronic time, dividing the degree-days by its respective phyllochron (Figure 4.12-IV and V).

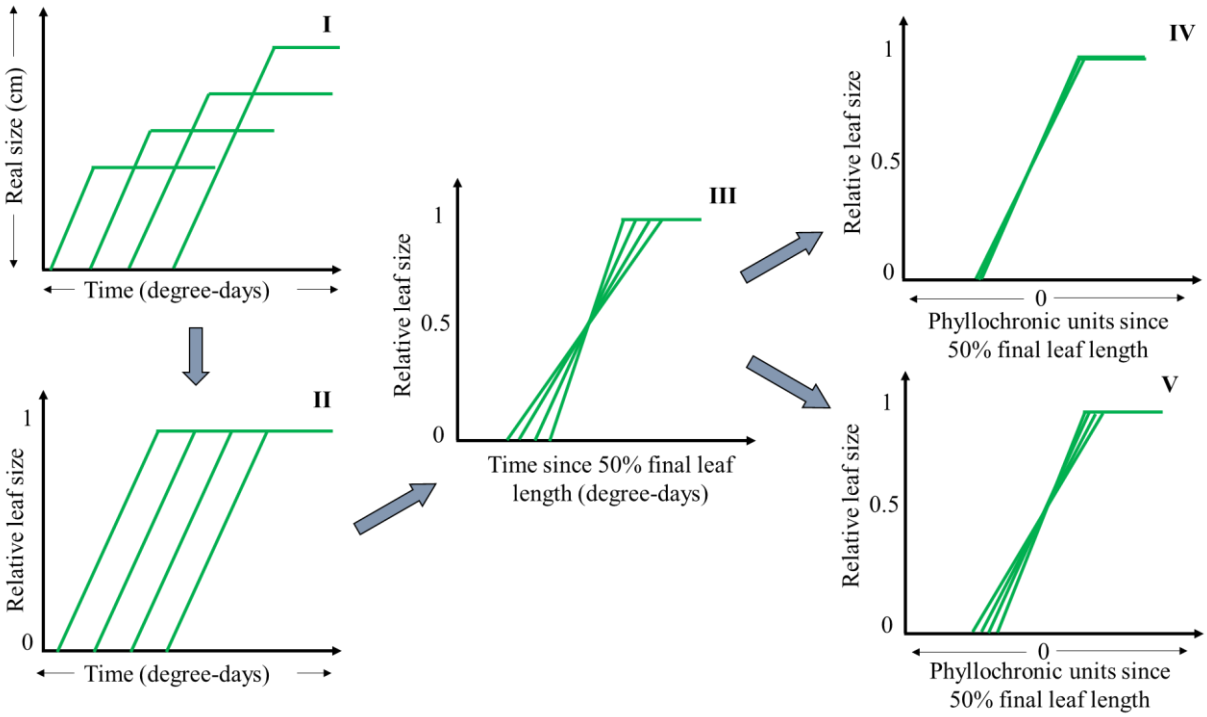

Figure 4.12. Diagram representing successive analysis to represent coordination of development between successive phytomers on main axis.

The analysis of coordination between successive phytomers was interpreted according to Figures 4.12 IV and V. When phytomers growth is coordinated, the duration of organ expansion presents a conservative pattern, regardless of leaf rank when expressed in phyllochronic time (Figure 4.12 IV). On the other hand, if there is divergence between successive phytomers growth when expressed in phyllochronic time, either there is no coordination between phytomers (Figure 4.12 V) or other factors need to be integrated in the coordination of successive phytomers.

4.5. Thermal time

The thermal time was expressed in growing degree-days (GDD, °C) including the period of nodes collection for seedlings production and transplantation. Thermal time was calculated using a base temperature of 10°C. Cumulative growing degree-days was calculated using the following equation:

$$GDD = \sum_{i}^{n} \left[\left(\frac{T\max + T\min}{2} \right) - Tbase \right];$$

Where:

- Tmax and Tmin are the maximum and minimum temperature recorded in a day, respectively;
- Tbase is the base temperature.

4.6. Plant nitrogen concentration

Nitrogen concentration was evaluated during Summer, Autumn and Spring on samples collected for destructive analysis. Samples were from cuts number 1, 4, 7 and 10. Samples were cut above soil surface, therefore comprising all shoot axes. Total-N and total-C concentrations were quantified on 0.5±1 g of dried and grounded samples through a C:N analyser (CN2000, LECO, Stockport, UK).

4.7. Statistical analyses

All calculations and statistical tests were performed using the R software (version 3.1.2; R Development Core Team, 2014). Rates of leaf appearance were calculated for the main and primary axes as the coefficient of the linear regression between thermal time and number of leaves. Phyllochron values were calculated as the reciprocal of the rates of leaf appearance. The temporal growth of plant organs was analyzed using a five-parameter hiperbolic function (Figure 4.13) fitted to the time series of organ growth measurements:

$$y = \left(\frac{1}{2.\theta} \right).\left[\alpha(t - tc) + y\max - \sqrt{(\alpha.(t - tc) + y\max)^2 - 4.\theta.\alpha.(t - tc).y\max} \right];$$

Where:

Ymax is the final length of the leaf, tc is the start time of the leaf length; α and θ are two constants. The parameter α represents the maximum growth rate which is reached at the first growth time (i.e. at time t = tb). The parameter θ indicates the convexity of the curve. This last parameter is strictly positive and lower or equal to 1. When this parameter is equal to 1,

the curve is formed by two straight lines of equations Y = α (t-tb) when t ≤ Ymax/(α-tb) and Y = Ymax when t> Ymax/(α-tb).

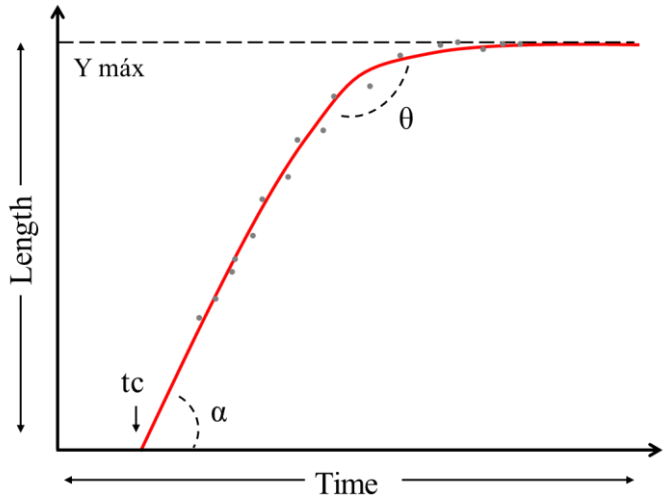

Figure 4.13. Graphical representation of the hyperbolic function used to model the kinetics of growth. Points represent cumulative length (i.e. leaf length or internode length) and red line represents hyperbola fitting.

The mathematical model of hiperbola is described by a non-equilateral formula (Thornley and Johnson, 1990). This adjustment allows to estimate the morphogenetic parameters, such as: LAR (leaf appearance rate), LER (leaf elongation rate) and LED (leaf elongation duration). The LER can be approximated directly by the value of α. Estimates of LED can be calculated as the time elapsed between *tc* and the time at which the organ reaches 95% of its final size, as follow:

$$t_{95\%} = tc + \left(\frac{0.95.y\max - 0.95^2.y\max.\theta}{0.05\alpha} \right)$$

Significant differences between means for plant traits were tested by performing analyses of variance (“aov” procedure). Analyses of covariance (ANCOVA, lm procedure) were used to test simultaneously for the effects of continuous and categorical variables and to compare the slopes and intercepts of the linear relationships.

5. RESULTS AND DISCUSSION

The Results and Discussion section is organized according to the two experimental hypotheses outlined in section 3.

5.1. IS THE COORDINATION OF LEAF DEVELOPMENT OBSERVED IN TEMPERATE FORAGE GRASSES VALID FOR TROPICAL FORAGE GRASSES?

5.1.1. RESULTS I

5.1.1.1. Nitrogen concentration

Nitrogen concentration was evaluated during all seasons of the year to investigate possible nitrogen deficiencies. Nitrogen concentration during Summer and Autumn gradually decreased as plant developed. This decline in N concentration was due to the well-known N dilution process (see Lemaire and Gastal 1997) occurring even for isolated plants. Lower nitrogen concentration was observed in Spring during the entire evaluation period (Figure 5.1.1). Therefore, for the same growth stage, i.e 1000 degree-days, N% was 1% in Spring, but 2% in Summer and Autumn, denoting a strong N deficiency. As plant grew during Spring, this difference decreased, and similar N concentrations were obtained at the end of each evaluation period, regardless of season of the year.

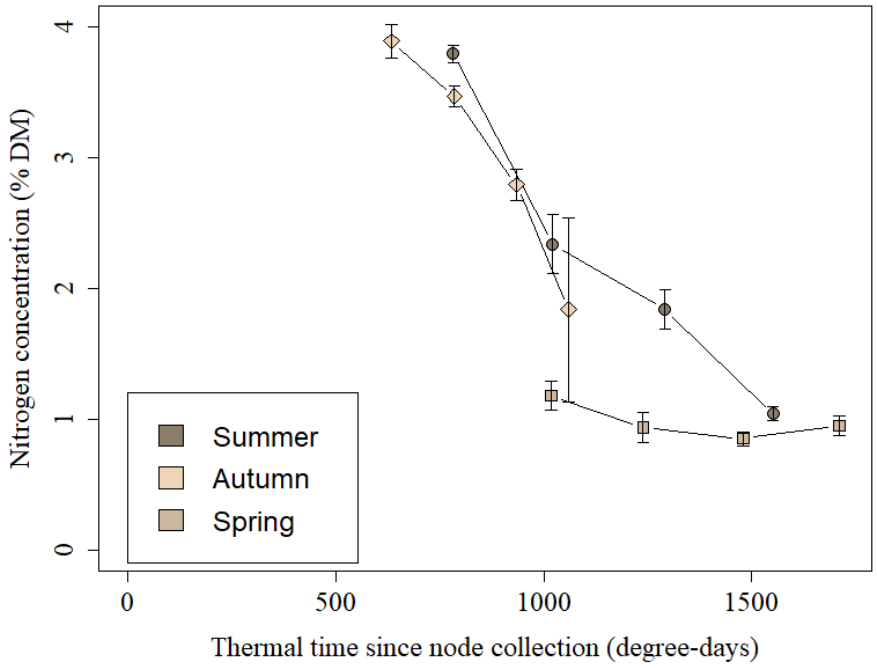

Figure 5.1.1. Nitrogen concentration in *Pennisetum purpureum* cv. Napier across seasons of the year expressed in percentage of the dry matter (% DM). Diamonds: Autumn (2016); circles: Summer (2016); squares: Spring (2015). Vertical bars indicate standard deviation of the mean.

5.1.1.2. Ontogenetic development on the main axis

5.1.1.2.1. Dynamics of leaf growth

The dynamics of successive leaves growth appearing on the main axis of *Pennisetum purpureum* cv. Napier was expressed in degree-days. When a leaf emerges, it elongates until reaching its final size and remains green until the start of senescence. The following diagram represents leaf tissue production on the main axis across the three seasons of the year in this study (Figures 5.1.2, 5.1.3 and 5.1.4).

During Summer, the average final leaf length increased for successive leaves from phytomer 10 to 20 (Figure 5.1.2). On the other hand, during Autumn, the final leaf length increased from phytomer 9 to 11 and then decreased to the last phytomer produced by the apical meristem, leaf 14, after which flowering occurred (Figure 5.1.3). During Spring, there was a progressive increase in final leaf length from phytomer 10 to 13, followed by a decrease from phytomer 13 to 17 and then another increase from phytomer 17 to 19 (Figure 5.1.4).

Final leaf length was greater during Summer relative to Spring and Autumn. More than one leaf was expanding at the same time on the main axis, and larger number of

expanding leaves was observed for higher leaf ranks during Summer and Spring (Figure 5.1.2 and 5.1.4). The smallest number of leaves was observed during Autumn and leaf appearance ceassed after leaf 14 (approximately 580 degree-days), because of the onset of flowering on all plants (Figure 5.1.3).

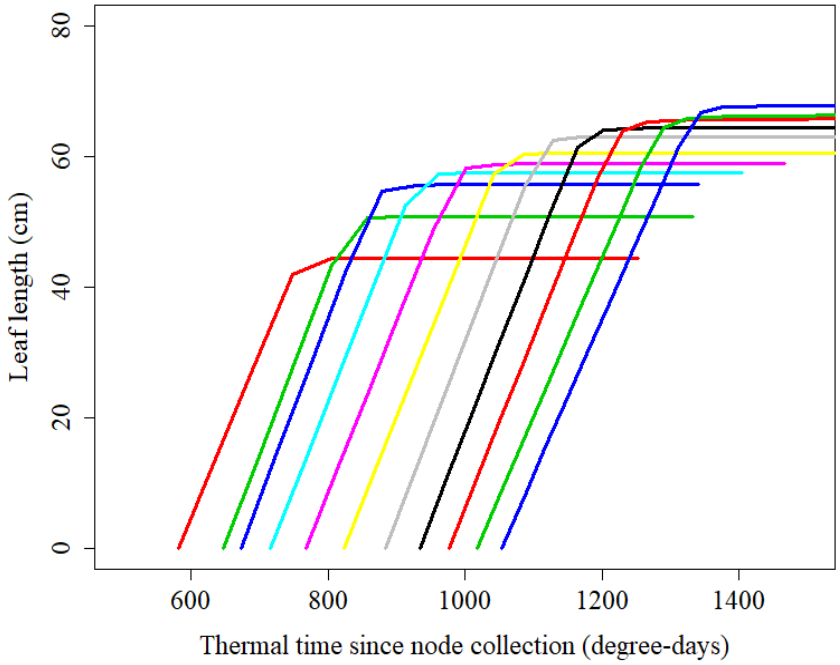

Figure 5.1.2. Time course of lamina length for successive leaves of *Pennisetum purpureum* cv. Napier during the Summer, 2016. The diagram shows individual leaves from phytomer 10 to 20 on the main axis, according to thermal time in degree-days (˚C).

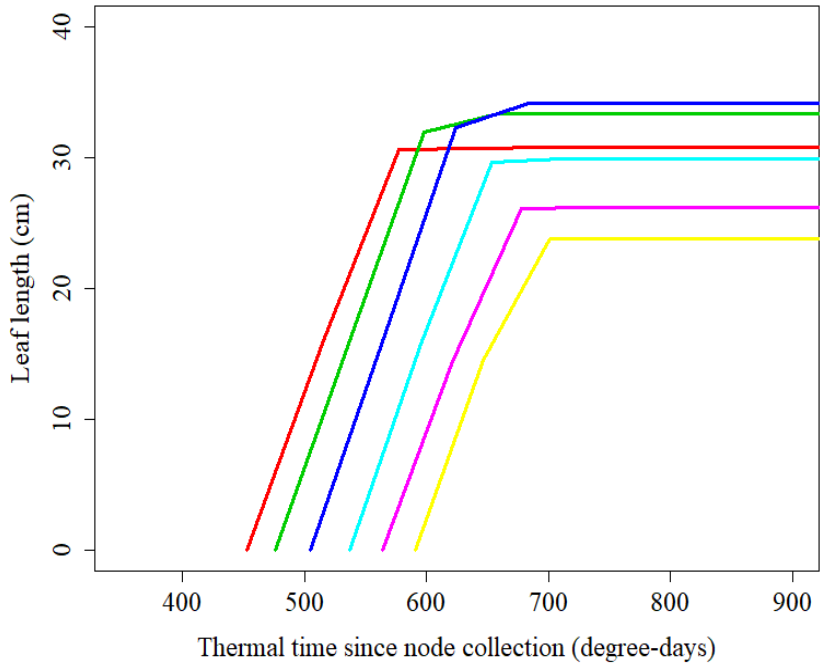

Figure 5.1.3. Time course of lamina length for successive leaves of *Pennisetum purpureum* cv. Napier during the Autumn, 2016. The diagram shows individual leaves from phytomer 9 to 14 on the main axis, according to thermal time in degree-days (˚C).

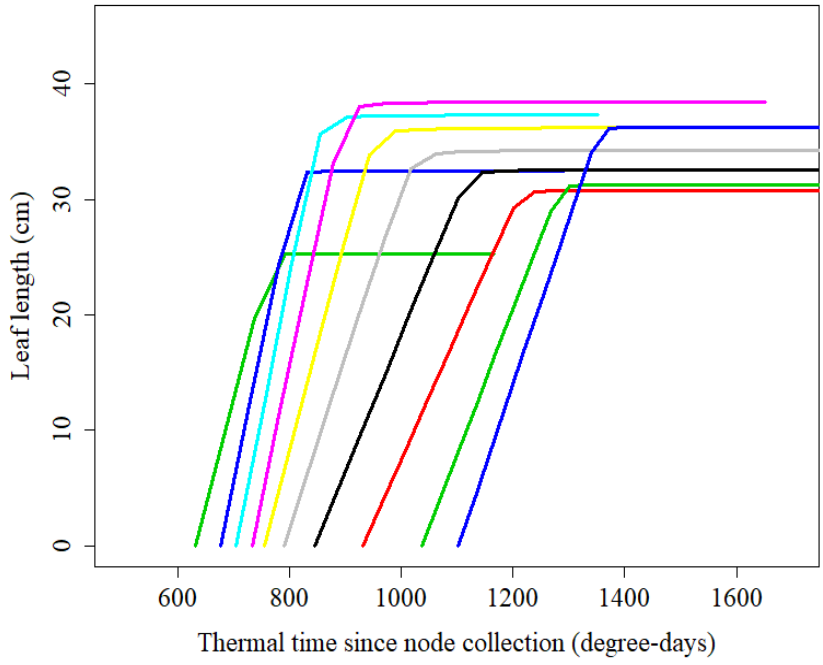

Figure 5.1.4. Time course of lamina length for successive leaves of *Pennisetum purpureum* cv. Napier during the Spring, 2015. The diagram shows individual leaves from phytomer 9 to 19 on the main axis, according to thermal time in degree-days (˚C).

The dynamics of successive leaves growth on the main axis was used to identify the other studied variables, namely: phyllochron, leaf elongation rate, leaf elongation duration and final leaf length, obtained by the hyperbolic curve adjusting on leaf growth, as presented in the Figure 4.13.

5.1.1.2.2. Leaf appearance rate (LAR)

The appearence of successive leaves on the main axis was first plotted against calendar days starting from the date of node collection (Figure 5.1.5). The appearance of leaf 10 occurred almost at the same time during Autumn and Summer, close to 35 days. The phyllochron, i.e. time elapsed between the emergence of successive leaves, was lower during Autumn (average of 1.83 day) relative to Summer (average of 3.05 days). Conversely, during Spring the time of appearance of leaf 10 was much longer, approximately 55 days, and the average phyllochron was greater relative to Summer and Autumn, approximately 3.86 days. In the vegetative phase, i.e. Summer and Spring, the same number of leaves was produced on the main axis in shorter period of time for Summer relative to Spring, 60 and 95 days, respectively (Figure 5.1.5). On the other hand, the limited amount of leaves produced during Autumn was related to the transition from the vegetative to the flowering stage. Leaf production ceassed after the appearance of leaf 14.

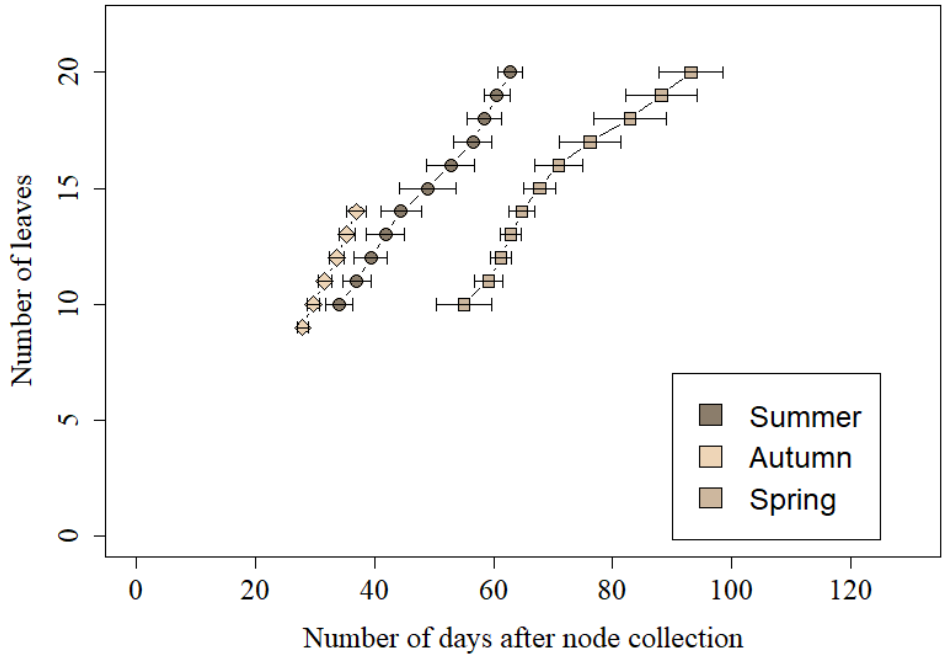

Figure 5.1.5. Timing of leaf appearance on the main axis of *Pennisetum purpureum* cv. Napier expressed in days. Diamonds: Autumn (2016); circles: Summer (2016); squares: Spring (2015). Horizontal bars indicate standard deviation of the mean.

To standardize the temperature effect on leaf appearance, the number of leaves on the main axis was plotted against thermal time, taking into account the base temperature of 10°C, starting from the date of node collection (Figure 5.1.6). The experimental period in thermal time corresponded to approximately 600, 1100 and 1200 degree-days for Autumn, Summer and Spring, respectively. During Autumn, leaf 10 appeared earlier, with approximately 450 degree-days, while during Summer and Spring it appeared later, with approximately 600 degree-days from the date of node collection.

New leaves appeared on the main axis at a constant rate, resulting in a linear relationship between the total number of leaves and thermal time during seasons of the year. Analysis of covariance performed on the regression slopes between the number of appeared leaves and thermal time (leaf appearance rate) showed significant season of the year effect (ANCOVA, $P<0.01$), with greatest values for Autumn, intermediate for Summer and lowest for Spring (Table 5.1.1). Mean phyllochron corresponded to 27.92, 47.38 and 58.64 degree-days for Autumn, Summer and Spring, respectively.

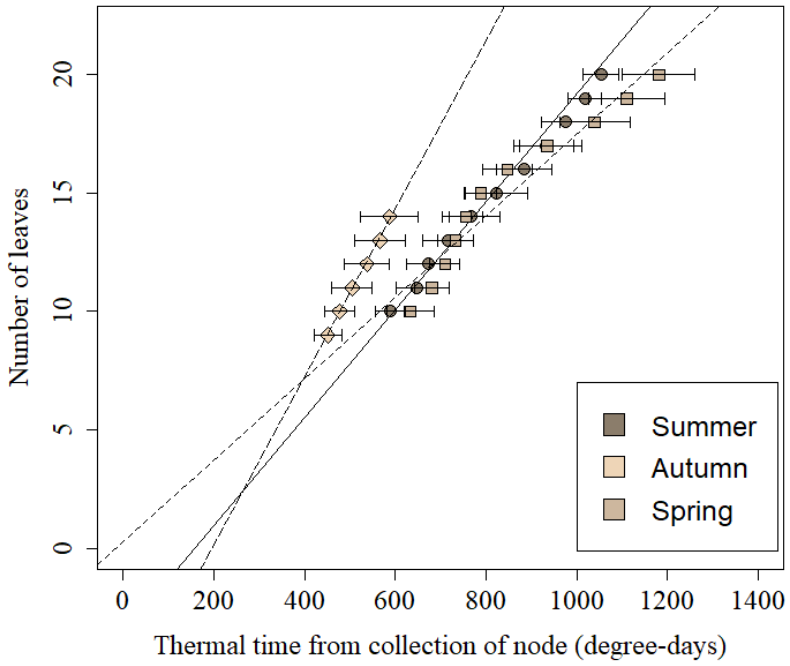

Figure 5.1.6. Timing of leaf appearance on the main axis of *Pennisetum purpureum* cv. Napier expressed in degree-days (˚C). Diamonds: Autumn (2016); circles: Summer (2016); squares: Spring (2015). Horizontal bars indicate standard deviation of the mean.

Table 5.1.1. Slope coefficient and coefficient of determination in the linear regression NL = α + LAR × DD, where NL = number of leaves, α is a constant and DD = degree-days (°C). The coefficient LAR describes leaf appearance rate (LAR) on the main axis of *Pennisetum purpureum* cv. Napier expressed in degree-days. Analysis of covariance was performed on LAR (P<0.01).

Season of the year	LAR	r^2
Summer	0.0203 B	0.99
	(0.00016)	
Autumn	0.0322 A	0.98
	(0.0031)	
Spring	0.0165 C	0.91
	(0.0020)	

Values in parentheses indicate standard error of the mean. Means followed by the same upper-case letter do not differ (P>0.05).

The thermal time at the emergence of the first leaf was not identified. Therefore, the number of leaves on the main axis was plotted against thermal time (degree-days in °C), by adjusting the linear regressions to start at the same point in all seasons (degree-days equal 0°C corresponded to 0 number of leaves for all seasons) and normalized by a common leaf appearance on the main axis for each season (Figure 5.1.7).

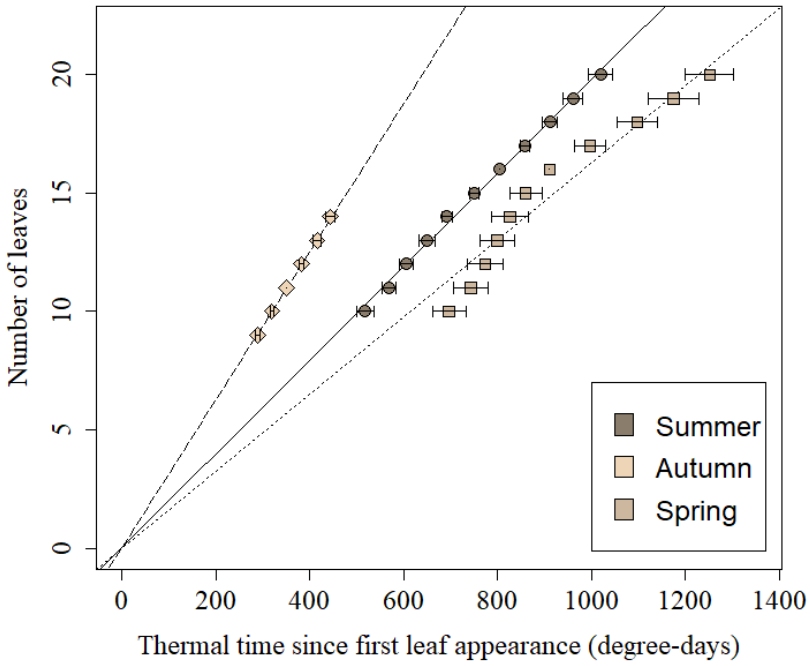

Figure 5.1.7. Leaf appearance on the main axis of *Pennisetum purpureum* cv. Napier expressed in degree-days (°C). Diamonds: Autumn (2016); circles: Summer (2016); squares: Spring (2015). For each season, the data were normalized according to a common event. In Summer-2016 and Spring-2015 the reference was the appearance of leaf 16, while in Autumn-2016 the reference was the appearance of leaf 11.

5.1.1.2.3. Leaf elongation rate (LER)

In general, LER on the main axis was constant during Summer and Autumn (Figure 5.1.8) for phytomers 10 to 20 and 9 to 14, respectively, with average values of 0.26 cm degree-day^{-1}. During Spring, LER was constant for phytomers 10 to 14, and then decreased abruptly until phytomer 16, remaining constant from then on until phytomer 20 (Figure 5.1.8). During Spring there was a variability of approximately 120% in LER, with recorded values ranging from 0.11 to 0.24 cm degree-day^{-1}.

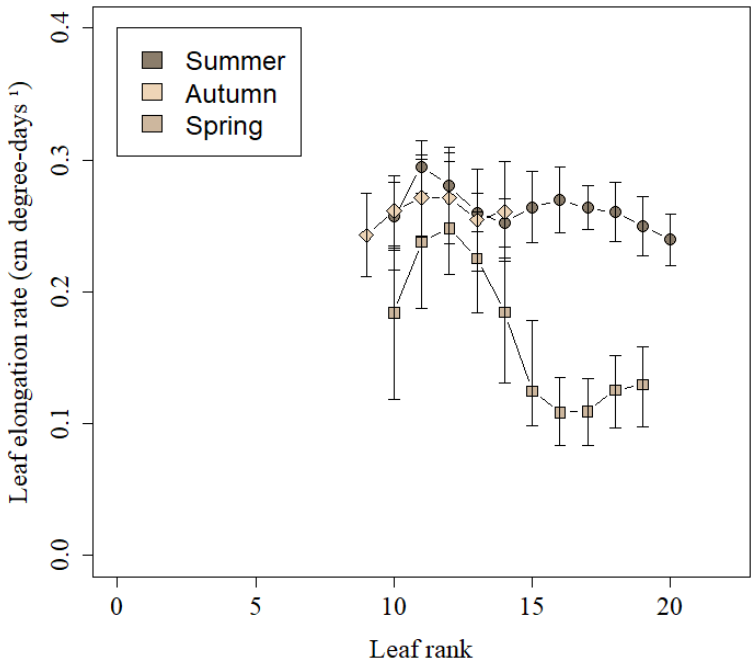

Figure 5.1.8. Leaf elongation rate (cm degree-days $^{-1}$) for *Pennisetum purpureum* cv. Napier expressed in degree-days (°C) for successive leaves on the main axis. Diamonds: Autumn (2016); circles: Summer (2016); squares: Spring (2015). Vertical bars indicate standard deviation of the mean.

5.1.1.2.4. Leaf elongation duration (LED)

The LED was first expressed in degree-days and increased according to leaf rank level on the main axis during Summer and Spring. Recorded values ranged from 180 to 280 and 130 to 280 degree-days for Summer and Spring, respectively. During Spring, when leaf rank was higher than 15, recorded values were constant and approximated 260 degree-days. On the other hand, when expressed in thermal time, a seasonality effect in LED was observed, with lower values recorded during Autumn regardless of leaf rank. During Autumn, the LED remained constant from leaf rank 9 to 11 (around 130 degree-days) and decreased until leaf rank 14 (average of 80 degree-days) (Figure 5.1.9).

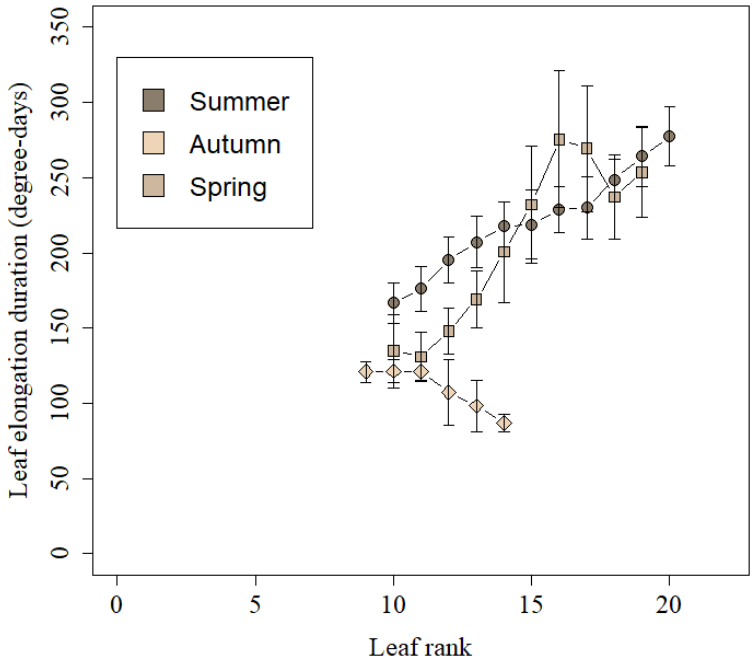

Figure 5.1.9. Leaf elongation duration for *Pennisetum purpureum* cv. Napier expressed in degree-days (°C) for successive leaves on the main axis. Diamonds: Autumn (2016); circles: Summer (2016); squares: Spring (2015). Vertical bars indicate standard deviation of the mean.

The LED was also expressed in phyllochronic time by dividing the thermal time by its corresponding phyllochron (Figure 5.1.10). In this sense, LED showed increasing values with increasing leaf rank level during Summer and Spring (Figure 5.1.10). During Summer, LED increased from phytomer 9 (average of 3.6 phyllochrons) to 20 (average of 5.2 phyllochrons). During Spring, LED incresead from leaf 9 to 16 (from 2.5 to 5.0 phyllochrons), and reached a plateau. Conversely, during Autumn, constant values of LED were obtained for leaf ranks 9 to 11, similar to Summer values (average of 4.2 phyllochrons). From leaf rank 11 to 14, values of LED decreased sharply until leaf 14 (average of 2.6 phyllochrons) (Figure 5.1.9).

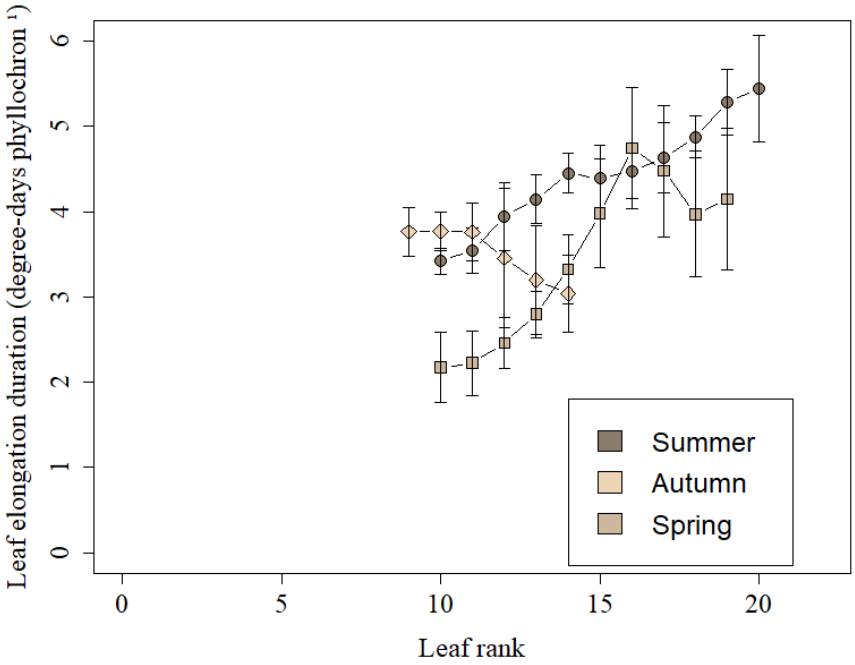

Figure 5.1.10. Leaf elongation duration (degree-days phyllochron^{-1}- phyllochronic units) for *Pennisetum purpureum* cv. Napier divided by phyllochron for successive leaves on the main axis. Diamonds: Autumn (2016); circles: Summer (2016); squares: Spring (2015). Vertical bars indicate standard deviation of the mean.

5.1.1.2.5. Final leaf length (FLL) and final sheath length

Final leaf length varied considerably between seasons of the year and phytomers on the main axis (Figure 5.1.11). The FLL increased according to leaf rank during Summer, varying from 42 cm for phytomer 10 to 71 cm for phytomer 20. During Autumn, leaf length decreased from phytomer 11 to 14, which may be attributed to flowering. During Spring, FLL increased from 22 cm (phytomer 10) to 40 cm (phytomer 13). For leaves above this level (phytomers 14 and higher), leaf length decreased until leaf rank 15, remaining constant up until phytomer 20.

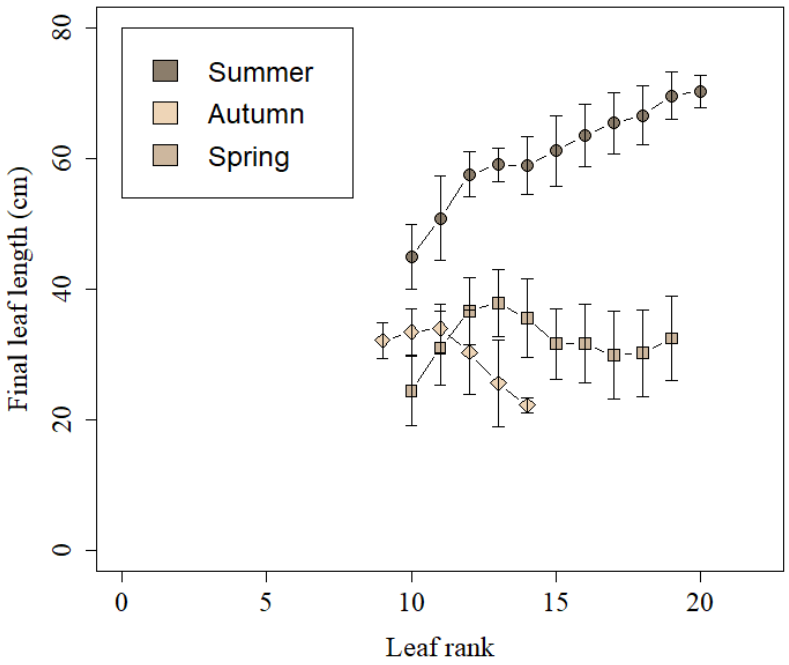

Figure 5.1.11. Final leaf length (cm) in *Pennisetum purpureum* cv. Napier for successive leaves on the main axis. Diamonds: Autumn (2016); circles: Summer (2016); squares: Spring (2015). Vertical bars indicate standard deviation of the mean.

Final sheath length increased across leaf ranks until phytomer 11, after which a plateau was reached, a common pattern observed during all seasons of the year. During Spring, values of sheath length increased until approximately 11 cm, whilst during Summer and Autumn, sheath length increased to approximately 13 cm (Figure 5.1.12).

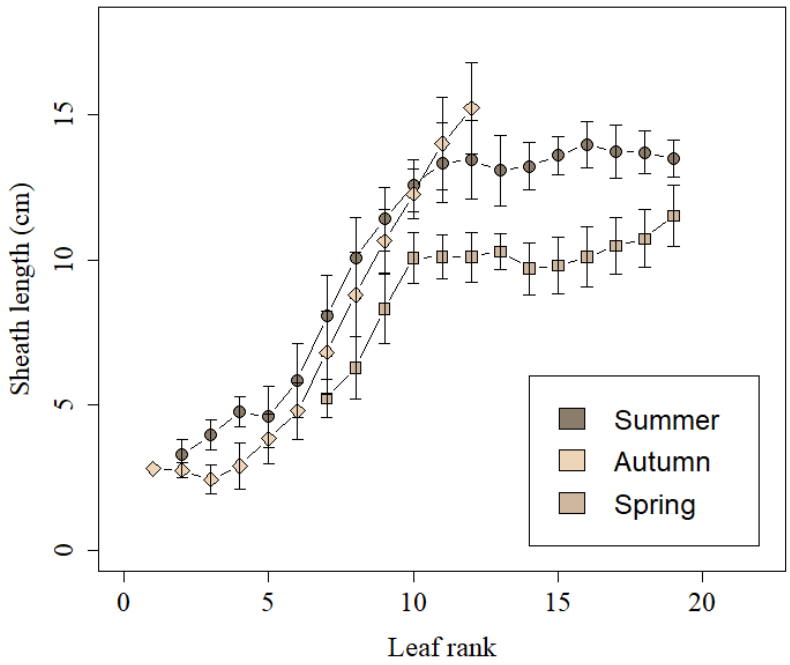

Figure 5.1.12. Final sheath length (cm) in *Pennisetum purpureum* cv. Napier for successive leaves on the main axis. Diamonds: Autumn (2016); circles: Summer (2016); squares: Spring (2015). Vertical bars indicate standard deviation of the mean.

5.1.1.2.6. Coordination of leaf growth

The analysis of coordination between the growth of successive leaves on the main axis of *Pennisetum purpureum* cv. Napier was obtained based on a series of graphs, according to the diagram presented in the Material and Methods Section (Figures 4.11 and 4.12). The coordination of development was tested in thermal time and phyllochronic time in order to identify the existence of seasonal effect on the coordination of leaf growth for all seasons of the year (Figures 5.1.13 and 5.1.14), and the effect of leaf rank during Summer (Figures 5.1.15 and 5.1.16), Autumn (Figures 5.1.17 and 5.1.18) and Spring (Figures 5.1.19 and 5.1.20). Analysis of covariance was performed on the regression slopes between the relative leaf length and time (thermal time and phyllochronic time) to compare the coordination between seasons, and the effect of leaf rank on the main axis for each season of the year, expressed in thermal time and phyllochronic units.

The coordination between growth of successive leaves on the main axis of *Pennisetum purpureum* cv. Napier was first analysed considering a common group of leaf ranks to compare the seasonal effect in the coordination, expressed in phyllochronic time. For all seasons, the intermediary group of leaves produced during the evaluation period was used.

During Summer and Spring, phytomers 14 to 17 were used, and during Autumn phytomers 9 to 11. When expressed in phyllochronic time, there was no difference (*P*=0.0827) between seasons of the year (Figures 5.1.13), representing the conservative coordination of leaf development.

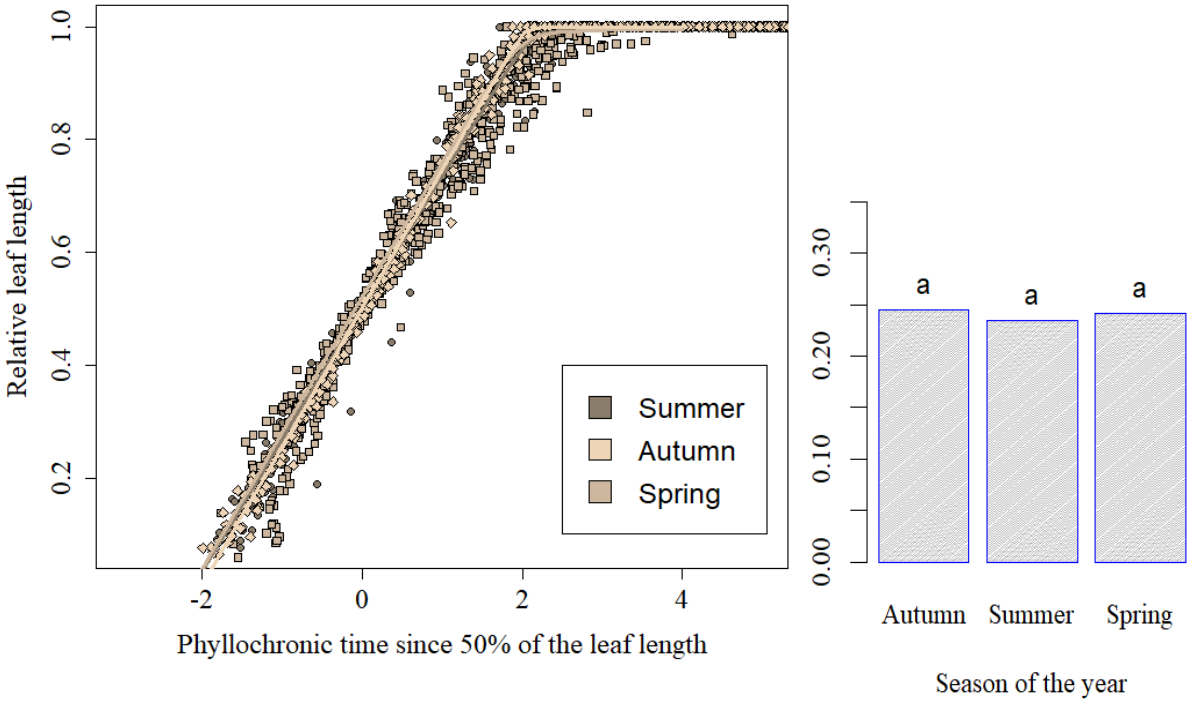

Figure 5.1.13. Kinetics of relative leaf length, expressed in phyllochronic time, on the main axis for *Pennisetum purpureum* cv. Napier across seasons of the year. In Summer and Spring, phytomers 14 to 17 were used, and in Autumn phytomers 9 to 11. The figure on the right side represents the ANCOVA ($p<0.001$) analysis performed on the maximum relative leaf elongation.

However, when expressed in thermal time, divergences were observed across seasons of the year (Figure 5.1.14). Therefore, the lack of synchronism between the curves characterizes a seasonal effect on leaf growth dynamics between seasons of the year.

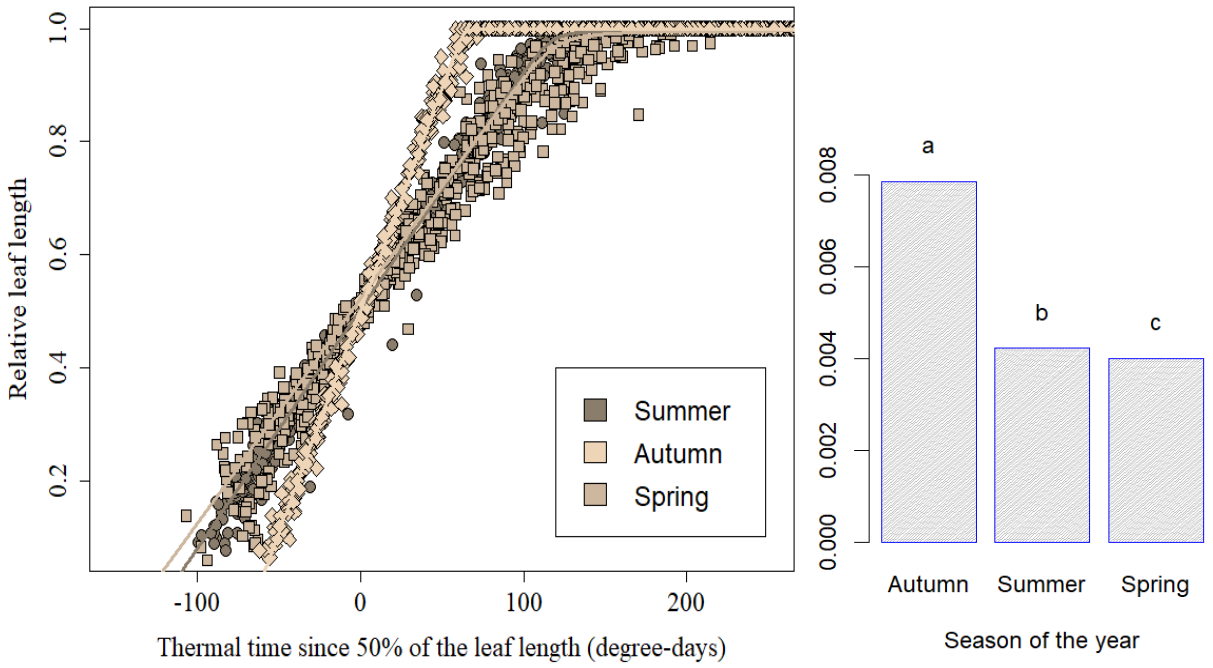

Figure 5.1.14. Kinetics of relative leaf length, expressed in thermal time (degree-days (°C)), on the main axis for *Pennisetum purpureum* cv. Napier across seasons of the year. In Summer and Spring, the phytomers 14 to 17 were used, and in Autumn phytomers 9 to 11. The figure on the right side represents the ANCOVA ($p<0.001$) analysis performed on the maximum relative leaf elongation.

Subsequently, the coordination of growth of successive leaves in each season of the year was analysed to characterize the coordination between leaf ranks on the main axis. For each season, leaf ranks were grouped into three categories according to leaf rank level on the main axis. During Summer and Spring, the three groups corresponded to: existing phytomers at the early-evaluation period (from leaf rank 10 to 12); existing phytomers at the mid-evaluation period (from leaf rank 13 to 16); and existing phytomers at the late-evaluation period (from leaf rank 17 to 20). Similarly, during Autumn, the three groups corresponded to: leaf rank 10 to 12; from leaf rank 13 to 16 and from leaf rank 17 to 20. For all seasons of the year there was a leaf rank effect (data calculated using both thermal and phyllochronic time). During Summer and Spring, leaf elongation duration (LED) was longer for leaf ranks 17 to 20, intermediate for leaf ranks 13 to 16 and shorter for leaf ranks 10 to 12 (Figures 5.1.15, 5.1.16, 5.1.19 and 5.1.20). On the other hand, during Autumn, LED was shorter for phytomers 17 to 20, the last phytomers produced before flowering (Figures 5.1.17 and 5.1.18).

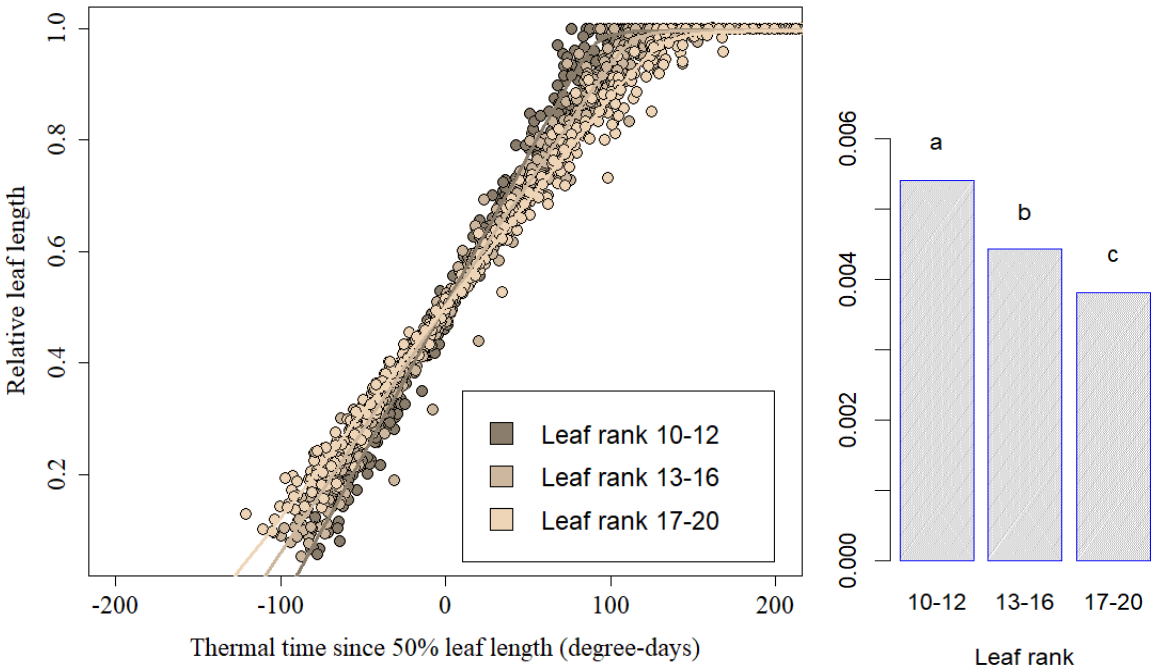

Figure 5.1.15. Kinetics of relative leaf length, expressed in thermal time (degree-days (°C)), on the main axis for *Pennisetum purpureum* cv. Napier in Summer. Dark grey color represents leaf ranks 10, 11 and 12; Dusk grey represents leaf ranks 13, 14, 15 and 16; Light grey represents leaf ranks 17, 18, 19 and 20. The figure on the right side represents the ANCOVA ($p<0.001$) analysis performed on the maximum relative leaf elongation.

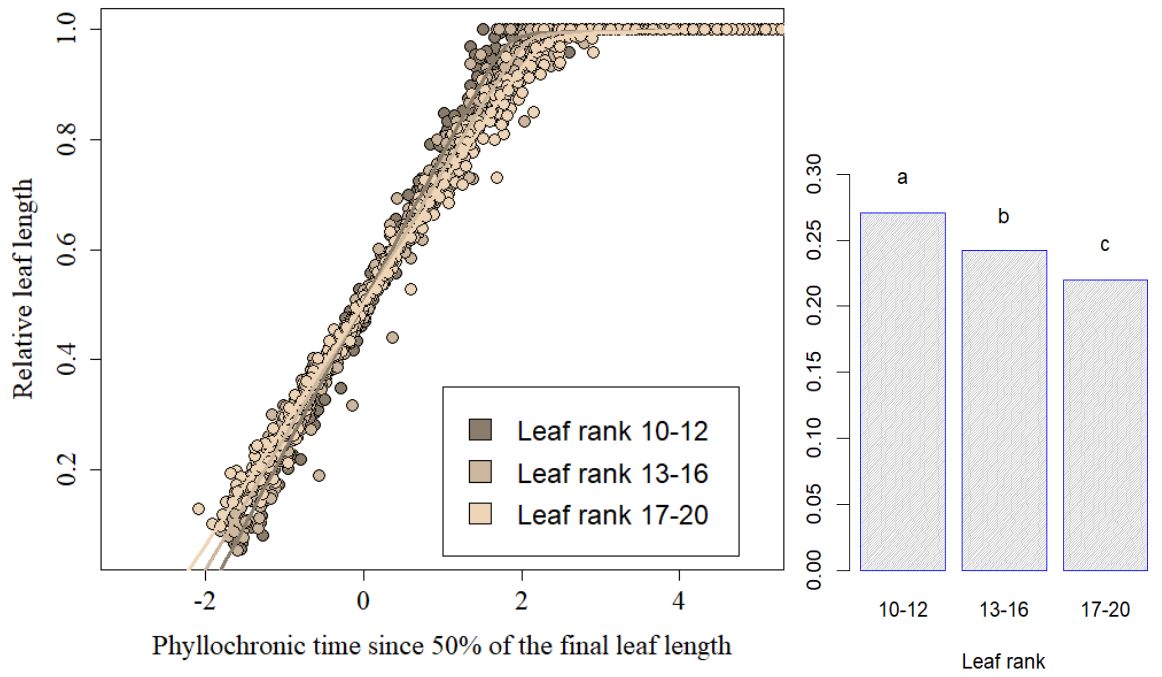

Figure 5.1.16. Kinetics of relative leaf length, expressed in phyllochronic time, on the main axis for *Pennisetum purpureum* cv. Napier in Summer. Dark grey color represents leaf ranks 9, 10, 11 and 12; Dusk grey represents leaf ranks 13, 14, 15 and 16; Light grey represents leaf ranks 17, 18, 19 and 20. The figure on the right side represents the ANCOVA ($p<0.001$) analysis performed on the maximum relative leaf elongation.

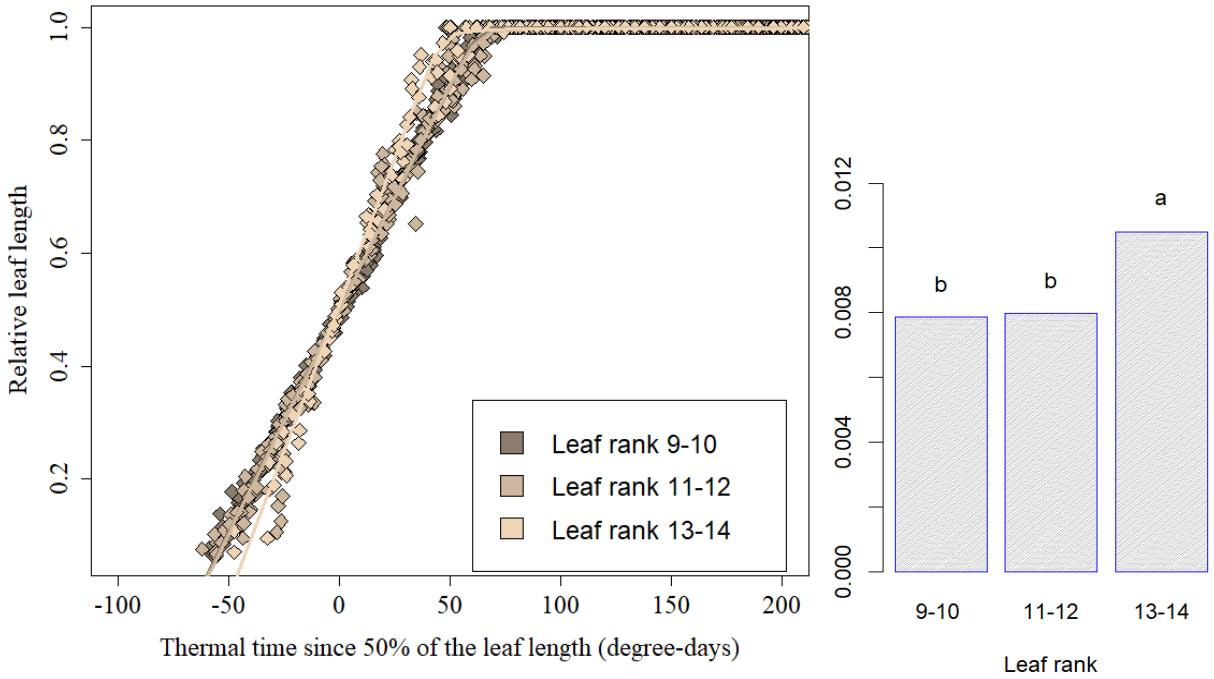

Figure 5.1.17. Kinetics of relative leaf length, expressed in thermal time (degree-days (°C)), on main the axis for *Pennisetum purpureum* cv. Napier in Autumn. Dark grey color represents leaf ranks 9 and 10; Dusk grey represents leaf ranks 11 and 12; Light grey represents leaf ranks 13 and 14. The figure on the right side represents the ANCOVA ($p<0.001$) analysis performed on the maximum relative leaf elongation.

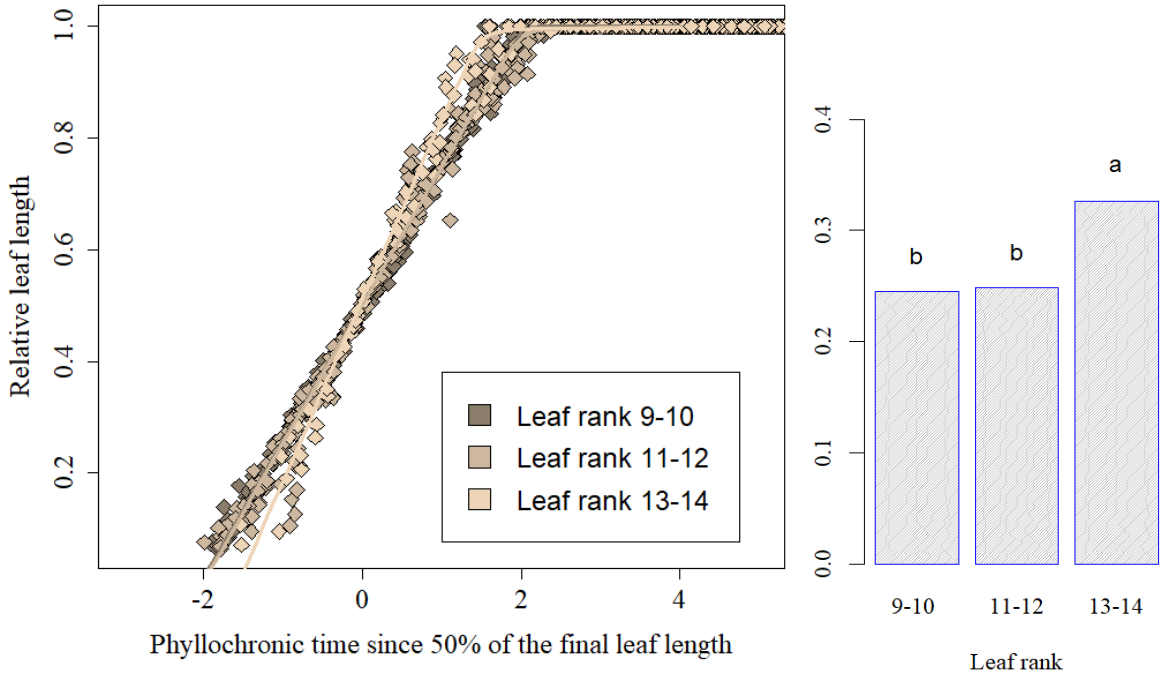

Figure 5.1.18. Kinetics of relative leaf length, expressed in phyllochronic time, on the main axis for *Pennisetum purpureum* cv. Napier in Autumn. Dark grey color represents leaf ranks 9 and 10; Dusk grey represents leaf ranks 11 and 12; Light grey represents leaf ranks 13 and 14.

The figure on the right side represents the ANCOVA ($p<0.001$) analysis performed on the maximum relative leaf elongation.

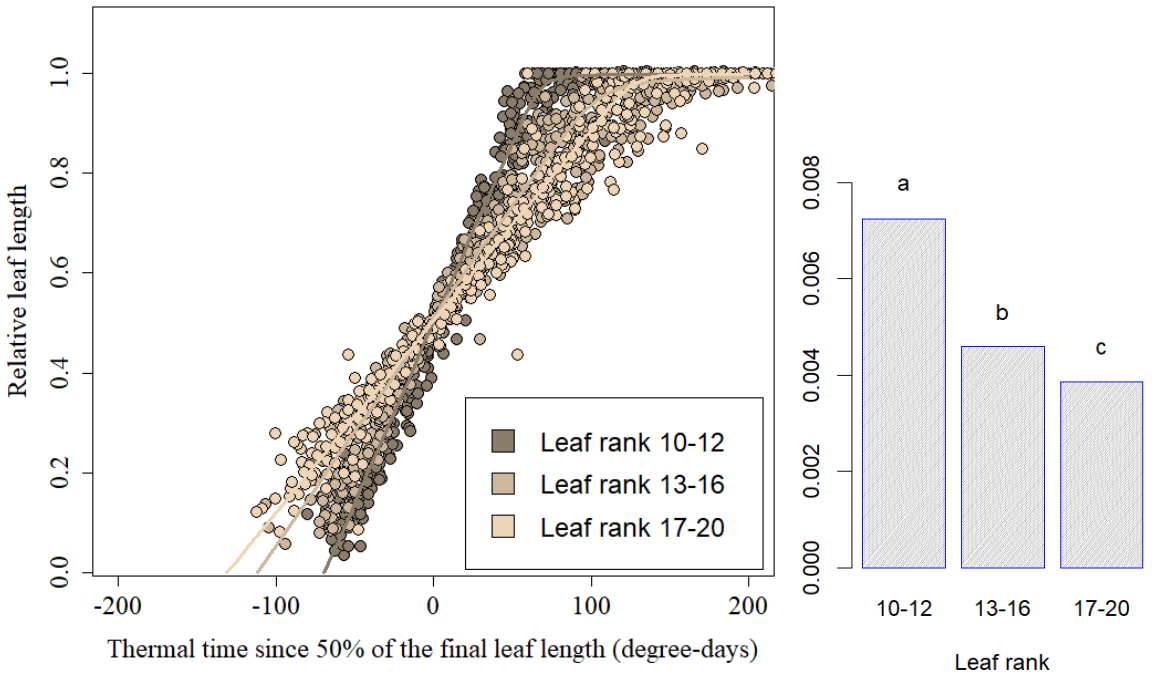

Figure 5.1.19. Kinetics of relative leaf length, expressed in thermal time (degree-days (°C)), on the main axis for *Pennisetum purpureum* cv. Napier in Spring. Dark grey color represents leaf ranks 10, 11 and 12; Dusk grey represents leaf ranks 13, 14, 15 and 16; Light grey represents leaf ranks 17, 18, 19 and 20. The figure on the right side represents the ANCOVA ($p<0.001$) analysis performed on the maximum relative leaf elongation.

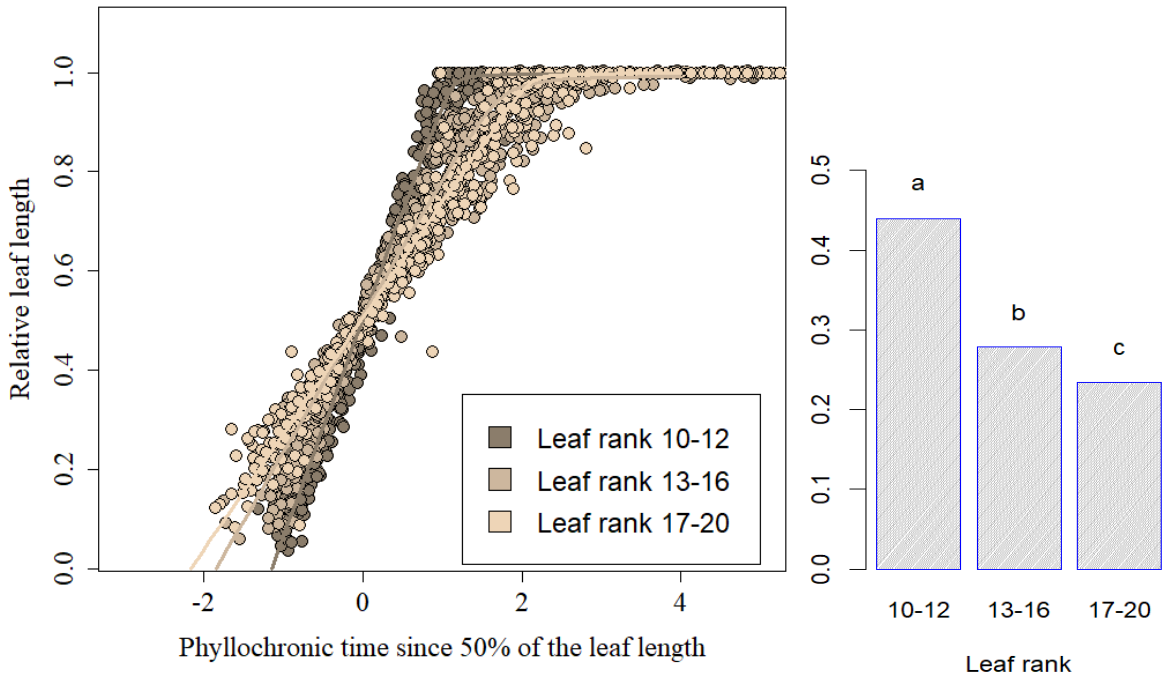

Figure 5.1.20. Kinetics of relative leaf length, expressed in phyllochronic time, on the main axis for *Pennisetum purpureum* cv. Napier in Spring. Dark grey color represents leaf ranks 9, 10, 11 and 12; Dusk grey represents leaf ranks 13, 14, 15 and 16; Light grey represents leaf ranks 17, 18, 19 and 20. The figure on the right side represents the ANCOVA ($p<0.001$) analysis performed on the maximum relative leaf elongation.

5.1.1.2.7. Number of expanding leaves

At the time of the longitudinal dissection of the axis, the rank number of the last expanded leaf (last leaf with visible ligule over the sheath tube) and the number of the younger primordium (leaf just after the apical meristem) were identified. This dataset was generated for Summer and Spring only, since during Autumn no new leaves were produced after the second desctructive analysis. Both response variables followed a linear relationship when expressed in degree-days on the main axis (Figures 5.1.21 and 5.1.22). Analysis of covariance was performed on the slope of the linear regressions, and no difference was found between curves ($P=0.716$).

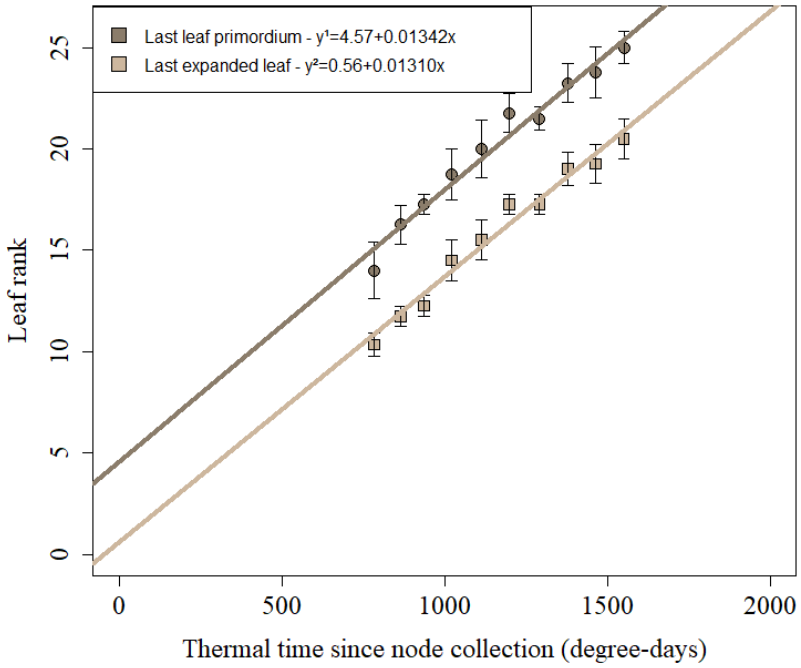

Figure 5.1.21. Relationship between leaf rank and thermal time (degree-days (°C)) since node collection date on the main axis of *Pennisetum purpureum* cv. Napier in Summer. Dark grey represents the younger leaf primordium (last leaf visible just after the apical meristem) and Light grey represents the last expanded leaf (last leaf with visible ligule).

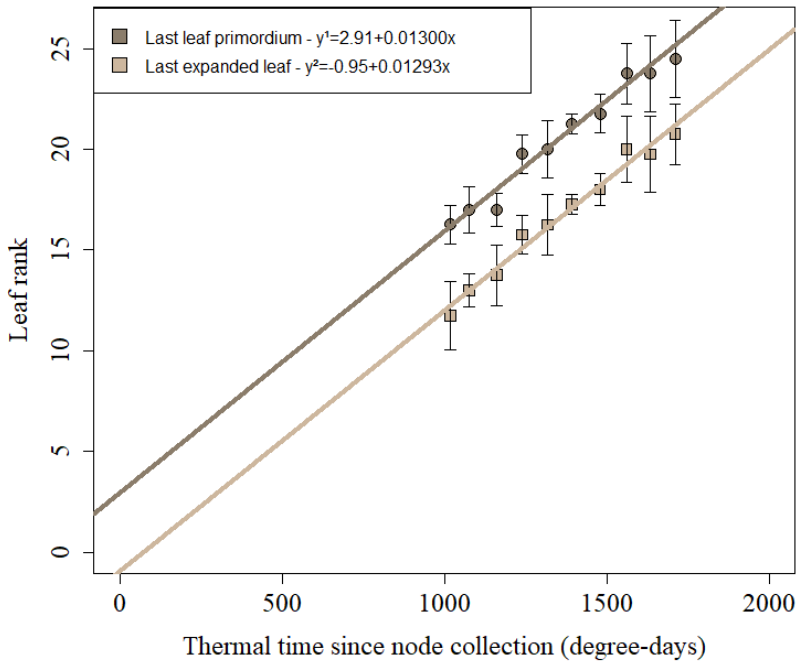

Figure 5.1.22. Relationship between leaf rank and thermal time (degree-days (°C)) since node collection date on the main axis of *Pennisetum purpureum* cv. Napier in Spring. Dark grey represents the younger leaf primordium (last leaf visible just after the apical meristem) and Light grey represents the last expanded leaf (last leaf with visible ligule).

5.1.1.3. Ontogenetic development and coordination between main and primary axes

5.1.1.3.1. Leaf appearance rate (LAR)

For all seasons of the year, plants systematically displayed a conspicuous branching. During Summer and Autumn, the first branch was observed on nodes 2 and 3, respectively, while during Spring the first branch arised from node 1 (Figures 5.1.23, 5.1.24 and 5.1.25). When considered the cumulative number of leaves on each axis over time, there was a progressive decrease in leaf number produced for each successive axis for all seasons of the year. During Summer, the number of leaves produced varied from 20 (on the main axis) to 4 (on the primary axis rank 11) (Figure 5.1.23). During Autumn, the number of leaves produced varied from 14 (on the main axis) to 4 (on the primary axis rank 8) (Figure 5.1.24), while during Spring, it varied from 20 (on the main axis) to 7 (on the primary axis rank 9) (Figure 5.1.25).

The first primary axis emerged during Summer after approximately 400 degree-days, while during Autumn and Spring the first primary axes appeared after 200 degree-days. As reported for the main axis, primary axis also presented linear relationship between number of leaves and degree-days. Analysis of variance performed on the regression slopes (LAR) between the number of leaves and thermal time showed significant effect of the axis rank for all seasons of the year ($P<0.01$) (Tables 5.1.2, 5.1.3 and 5.1.4). During Summer, there was no diference in LAR between primary axes 3 to 8. Moreover, higher values of leaf appearance rate were recorded for the topmost primary axes, at node positions 9, 10 and 11, with average of 0.029 leaf degree-day^{-1}. Similarly, during Autumn, higher values of LAR were recorded for axis 8 (average of 0.049 leaf degree-day^{-1}). Conversely, there was no diference in LAR between axes rank during Spring (Figure 5.1.24). These results indicate the existence of significant differences among axes for LAR.

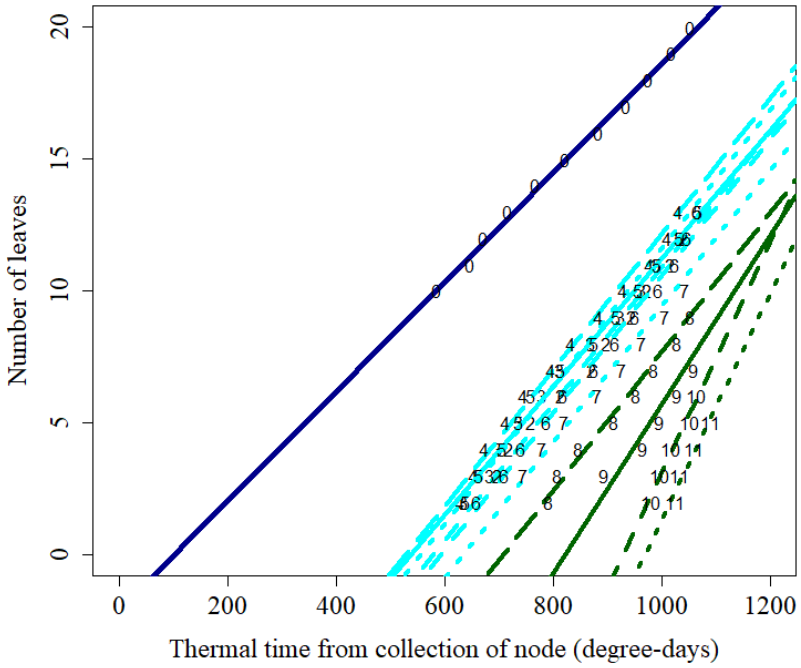

Figure 5.1.23. Timing of leaf appearance on the main and primary axes of *Pennisetum purpureum* cv. Napier expressed in degree-days (°C) in Summer (2016). Main axis (0); primary axes (2 to 11- refering to axis rank). Dark blue represents the main axis; Light blue represents primary axes branching close to soil surface (from 2 to 7); Dark green represents primary axes branching above soil surface, i.e. topmost axes (from 8 to 11).

Table 5.1.2. Slope coefficient and coefficient of determination of the linear regression NL = α + LAR.DD, where NL = number of leaves, α is a constant and DD = degree-days (°C). The coefficient LAR refers to leaf appearance rate (LAR) on the main axis and primary axes of *Pennisetum purpureum* cv. Napier expressed in degree-days in Summer. Analysis of covariance was performed on LAR (P<0.01).

Summer	LAR	r^2
Main axis	0.020 C	0.98
	(0.0016)	
Axis rank 2	0.023 BC	0.64
	(0.0019)	
Axis rank 3	0.023 BC	0.76
	(0.0016)	
Axis rank 4	0.023 BC	0.86
	(0.0020)	
Axis rank 5	0.023 BC	0.93
	(0.0023)	
Axis rank 6	0.023 BC	0.94
	(0.0020)	
Axis rank 7	0.022 BC	0.94
	(0.0025)	
Axis rank 8	0.024 B	0.91
	(0.0035)	
Axis rank 9	0.028 A	0.67
	(0.0051)	
Axis rank 10	0.030 A	0.50
	(0.0075)	
Axis rank 11	0.016 A	0.40
	(0.0093)	

Values in parentheses indicate standard error of the mean. Means followed by the same upper case letter are not different (P>0.05).

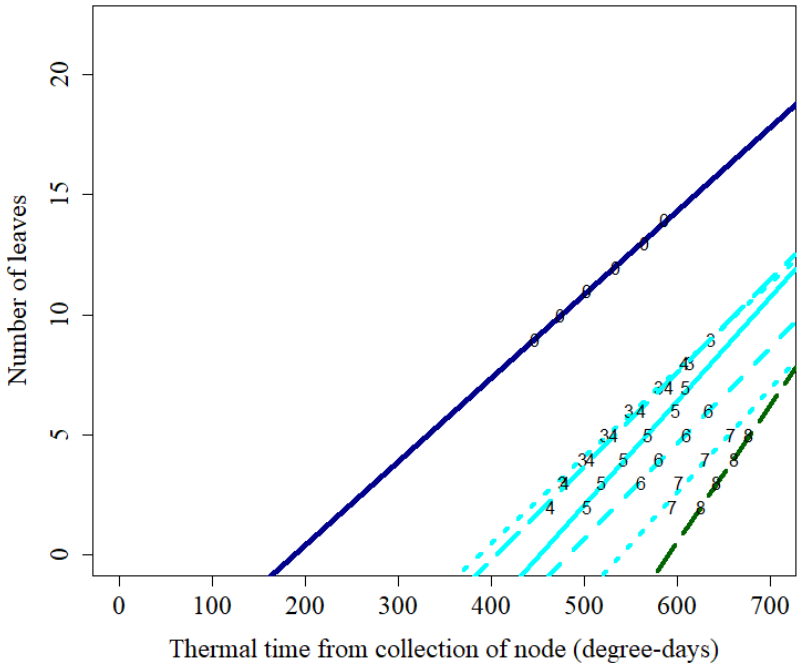

Figure 5.1.24. Timing of leaf appearance on the main and primary axes of *Pennisetum purpureum* cv. Napier expressed in degree-days (°C) in Autumn (2016). Main axis (0); primary axes (1 to 8- refering to the axis rank). Dark blue represents the main axis; Light blue represents primary axes branching close to soil surface (from 3 to 7); Dark green represents primary axes branching above soil surface, i.e. topmost axes (8).

Table 5.1.3. Slope coefficient and coefficient of determination of the linear regression NL = α + LAR.DD, where NL = number of leaves, α is a constant and DD = degree-days (°C). The coefficient LAR refers to leaf appearance rate (LAR) on the main axis and primary axes of *Pennisetum purpureum* cv. Napier expressed in degree-days in Autumn. Analysis of covariance was performed on LAR (P<0.01).

Autumn	LAR	r^2
Main axis	0.032 D	0.98
	(0.0030)	
Axis rank 3	0.034 CD	0.73
	(0.0055)	
Axis rank 4	0.036 CD	0.90
	(0.0054)	
Axis rank 5	0.040 BC	0.76
	(0.0088)	
Axis rank 6	0.042 B	0.80
	(0.0057)	
Axis rank 7	0.042 B	0.70
	(0.0076)	
Axis rank 8	0.049 A	0.67
	(0.0129)	

Values in parentheses indicate standard error of the mean. Means followed by the same upper case letter are not different (P>0.05).

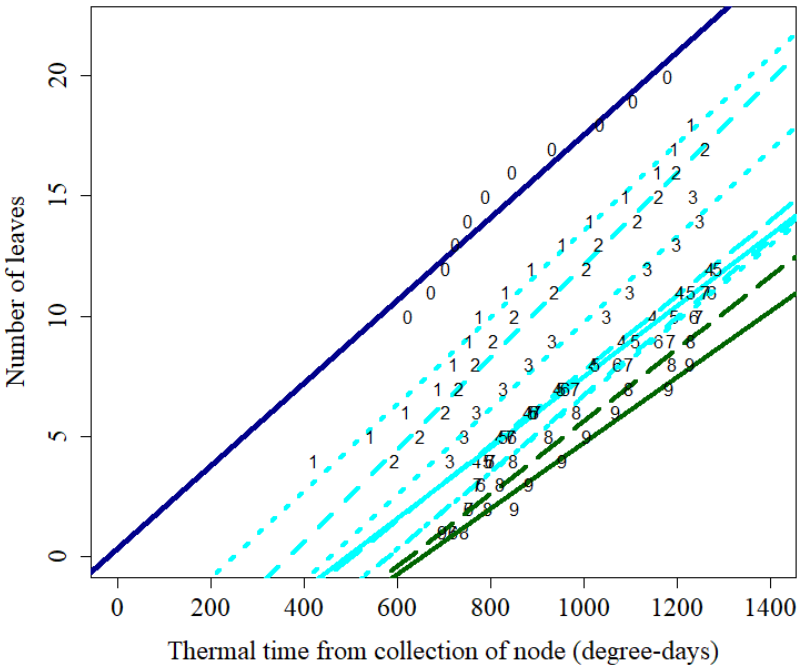

Figure 5.1.25. Timing of leaf appearance on the main and primary axes of *Pennisetum purpureum* cv. Napier expressed in degree-days (°C) in Spring (2016). Main axis (0); primary axes (1 to 9- refering to axis rank). Dark blue represents the main axis; Light blue represents primary axes branching close to soil surface (from 1 to 7); Dark green represents primary axes branching above soil surface, i.e. topmost axes (from 8 and 9).

Table 5.1.4. Slope coefficient and coefficient of determination of the linear regression NL = α + LAR.DD, where NL = number of leaves, α is a constant and DD = degree-days (°C). The coefficient LAR refers to leaf appearance rate (LAR) on the main axis and primary axes of *Pennisetum purpureum* cv. Napier expressed in degree-days in Spring. Analysis of covariance was performed on LAR (P<0.01).

Spring	LAR	r^2
Main axis	0.0164 A	0.91
	(0.00129)	
Axis rank 1	0.0159 AB	0.80
	(0.00242)	
Axis rank 2	0.0157 AB	0.75
	(0.00228)	
Axis rank 3	0.0141 BCD	0.79
	(0.00271)	
Axis rank 4	0.0120 E	0.72
	(0.00281)	
Axis rank 5	0.0120 DE	0.77
	(0.00186)	
Axis rank 6	0.0140 BCDE	0.79
	(0.00133)	
Axis rank 7	0.0145 BC	0.87
	(0.00206)	
Axis rank 8	0.0135 CDE	0.81
	(0.00248)	
Axis rank 9	0.0121 DE	0.69
	(0.00319)	

Values in parentheses indicate standard error of the mean. Means followed by the same upper case letter are not different (P>0.05).

5.1.1.3.2. Leaf elongation rate (LER)

The analysis of leaf elongation rate on the main and primary axes was perfomed across seasons of the year in two different manners. Firstly, LER was plotted against leaf rank of the main axis, i.e. using the main axis as a reference, to visualize LER at a specific time common to all axes. Secondly, LER was plotted against leaf rank on each axis to visualize successive changes in LER according to leaf rank on the main and primary axes.

During Summer, when LER was plotted against leaf rank on the main axis, a successive increase in LER for primary axes rank 2 to 7 was reported to a maximum value of approximately 0.26 cm degree-days^{-1}. On the other hand, lower values were reached for the topmost axes (primary axes rank 8 to 11) (Figure 5.1.26).

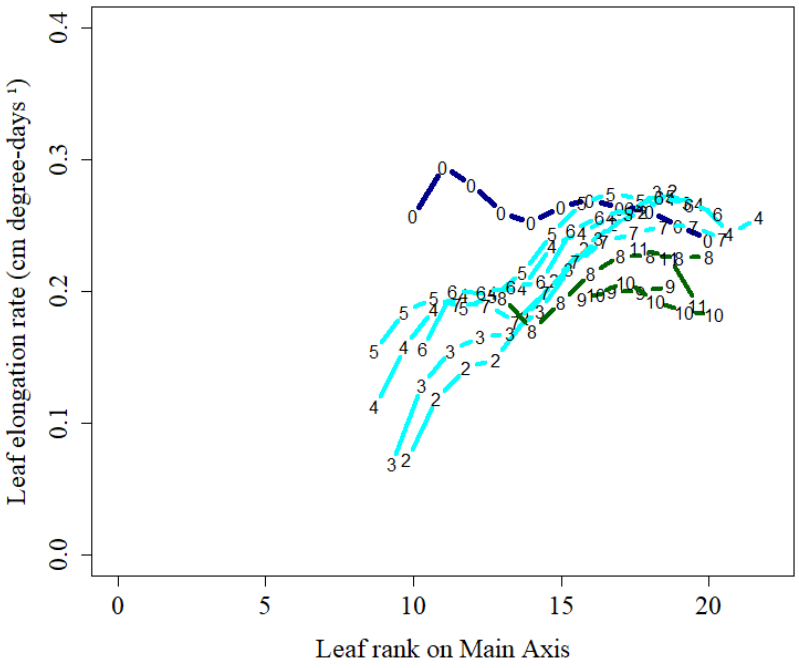

Figure 5.1.26. Leaf elongation rate (cm degree-days^{-1}) on the main and primary axes of *Pennisetum purpureum* cv. Napier relative to leaf rank on the main axis, in Summer (2016). Main axis (0); primary axes (1 to 11- refering to axis rank). Dark blue represents the main axis; Light blue represents primary axes branching close to soil surface (from 2 to 7); Dark green represents primary axes branching above soil surface, i.e. topmost axes (from 8 to 11).

When data were plotted against the leaf rank of each axis, it was possible to visualize the ontogenetic changes for successive phytomers in each axis. Although there was no difference in LER for leaf ranks 10 to 20 on the main axis during Summer, as reported earlier in Figure 5.1.8, when the analysis was expressed in leaf rank on the axes of successive primary axes that arised during the evaluation period, it was possible to observe a consistent increase in LER with increasing leaf rank (Figure 5.1.27). Values of LER incresead from 0.05 to 0.3 cm degree-days^{-1} until reaching a plateau (approximately 0.26 cm degree-days^{-1}). For primary axis rank 8, 9, 10 and 11, lower values were observed for LER across levels of leaf rank.

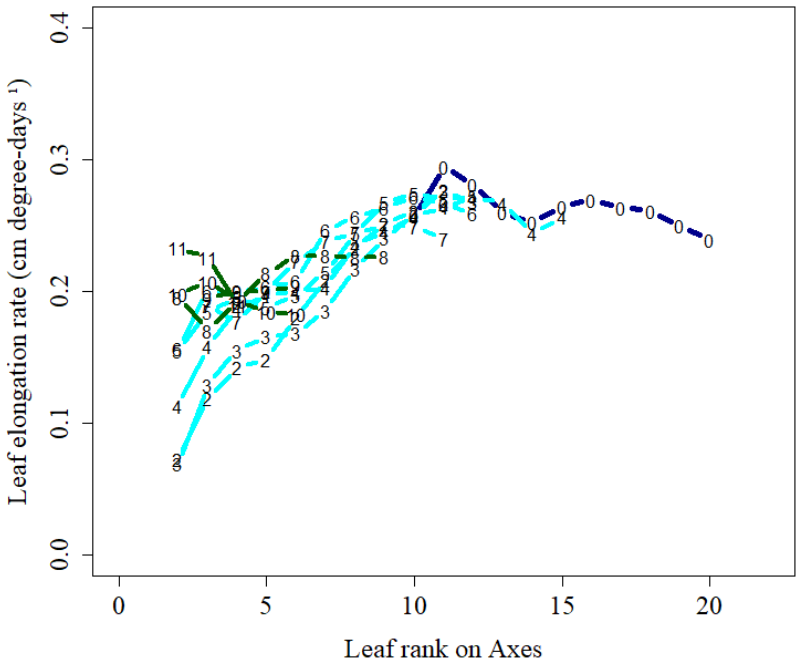

Figure 5.1.27. Leaf elongation rate (cm degree-days^{-1}) on the main and primary axes of *Pennisetum purpureum* cv. Napier expressed in degree-days (°C) in Summer (2016). Main axis (0); primary axes (1 to 11- refering to axis rank). Dark blue represents the main axis; Light blue represents primary axes branching close to soil surface (from 2 to 7); Dark green represents primary axes branching above soil surface, i.e. topmost axes (from 8 to 11).

During Autumn, although there were no differences in LER for leaf rank 9 to 14 on the main axis (Figure 5.1.7), when the analysis was performed on primary axes, it was possible to visualize a consistent increase in LER as leaf rank increased (Figure 5.1.28 and 5.1.29). The values of LER varied from 0.06 to 0.3 cm degree-days^{-1}. However, primary axis rank 8 showed decreasing LER values as leaf rank increased.

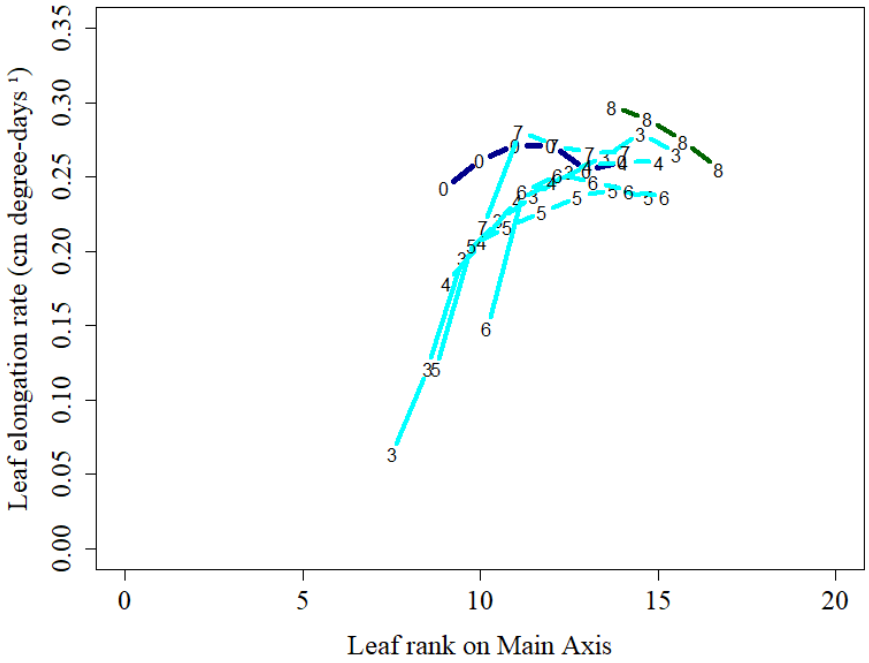

Figure 5.1.28. Leaf elongation rate (cm degree-days^{-1}) on the main and primary axes of *Pennisetum purpureum* cv. Napier relative to leaf rank on the main axis, in Autumn (2016). Main axis (0); primary axes (1 to 11- refering to axis rank). Dark blue represents the main axis; Light blue represents primary axes branching close to soil surface (from 3 to 7); Dark green represents primary axes branching above soil surface, i.e. topmost axis (8).

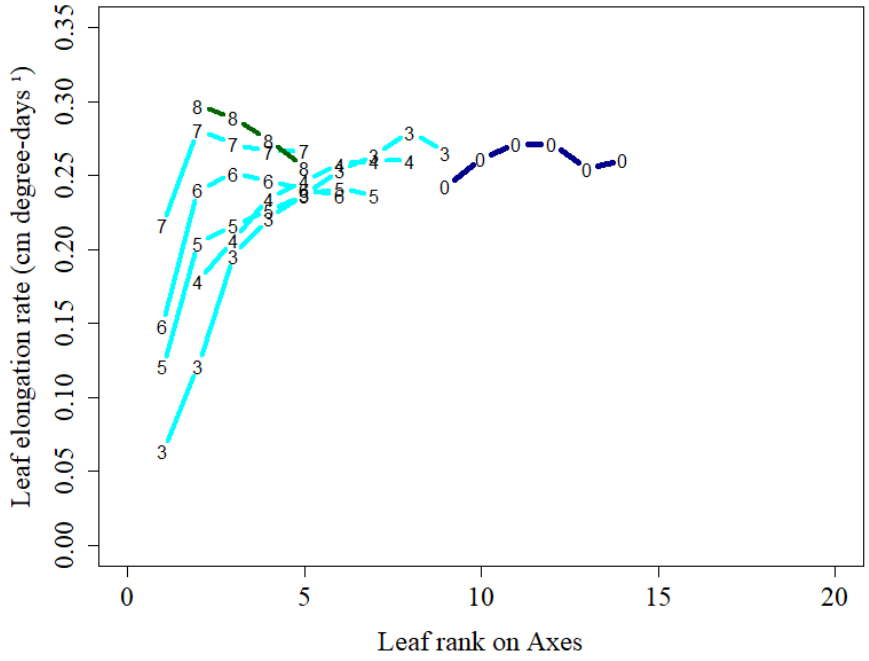

Figure 5.1.29. Leaf elongation rate (cm degree-days^{-1}) on the main and primary axes of *Pennisetum purpureum* cv. Napier expressed in degree-days (°C) in Autumn (2016). Main axis (0); primary axes (1 to 8 - refering to axis rank). Dark blue represents the main axis; Light blue represents primary axes branching close to soil surface (from 3 to 7); Dark green represents primary axes branching above soil surface, i.e. topmost axis (8).

During Spring, the dynamics of LER on successive leaf ranks of primary axes showed a distinct pattern relative to that observed during Autumn and Summer. When data were plotted against leaf rank on the main axis, all primary axes showed the same fluctuation in LER at the same time (Figure 5.1.30). However, when plotted against leaf rank for each axis, dissimilarities were observed among axes (Figure 5.1.31). These results indicate that the fluctuation observed in LER across leaf ranks for all primary axes was related to the time phytomer developed and not to a response relative to the ontogenetic development.

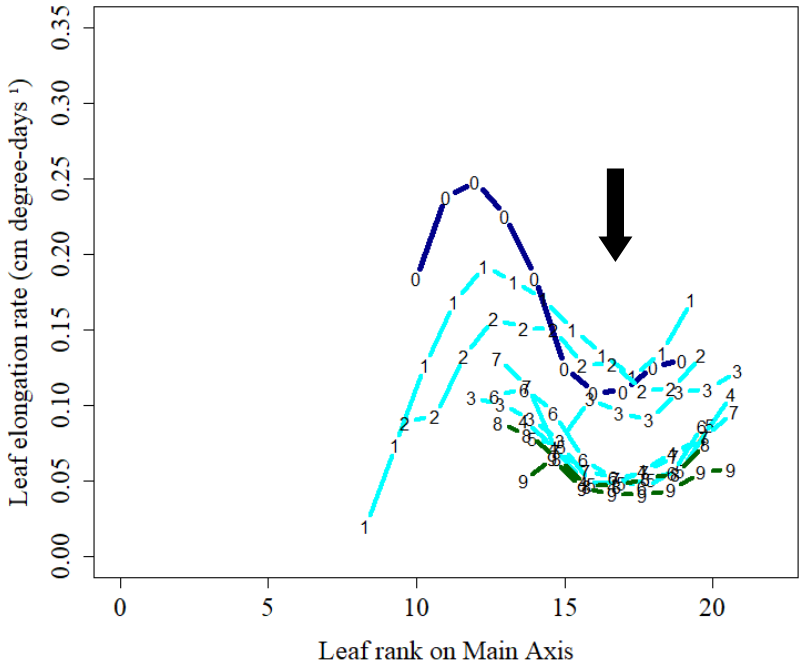

Figure 5.1.30. Leaf elongation rate (cm degree-days^{-1}) on the main and primary axes of *Pennisetum purpureum* cv. Napier relative to leaf rank of the main axis, in Spring (2016). Main axis (0); primary axes (1 to 11- refering to axis rank). Vertical arrow indicate the depression in LER common to all axes. Dark blue represents the main axis; Light blue represents primary axes branching close to soil surface (from 1 to 7); Dark green represents primary axes branching above soil surface, i.e. topmost axes (8 and 9).

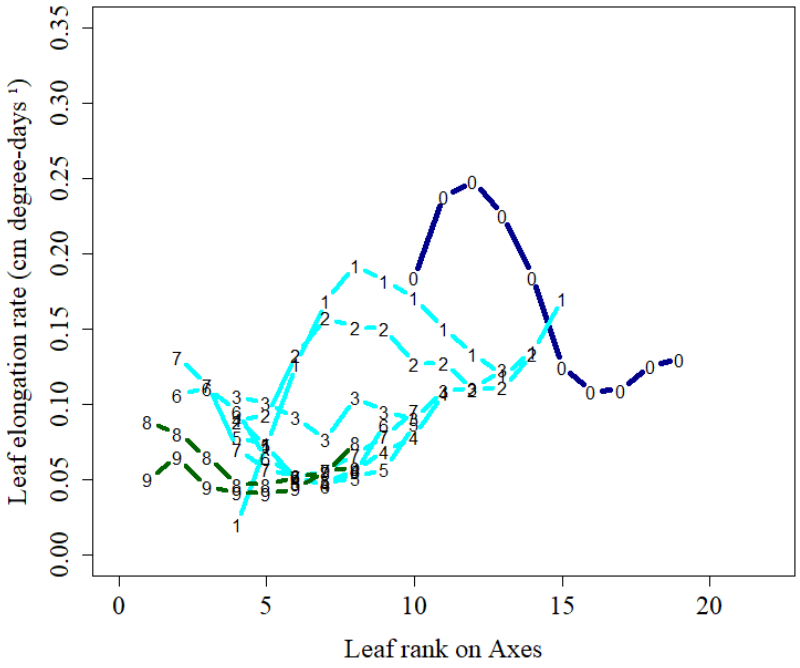

Figure 5.1.31. Leaf elongation rate (cm degree-days^{-1}) on the main and primary axes of *Pennisetum purpureum* cv. Napier relative to leaf rank on axes, in Spring (2015). Main axis (0); primary axes (1 to 9 - refering to axis rank). Dark blue represents the main axis; Light blue represents primary axes branching close to soil surface (from 1 to 7); Dark green represents primary axes branching above soil surface, i.e. topmost axes (8 and 9).

5.1.1.3.3. Leaf elongation duration (LED)

The analysis of LED was first presented considering leaf rank on the main axis. Secondly, LED was plotted according to leaf rank on each axis to visualize the successive changes in LED according to leaf rank on the main and primary axes.

The LED consistently increased with leaf rank during Summer, expressed in thermal time (Figures 5.1.32 to 5.1.33), with values varing from 60 to 250 degree-days. The successive changes in LED follow the same pattern for primary axes from rank 2 to 7, while primary axes rank 8, 9 and 10 presented higher discrepancy, but reaching the same values of other primary axes for the last leaf ranks.

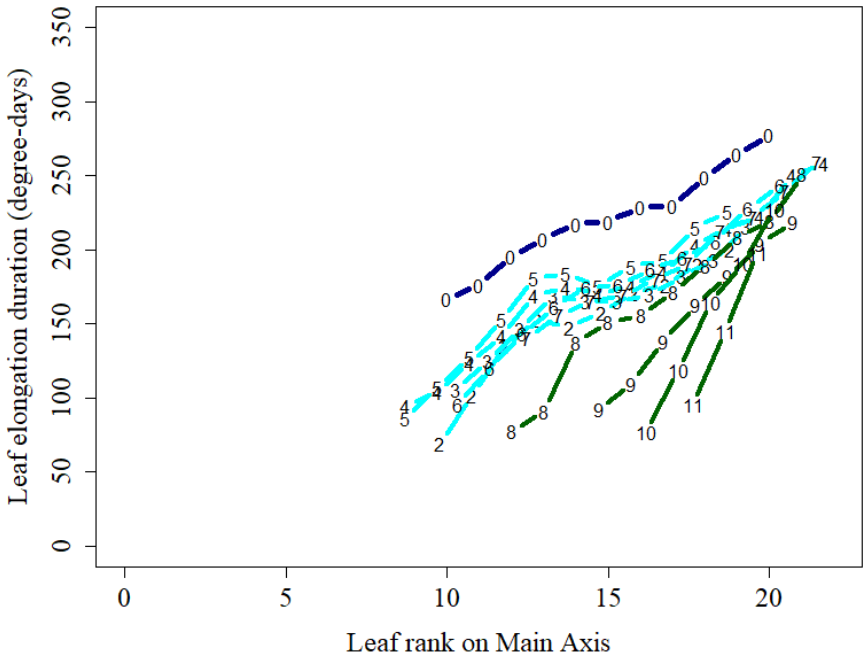

Figure 5.1.32. Leaf elongation duration (degree-days) on the main and primary axes of *Pennisetum purpureum* cv. Napier relative to leaf rank on the main axis, in Summer (2016). Main axis (0); primary axes (1 to 11- refering to axis rank). Dark blue represents the main axis; Light blue represents primary axes branching close to soil surface (from 2 to 7); Dark green represents primary axes branching above soil surface, i.e. topmost axes (from 8 to 11).

Values of LED increased successively according to leaf rank based on leaf rank on the axes. The topmost primary axes, i.e. axis ranks 8, 9, 10 e 11, presented higher changes from one leaf rank to another (Figure 5.1.33).

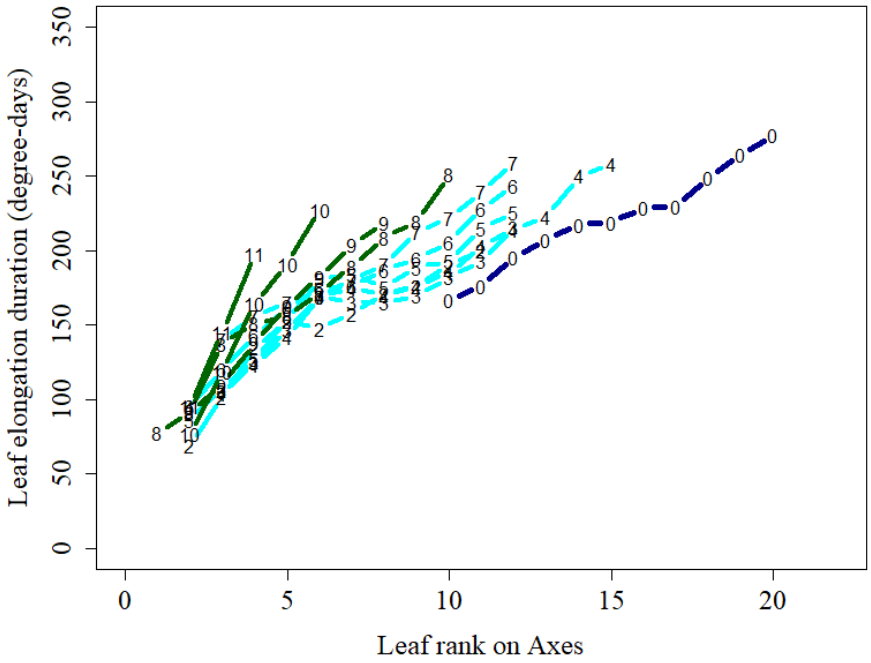

Figure 5.1.33. Leaf elongation duration (degree-days) on the main and primary axes of *Pennisetum purpureum* cv. Napier expressed in thermal time (degree-days (°C)) in Summer (2016). Main axis (0); primary axes (1 to 11 - refering to leaf rank of main axis). Dark blue represents the main axis; Light blue represents primary axes branching close to soil surface (from 2 to 7); Dark green represents primary axes branching above soil surface, i.e. topmost axes (from 8 to 11).

During Autumn, LED increased according to leaf rank, and then decreased for the last 3-4 phytomers produced before flowering. When expressed according to leaf rank on the main axis, LED values showed a strong synchronism with time of flowering for primary axes rank 3 to 6, with a maximum value of approximately 120 degree-days, similar to that observed for the main axis. On the other hand, smaller LED values were obtained for primary axis rank 8, with the maximum value close to 90 degree-days (Figure 5.1.34).

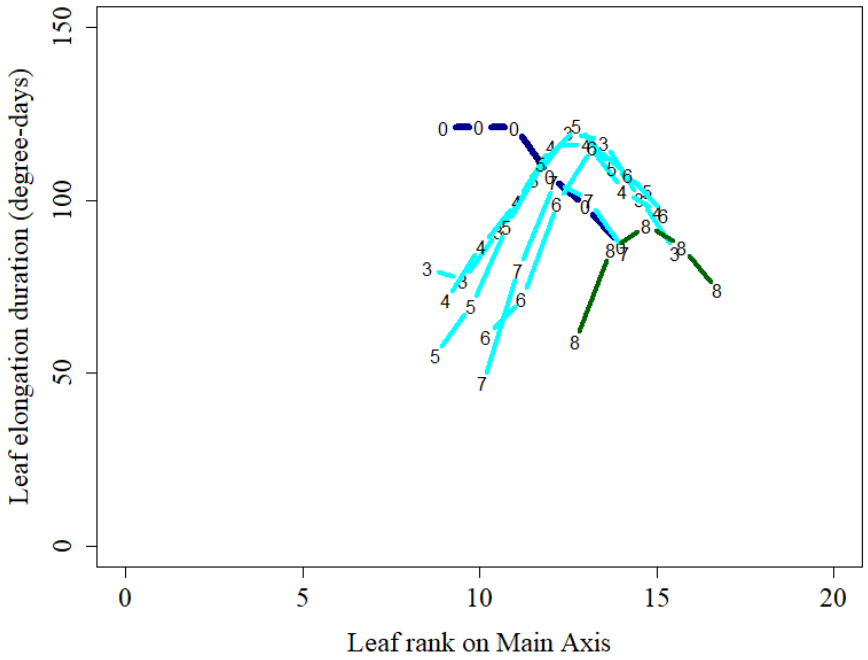

Figure 5.1.34. Leaf elongation duration (degree-days) on the main and primary axes of *Pennisetum purpureum* cv. Napier relative to leaf rank on the main axis, in Autumn (2016). Main axis (0); primary axes (3 to 8- refering to leaf rank of main axis). Dark blue represents the main axis; Light blue represents primary axes branching close to soil surface (from 3 to 7); Dark green represents primary axes branching above soil surface, i.e. topmost axis (8).

When LED was plotted against the leaf rank on each axis, a synchronism between successive primary axes in terms of increasing leaf rank and corresponding increase in LED was observed. In all axes, flowering was observed, so that the highest leaf rank for each axis was represented by the last leaf (flag leaf). Successive primary axes rank presented reducing number of leaves produced; i.e. primary axes rank 3, 4, 5, 6, 7 and 8 produced 9, 8, 7, 6, 5 and 5 leaves before flowering (Figure 5.1.35).

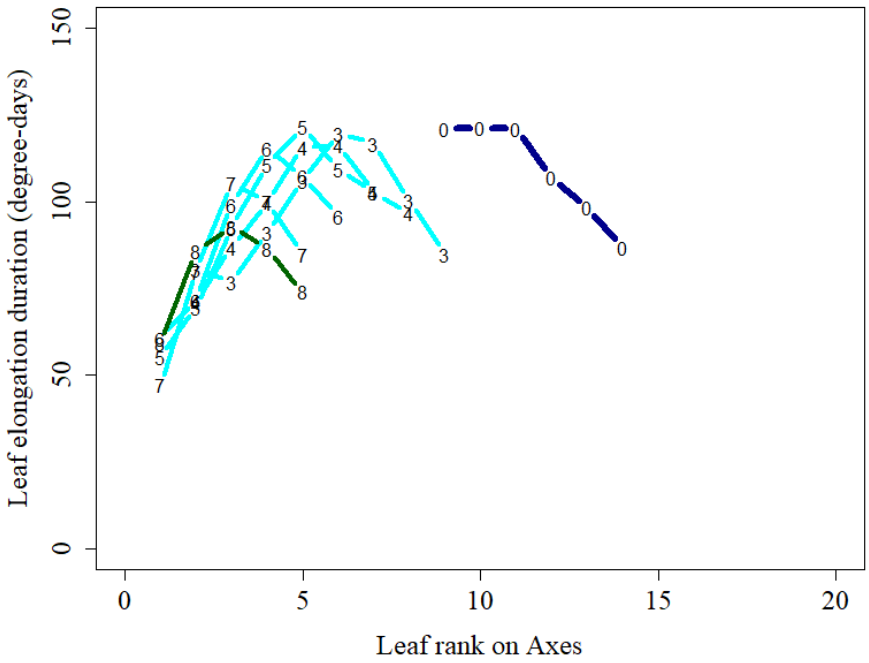

Figure 5.1.35. Leaf elongation duration (degree-days) on the main and primary axes of *Pennisetum purpureum* cv. Napier expressed in leaf rank on axes, in Autumn (2016). Main axis (0); primary axes (3 to 8- refering to leaf rank of main axis). Dark blue represents the main axis; Light blue represents primary axes branching close to soil surface (from 3 to 7); Dark green represents primary axes branching above soil surface, i.e. topmost axis (8).

During Spring, within leaf ranks, LED values increased successively when plotted against leaf rank on the main axis. The LED values reached a plateau at approximately 250 degree-days for all axes (Figure 5.1.36).

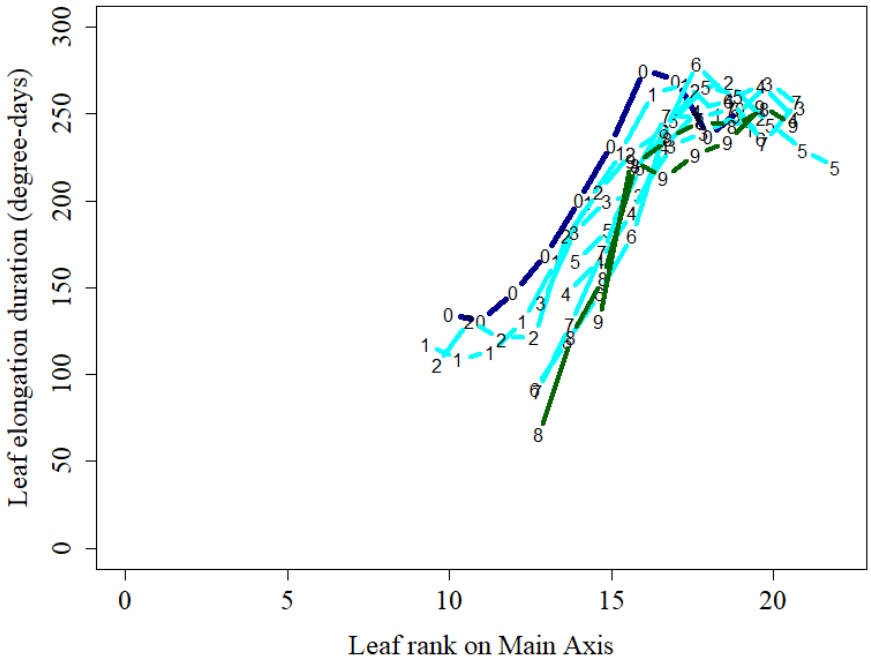

Figure 5.1.36. Leaf elongation duration (degree-days) on the main and primary axes of *Pennisetum purpureum* cv. Napier relative to leaf rank on the main axis, in Spring (2015). Main axis (0); primary axes (1 to 9 - refering to leaf rank on the main axis). Dark blue represents the main axis; Light blue represents primary axes branching close to soil surface (from 1 to 7); Dark green represents primary axes branching above soil surface, i.e. topmost axes (8 and 9).

When expressed in thermal time and plotted against leaf rank of each axis, LED values were greater for higher leaf ranks, until reaching a plateau, of approximately 250 degree-days. Higher primary axis ranks reached greater LED values earlier in shoot development (Figure 5.1.37).

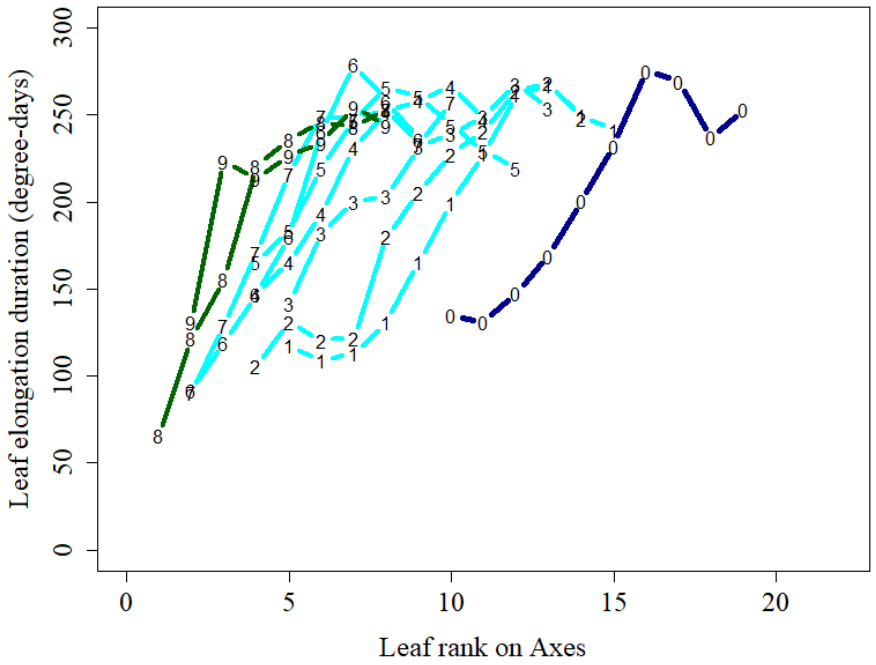

Figure 5.1.37. Leaf elongation duration (degree-days) on the main and primary axes of *Pennisetum purpureum* cv. Napier expressed in degree-days in Spring (2015). Main axis (0); primary axes (1 to 9 - refering to leaf rank of main axis). Dark blue represents the main axis; Light blue represents primary axes branching close to soil surface (from 1 to 7); Dark green represents primary axes branching above soil surface, i.e. topmost axes (8 and 9).

5.1.1.3.4. Final leaf length (FLL)

There was an increase in FLL according to leaf rank for all axes during Summer, with values ranging from 6 to 70 cm. Considering the same leaf rank, successive greater values of FLL were observed for higher axis ranks (Figure 5.1.38).

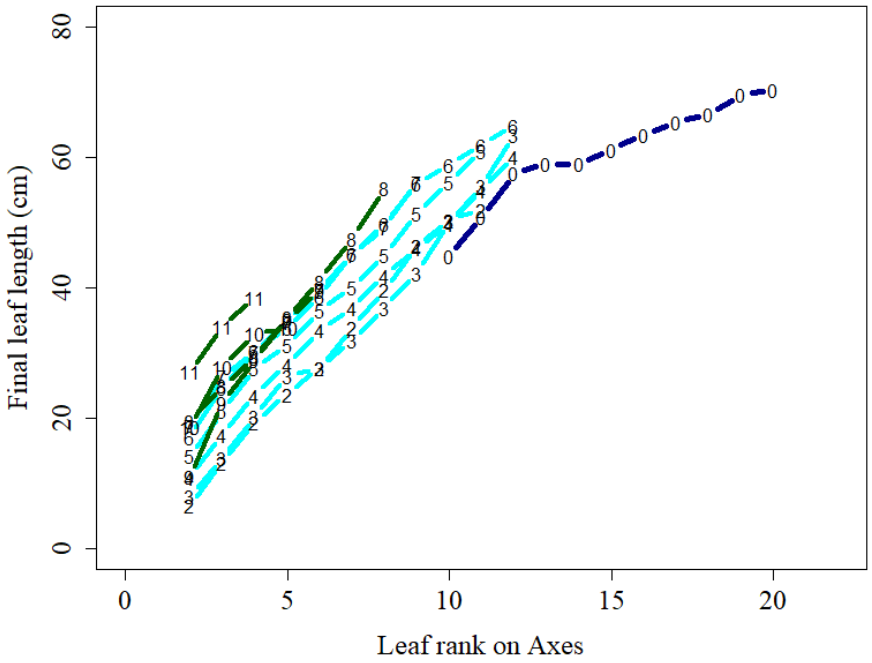

Figure 5.1.38. Final leaf length (cm) on the main and primary axes of *Pennisetum purpureum* cv. Napier in Summer (2016). Main axis (0); primary axes (1 to 11 - refering to leaf rank of main axis). Dark blue represents the main axis; Light blue represents primary axes branching close to soil surface (from 2 to 7); Dark green represents primary axes branching above soil surface, i.e. topmost axes (from 8 to 11).

During Autumn, the FLL of successive leaf rank presented a bell-shaped curve for all axes. The greater leaf length for each axis depended on the final number of phytomers and, generally, the reduction in final leaf length occurred for the last three phytomers (Figure 5.1.39).

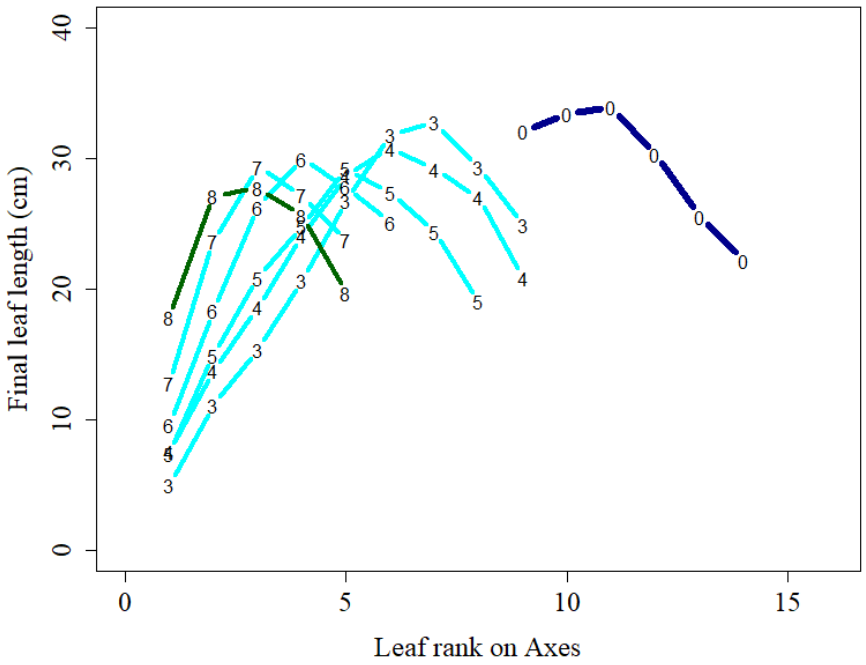

Figure 5.1.39. Final leaf length (cm) on the main and primary axes of *Pennisetum purpureum* cv. Napier in Autumn (2016). Main axis (0); primary axes (1 to 8 - refering to leaf rank of main axis). Dark blue represents the main axis; Light blue represents primary axes branching close to soil surface (from 3 to 7); Dark green represents primary axes branching above soil surface, i.e. topmost axis (8).

As FLL derives from the product between LED and LER, the same pattern of fluctuation in FLL was observed for all axes. Values of FLL varied considerably among axes, with greater values observed for the main axis and smaller values for successive primary axes (Figure 5.1.40).

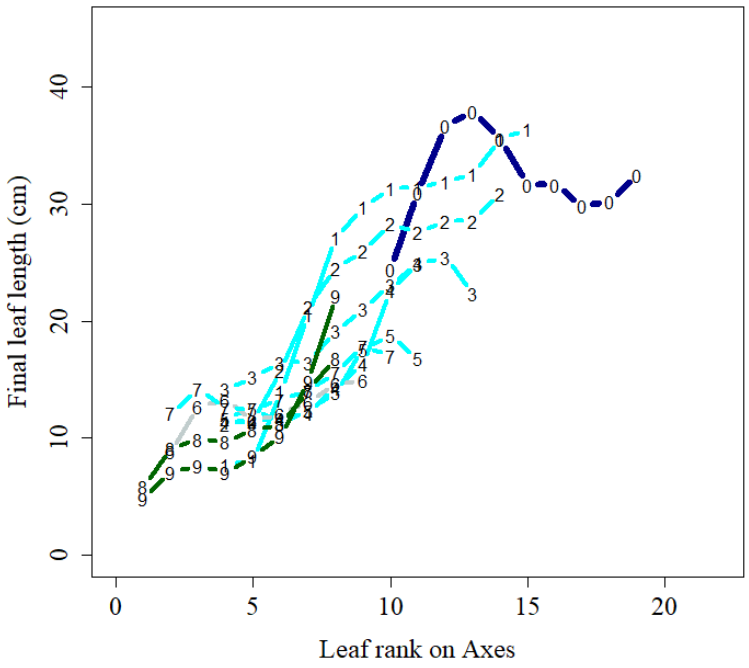

Figure 5.1.40. Final leaf length (cm) on the main and primary axes of *Pennisetum purpureum* cv. Napier in Spring (2016). Main axis (0); primary axes (1 to 9 - refering to leaf rank of main axis). Dark blue represents the main axis; Light blue represents primary axes branching close to soil surface (from 1 to 7); Dark green represents primary axes branching above soil surface, i.e. topmost axes (8 and 9).

5.1.2. DISCUSSION I

Growth conditions

Based on experimental data the ontogenetic development of *Pennisetum purpureum* cv Napier (elephant grass) was assessed under a large range of growth conditions. This information allowed the elucidation of the seasonality effect on vegetative (Summer and Spring) and reproductive phases of development (Autumn). Summer was the season with the most appropriated set of climatic growth factors, i.e. constant elevated temperature and high global radiation, well distributed pluvial precipitation and longer daylength since node collection date to the end of the evaluation period.

In Spring, the first of the three evaluation seasons, after the experimental period, it was necessary to add more substrate to fill up the tanks, indicating that tanks were not compacted enough. The lack of compactation could have affected root development and nutrients and water retention in the soil. In addition, plant nodes were collected during Winter (July, 27, 2015), and remained for a long time in cold weather (almost two months) until the climatic growth factors improved (from 21 September to 28 November). These conditions might have resulted on a delay in days for seedling emergence relative to Summer and

Autumn (Figure 5.1.5). Under lower temperatures, plants accumulate reserves and present higher concentration of carbohydrates and proteins (Taiz and Zeiger, 2010), which stimulate plant growth later on in the growing season when favorable climatic conditions are reinstated. This pattern is supported by the intense branching observed in Spring in a short period of time since first node appearance (Spring was the only season of the year when axis rank 1 was observed - Figure 5.1.25). Moreover, plants experienced an important N deficiency in the beginning of Spring (Figure 5.1.1). This deficiency might have greatly disturbed the plants'ontogenetic pattern at that time of the year.

During Autumn, climatic conditions were considerably different from Spring and Summer, with a much lower temperature, lower global radiation and shorter daylength (Figures 4.5 and 4.6). As a consequence, the main axis and all the primary axes evaluated during Autumn got into the flowering stage. Floral induction occurs in response to suitable day length or photoperiod conditions, and is influenced by climatic growth factors, such as temperature and soil moisture (Vincente-Chandler, 2001). Most tropical grasses are either day neutral or short-day in response to flowering (Burson and Young, 2001; West and Pitman, 2001). A tipical response of short-day plants was observed for elephant grass, since flowering was observed during Autumn on all axes, a time of the year when days are shorter and air temperature is cooler.

Therefore, seasonality effects on growth dynamics of successive leaves may be reported, as described in the Figures 5.1.2, 5.1.3 and 5.1.4. The parameters obtained by adjusting the hiperbola curve on leaf growth measurements allowed the assessement of morphogenetic variables such as leaf appearance rate (LAR), leaf elongation rate (LER) and leaf elongation duration (LED). Time was expressed in thermal time, considering a base temperature of 10°C, and in phyllochronic units. The use of phyllochronic units reduced the variation associated with temporal unit (such as chronologic and thermal time, heating units, photothermal units, etc) by considering a plant as a repeated regular production of organs, which is "the basic building block of grass growth" (Wilhelm and McMaster, 1995).

Ontogenetic development on the main axis

Dynamics of plant form generation and expansion in space, i.e. morphogenesis (Chapman and Lemaire, 1993), is usually studied in forage plants through analyses of variables such as leaf appearance rate, leaf elongation rate and leaf elongation duration. These characteristics, in turn, are influenced by weather conditions and by the light enviroment

within the sward canopy resulting from the interactions among individual plants (Lemaire and Chapman, 1996).

Leaf appearance in grasses starts with production of cells that encircles the apical dome in the outer layers of shoot apical meristem, which is mostly influenced by temperature and nitrogen status (Skinner and Moore, 2007). For all seasons of the year, the successive appearance of leaves presented a linear relationship on a thermal time basis, indicating that temperature was a direct determinant of the phyllochron, as reported for other forage grasses (Andrieu et al., 2006; Birch et al., 2007; Lafarge and Andrieu, 2002; McMaster et al., 2003; Zhu et al., 2014). The effect of temperature on plant functioning is brought about by the action on enzymatic activities, altering the conformation of the enzymes, and directly affecting the velocity of chemical reactions (Bonhome, 2000). Although temperature is the major contributor to LAR, seasonality effect was reported (LAR varying from 0.0165 to 0.0322 leaf per degree-day in Spring and Autumn, respectively – Table 5.1.1). However, even considering time in degree-days, differences in LAR were observed between seasons of the year. These results suggest that LAR does not solely depend on temperature, but also possibly on radiation or daylength. Egle et al. (2015) also reported seasonality effects on LAR for different rice genotypes. The LAR is primarily influenced by temperature but also by many other environmental factors such as water or nutrient availability and light quality (Wilhelm and McMaster, 1995). During the vegetative phase, higher LAR during Summer relative to Spring can be justified by higher temperatures, longer daylength and greater global radiation (Figure 4.5 and 4.6). On the other hand, high LAR was reported in Autumn, when plants were commited to flowering (Table 5.1). The increased LAR in Autumn was presumably consequence of rapid stem elongation and smaller leaves requiring less time to expand (Warrington and Kanemasu 1983) due to the reproductive growth.

In grasses, LAR is a key variable, since it influences other structural characteristics of the plant (Lemaire and Chapman, 1996). In temperate forage grasses, LAR is directly influenced by temperature but also depends on the length of the sheath tube (Cruz and Boval, 2000), which determines LER and LED. There is an interdependency among LER, LED and LAR in terms of control of plant growth (Bahamani et al., 2000). The growth of cells following its production, at the apical meristem region, progresses through cell expansion. In that sense, rate and duration of cell expansion determine final leaf length. In grasses, leaf elongation occurs inside the sheath tube, enclosed by the whorl of mature sheaths (Skinner and Nelson, 1995). When leaf tip reaches the atmosphere over the whorl, formation of the ligule begins, and the leaf diferenciates in two parts: blade and sheath (Skinner and Nelson,

1994). Therefore, longer sheath tube results in increased cell production and greater number of cells elongating at a given time, resulting in higher LER and longer LED. For elephant grass, during Summer and Autumn, within the range of leaf ranks evaluated (10 to 20 and 9 to 14, respectively), LER was constant, as was sheath length (Figure 5.1.12). On the other hand, LED (calculated in degree-days) inscreased as leaf rank increased on the main axis during Summer (Figure 5.1.9), explaining the concomitant increase in final leaf length (FLL).

For temperate forage grasses, usually LAR decreases as leaf rank increases, with corresponding increase in LED. The decrease in LAR is compensated by longer leaf length (Duru and Ducrocq, 2000a). The size of the sheath tube determines the length of elongation zone by regulating the number of cells produced (Begg and Wright, 1962). The reason is that leaf tip emergence corresponds to the formation of the ligule and stop cell production of the blade (Skinner and Nelson, 1995), preceded by cell expansion phase. This explains the proportional relationship usually found between leaf blade and leaf sheath length (Duru and Ducroq, 2000a). In this sense, as temperate grasses grow, the sheath tube length increases, leading to increased phyllochron due to longer time elapsed for the leaf tip to reach the atmosphere, i.e. increasing period of leaf elongation (Duru et al., 1993; Miglietta, 1991; Skinner and Nelson, 1994). The importance of the leaf sheath tube length in determining leaf dimensions was previously demonstrated in the literature by several authors (Casey et al., 1999; Wilson and Laidlaw, 1985) by modifying the length of the sheath tube artificialy and through cutting. Such responses have been characterized as a general developmental pattern for temperate forage grasses by Lemaire and Chapman (1996). Therefore, increases in FLL of successive phytomers occurs until the sheath tube reachs its maximum length, reaching a plateau from phytomer 12 onwards.

In elephant grass, FLL increased from leaf rank 10 to 20 without changing the length of leaf sheath (Figure 5.1.12), most likely due to the increased LED of higher rank leaves. Considering a constant phyllochron through the development of elephant grass, the increase in FLL could be attributed to the increased number of visible expanding leaves as leaf rank increased. In fact, even in a phyllochronic time basis, LED increased from 3 to 5 phyllochron units during Summer (Figure 5.1.10). Increased LED in a phyllochronic time basis means more leaves expanding at the same time on higher rank leaves. This was a key characteristic determining leaf length in *Pennisetum purpureum* cv. Napier, which has not been reported in the literature for any other C4 perennial tropical grass. The measurement of LAR is obtained after tip emergence over the whorl; however, more leaves could have been produced by the apical meristem and would not have been accounted for because they were still placed within

the sheath tube. Formation of leaf primordia could happen faster than leaf appearance over the whorl, resulting in accumulation of leaf primordia at the apex (Williams, 1960; Skinner and Nelson, 1995). When the last leaf primordium and last expanded leaf were plotted against thermal time, although no statistical difference was found between the slopes of the curves (Figures 5.1.21 and 5.1.22), the slight difference in regression slope indicates that a greater number of leaves was expanding (including visible leaf primordium) with time. It is worth to note that plasthocronic index was not directly assessed and would be interesting to investigate if it is proportional to phyllochronic index, as reported for temperate forage grasses (Nelson, 2000). Robin (2011) reported that LED of an individual leaf is not necessarily equal to the interval between leaf appearances, although closely related. Sartie (2006) observed interval between ligule appearances to be greater than the interval between leaf appearances, indicating that FLL increased for successive leaves and LED was greater than the appearance of successive leaves. These results suggest that the plasthocronic unit could be more appropriate to analyse the development of elephant grass, however, further studies are needed to investigate these relations.

The linear relationship between number of leaves and thermal time was also reported for several annual grasses, like rice (Lafarge and Tardieu, 2002), maize (Warrington and Kanemasu, 1983) and millet (Ong, 1983). However, in those studies, FLL represented a bell-shaped curve for leaf position on the main axis, essentially linked to differences in the duration of the elongation phase rather than to differences in elongation rate. The duration of the linear phase decreased with leaf position in the last-formed leaves, due to a simultaneous cessation of elongation with the transition to the flowering phase. This pattern was analogous to the pattern observed during Autumn for elephant grass in this study, when for a constant LER (Figure 5.1.8), LED decreased as leaf rank increased in both on a degree-day basis (Figure 5.1.9) and on a phyllochronic time basis (Figures 5.1.10), leading to decreased FLL (Figure 5.1.11) until the last leaf produced before flowering.

Coordination of leaf development

Kinetics of leaf development for a selected group of leaf ranks during the three evaluation seasons showed highly stable expansion dynamics when expressed on a phyllochronic basis (Figure 5.1.13). The same coordination was not found on a thermal time basis (Figure 5.1.14), which can be explained by the seasonality effect of plant growth, as mentioned above. These results support the existence of a general pattern of development common to all seasons of the year, indicating that the coordination of organ growth was

conserved irrespectively of evaluation season for a selected group of leaf ranks. Concerning the timing of leaf development, the coordination of development is supported by the synchrony of the kinetics using a phytomer based origin (Fournier et al., 2005). The synchrony between growth curves means that independently of the variability in thermal time, leaf elongation was triggered by the same emergence event during the different evaluation seasons.

On the other hand, when different groups of leaf ranks were analysed within evaluation seasons, dissimilarities between leaf rank groups were observed on a degree-day time scale or even using a phytomer-based time origin. During Summer and Spring, leaf elongation duration was longer for leaf ranks 17-20 relative to leaf ranks 10-12 (Figure 5.1.15 and 5.1.19). The divergence in maximum relative elongation rates indicates differences in the timing of organ growth (Faverjon et al., 2017). Dissimilarities in kinetics of leaf growth were also reported during Autumn (Figure 5.1.16). However, lower values of maximum leaf elongation rate were observed for leaf ranks 13-14. As reported earlier, during Autumn, all axes were commited to flowering, and such divergences could be explained by the cessation of leaf production and decreased sheath tube length by displacement of the apical meristem.

When shynchrony is observed, the organogenesis of growth can be used to characterize ontogenetic development and to predict changes according to plant development. Otherwise, as reported for different leaf ranks on the main axis, further studies are needed to investigate the determinants of changes according to leaf rank in order to integrate the response in a conceptual model of coordination between kinetics of leaf growth.

Coordination of development on the axes

The overall shoot architecture of a plant is derived from the primary shoot apical meristem activity that suports the main axis. Along with that, activity of the additional axillary meristems (Shimizu-Sato and Mori, 2001) build the shoot structure of the plant by recruiting a series of connected axes generations referred to as hierarchies of branches (Langer, 1979). The production of axillary axes is one of the most important characteristics related to plant plasticity and usually presents great recruitment of axes under high availability of light and resources (Aguilar Martinez et al., 2007; Baldissera et al. 2014; Kebrom et al., 2013). During the development of elephant grass, for all seasons of the year, plants systematically displayed a conspicuous branching pattern (Figures 5.1.23, 5.1.24 and 5.1.25). The first primary axis took longer to appear. During Summer, the first node branching appeared approximately after 200 degree-days, while during Spring and Autumn first

branching occurred at approximately 400 degree-days. The delayed appearance of the first axis was related to internal carbon status of the plants and assimilate acquisition, a phenomenon called “assimilate availability” (Moulia et al., 1999; Lafarge et al., 2002). After the establishment of seedlings, plants first produce assimilates to support their growth while storing assimilates in the reserve organs. As soon as they have sufficient assimilates, they supply nutrients and growth substances for several active growing sinks. This pattern was also reported for rice (Jaffuel and Dauzat, 2005) and maize (Moulia et al., 1999).

The linear relationship between number of leaves and thermal time described above for the main axis was also observed for primary axes. However, two distinct groups of axes could be identified according to LAR during Summer and Autumn. Primary axes positioned above the soil surface, i.e. topmost axes, and axes located close to soil surface. The first showed significantly higher LAR than the second (Tables 5.2, 5.3 and 5.4). The higher LAR for topmost axes was also reported by Moulia et al. (1999) for maize. The authors mentioned that it is not clear whether this is due to their type of differentiation or position on the main axis. One possible hypothesis is that stems are important reserve organs, especially in the base region (Speck and Burgert, 2011) and could provide instantaneous availability of resources to support faster growth of the topmost axes. In addition, as topmost axes do not produce roots, resources should be provided exclusively to shoot, especialy for leaves. It is important to note that plants’ growth increases over time due to increased leaf area and amount of intercepted light. When the topmost axes arised, the leaf area of the plant was higher and the carbon input greater than initially, optimizing growth of the whole plant, and consequently recruitment of tillers. During Spring, the same pattern was not observed, which could be related to the timing of branching on the main axis, consequence of the nitrogen deficiency, as described above.

The development for primary axes generally followed a shynchronization of development for successive axis ranks, and was similar to the pattern described for the main axis. However, primary axes were evaluated since the appearance of the first leaves, and it was possible to follow changes in successive leaf ranks since the beggining of axis development. When analyzing the morphogenetic characteristic of axes, the hierarchy and synchronization of growth could be perceived by gradual changes occurring on successive leaf ranks. During Summer, LER regularly increased with increasing leaf rank on the axes and reached a plateau, with maximum value depending on the axes (Figure 5.1.26). The internal coordination between LER was mainly a response of gradual changes from one leaf to another, also reported by Egle et al. (2015). Conversely, LED increased with increasing leaf rank at a higher rate for the topmost primary axes, leading to an increase in FLL (Figure

5.1.38). FLL increased with leaf rank on all axes, and was higher on successive axes rank for a given leaf rank, i.e. FLL on the axes rank *n*+1 is higher than FLL on the axes *n* for the same leaf rank. This result is in line with the findings of Lestienne et al. (2002) for *Lolium perenne*, and could be explained by the effect of the preceding leaf sheath length where the first leaf arised. The first leaf of primary axes was influenced by an increased sheath length on the main axis.

The morphogenetic characteristics reported for successive axes have not been reported in the literature for any perennial C4 tropical forage grasses and remains to be investigated wether there are other intrinsic aspects of development on the main axis responsible for diferences between axes branching close to soil surface and topmost axes. During Spring, the analyses of successive changes in LER according to leaf rank did not follow the same patern as observed during Summer and Autumn (Figure 5.1.31), certainly due to the nitrogen deficiency at that time of the year, as reported above.

During Autumn, while LER increased to a plateau and remained stable for higher leaf ranks, LED decreased for the last leaf ranks, resulting in a bell-shaped curve of FLL with leaf rank (Figure 5.1.39). This pattern is typical for flowering grasses, such as maize (Birch et al., 2007) and rice (Egle et al., 2015; Lafarge and Tardieu, 2002). The reduction of leaf length in Autumn can be attributed to shortening of the sheath tube length and reduced number of expanding leaves, since leaves stop elongating with the onset of the flowering period.

The results obtained in this study clearly show that the process determining morphogenesis of elephant grass during the vegetative phase differs from the classic pattern described for temperate forage grasses, as presented by Lemaire and Chapman (1996). As the number of visible leaves expanding simultaneously increased with increasing leaf rank, leaf size was not a constant function of leaf elongation and leaf appearance rate as stated by Equation 3 (FLL = a x LER x Ph; where “a” is the number of expanding leaves) presented in section 2.2. The continuous increase in LED with increasing phytomer rank, accompanied by the constant LAR and stable LER have not been reported for any perennial C4 tropical forage grass. This pattern is crucial for understanding plant behaviour and its morphogenetic adaptation to environmental changes, competition with neighbouring plants and defoliation management. However, some questions still need to be investigated to better elucidade the main points in ontogenetic development of elephant grass, such as: i) What are the determinant factors of the non-coordination between leaf ranks on the main axis? ii) How does the plant change the number of expanding leaves? Is there a genetic trait related to

ontogeny or the LED should be analysed at the level of plastochronic index? iii) What are the determinants of higher LAR for the topmost primary axes?

5.1.3. CONCLUSION I

The ontogenetic development described for elephant grass during the vegetative phase diverge from that of temperate forage grasses, with an independent increase of LED leading to increased number of visible expanding leaves and consequently FLL. The seasonality effect was observed in the ontogenetic development of plants and suggests that factors other than temperature should be integrated to analyse plant growth and development patterns.

The hierarchical organization was observed between main axis and successive primary axes, representing a strong synchronization among axes. However, for the topmost axes and higher leaf ranks on the main axis, the behavior is different and remains unclear whether there are some intrinsic aspects related to phytomer development of the main axis. This study brings new information on the morphogenetic program of elephant grass and provides a key element towards a better understanding of plant plasticity to environmental conditions. These results can potentially be used for functional–structural plant modelling.

5.2. IS INTERNODE ELONGATION COORDINATED WITH LEAF DEVELOPMENT ONTOGENY? IF SO, HOW IS THIS COORDINATION OPERATED?

In this section, in complement to the leaf development described above, the relationship between stem elongation in main and primary axes is demonstrated. Additionally, the coordination between leaf and internode growth is elucidated.

5.2.1. RESULTS II

The apical meristem height increased progressively with thermal time for all seasons, due to elongation of intercalary meristems that produced the internodes. Stem elongation started at approximately 600, 780 and 1000 degree-days following node collection during Autumn, Summer and Spring, respectively (Figure 5.2.1). During Summer, stem elongation

began earlier and reached higher values of apical meristem height than during Spring (approximately 80 and 60 cm, respectively). The displacement of apical meristem was much faster during Autumn than Summer and Spring. During Autumn only the first three sampling dates were used to measure and identify apical meristem height on the main axis, because of flowering.

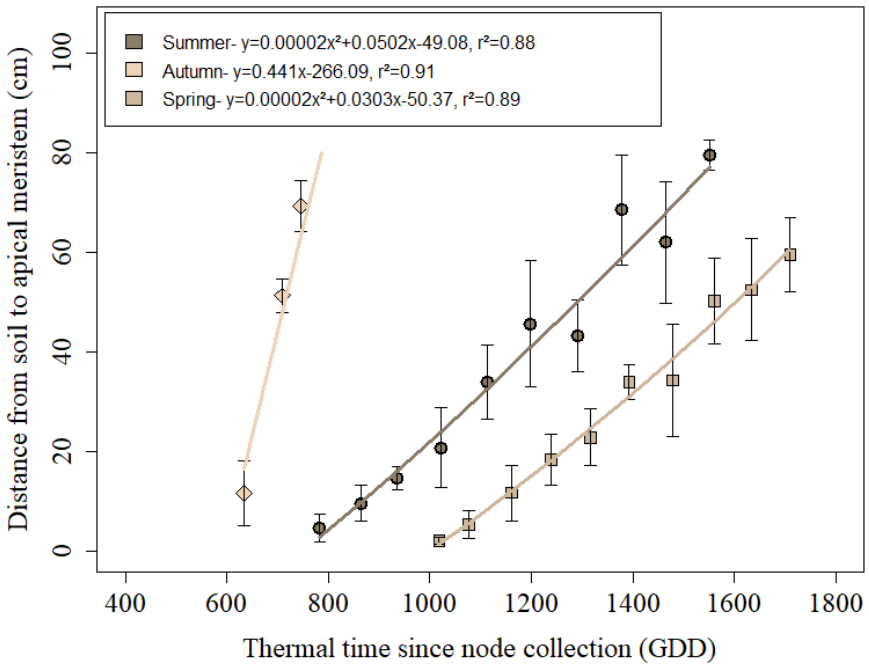

Figure 5.2.1. Apical meristem height (cm) in *Pennisetum purpureum* cv. Napier plotted against thermal time (degree-days (°C)) since node collection on the main axis. Each point represents one sampling date for destructive evaluations. Diamonds: Autumn (2016); circles: Summer (2016); squares: Spring (2015). Vertical bars indicate standard deviation of the mean.

Apical meristem height showed a similar starting point of elongation during Summer and Spring, when expressed on a shoot development stage basis, i.e. number of emerged leaves on the axis (Figure 5.2.2). The rapid displacement of the apex started approximately after leaf 13 appearance and increased successively following a quadratic polynomial curve. During Autumn, a curve was not fitted since plants were rapidly flowering, and only two leaves were produced during the period of destructive evaluations. As mentioned in the material and methods section, in Summer and Autumn, the first desctructive analyses were performed 15 days earlier than in Spring, starting with leaves from rank 11. During the evaluation period, approximately 25 and 26 leaves were produced during Summer and Spring, respectively.

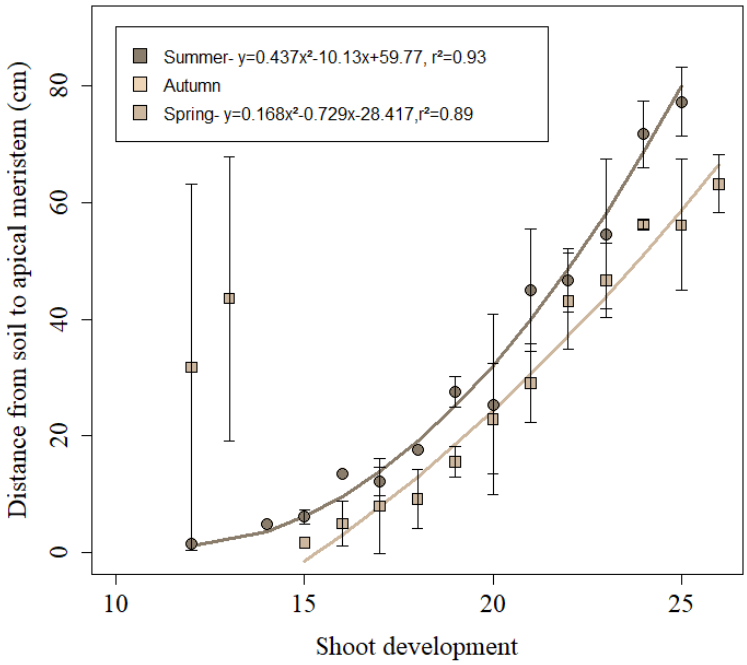

Figure 5.2.2. Apical meristem height (cm) in *Pennisetum purpureum* cv. Napier plotted against shoot development, i.e. number of emerged leaves, on the main axis. Each point represents one sampling date for destructive evaluations. Diamonds: Autumn (2016); circles: Summer (2016); squares: Spring (2015). Vertical bars indicate standard deviation of the mean.

A linear equation was fitted between the number of internodes and shoot development, i.e. number of emerged leaves (Fig 5.2.3). A similar curve was obtained for Summer and Spring, with the same number of internodes produced. Stem elongation was reported from the shoot development 14 and 17 during Summer and Spring, respectively. The x-intercept of the fitted curves indicates that the start of internode elongation occured approximately after shoot development 13. During Autumn, at the first desctructive analyses sampling, stem elongation had already started, and only three leaves were observed. Therefore, it was not possible to follow the progressive internode elongation and its relationships with shoot development.

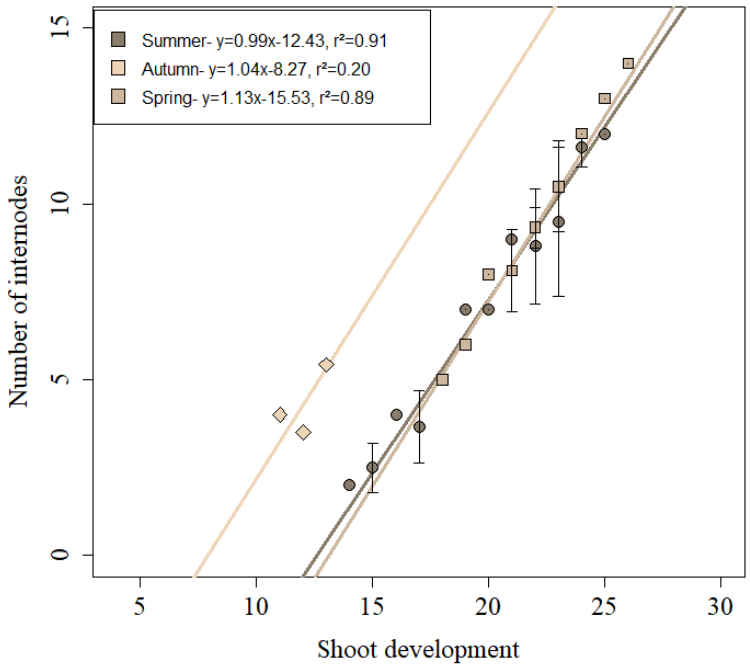

Figure 5.2.3. Number of internodes observed in *Pennisetum purpureum* cv. Napier plotted against shoot development, i.e. number of emerged leaves, on the main axis. Diamonds: Autumn (2016); circles: Summer (2016); squares: Spring (2015). Vertical bars indicate standard deviation of the mean.

For all seasons of the year, internode elongation progressed from phytomer 8 until reaching a maximum size in phytomer 12-13 (Figure 5.2.4). During Spring and Summer, the internode 8 elongated only a few centimeters (approximately 2 cm), whilst during Autumn it elongated 5 cm. Similar pattern of internode elongation was found during Summer and Spring, with a maximum internode size of approximately 8 to 10 cm from phytomer 13 onwards. During Autumn, the maximum internode lenght was around 21 cm, more than twice the values recorded during Summer and Spring.

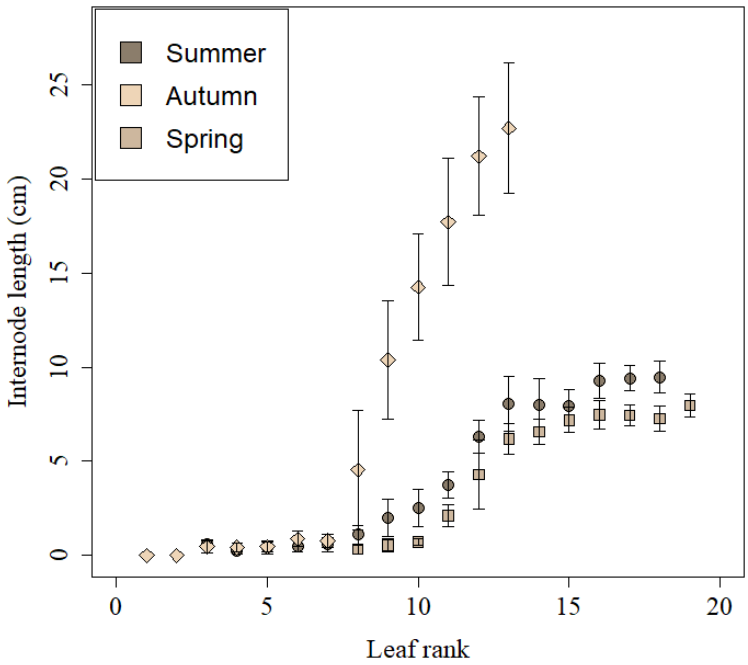

Figure 5.2.4. Final length of the internode (cm) plottted against leaf rank on the main axis of *Pennisetum purpureum* cv. Napier. Diamonds: Autumn (2016); circles: Summer (2016); squares: Spring (2015). Vertical bars indicate standard deviation of the mean.

The progressive increase in internode length with thermal time is shown in Figures 5.2.5, 5.2.6 and 5.2.7 for Summer, Autumn and Spring seasons, respectively. These results show a pattern of sigmoidal growth of internodes from phytomer 8. During Spring, because destructive evaluations were performed later than during Summer and Autumn, results are presented solely for phytomers above leaf rank 10. Graphs additionally show the sequential commencement of internode extension and the maximum value of internode elongation reached from leaf rank 13 onwards for all seasons. Higher values of internode length were recorded in Autumn, with maximum value of approximately 20 cm, whilst during Summer and Autumn maximum values corresponded to around 10 and 8 cm, respectively.

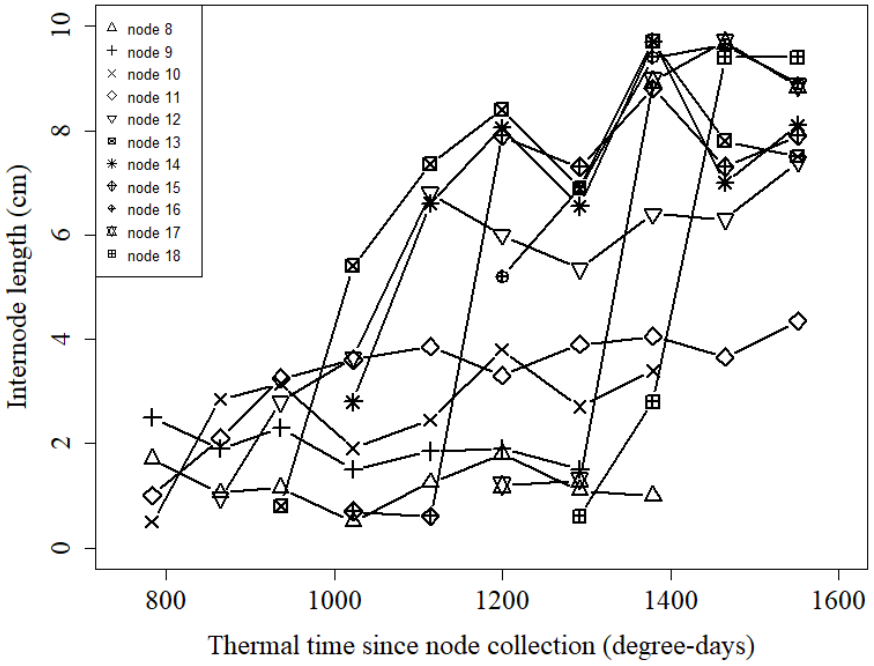

Figure 5.2.5. Median internode length (cm) of *Pennisetum purpureum* cv. Napier plotted against thermal time (degree-days (°C)) on the main axis, since node collection in Summer. Each line represents one node.

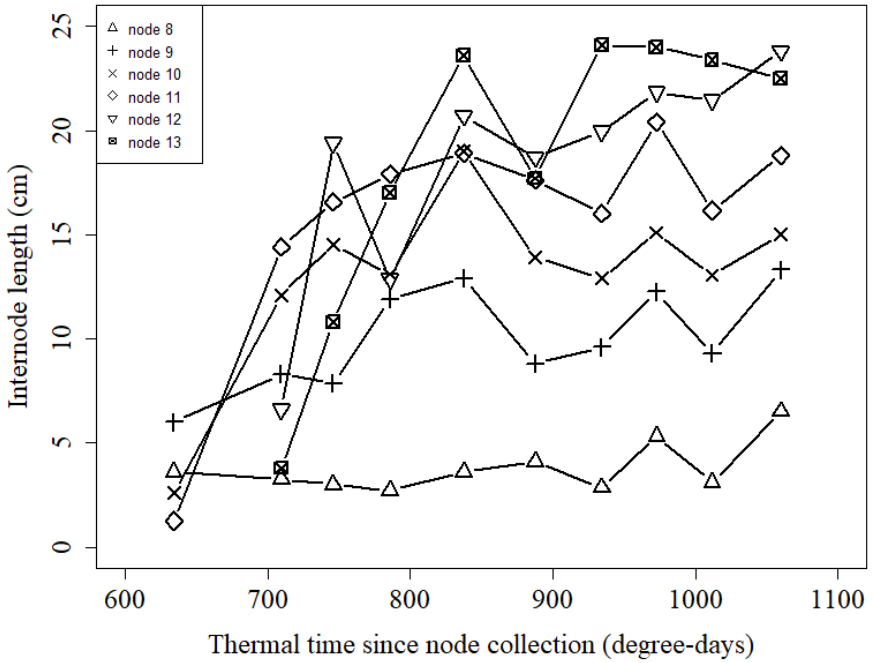

Figure 5.2.6. Median internode length (cm) of *Pennisetum purpureum* cv. Napier plotted against thermal time (degree-days (°C)) on the main axis, since node collection in Autumn. Each line represents one node.

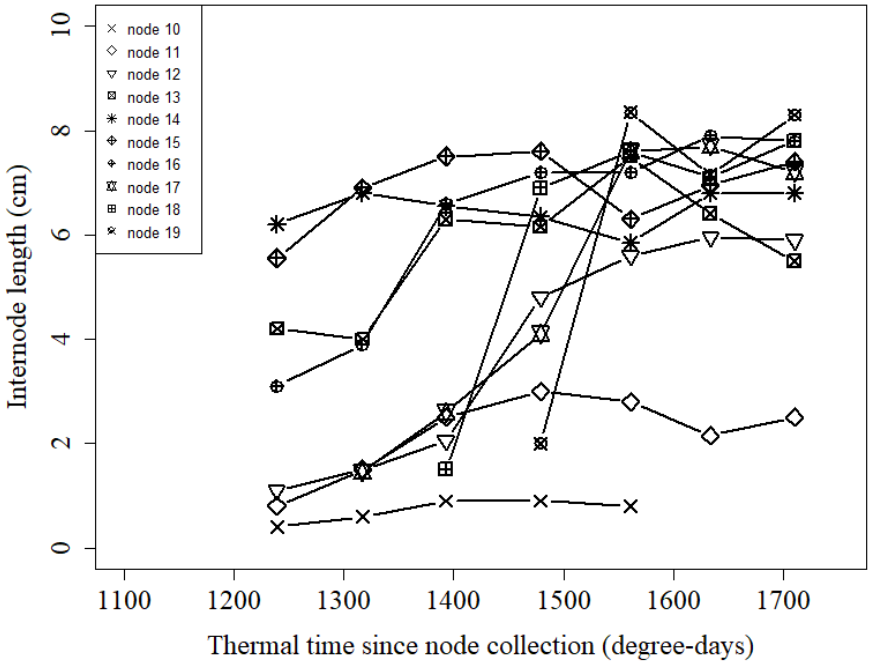

Figure 5.2.7. Median internode length (cm) of *Pennisetum purpureum* cv. Napier plotted against thermal time (degree-days (°C)) on the main axis, since node collection in Spring. Each line represents one node.

The timing of relative leaf blade and internode elongation was plotted against phyllochronic time starting at 50% of leaf length during Summer and Spring (Figure 5.2.8). A strict coordination of growth kinetics was observed for leaf blade and internode length. The beginning of internode elongation was synchronized with the end of the relative leaf blade elongation. Internode elongation started systematically approximately 5.0 phyllochrons after leaf initiation. This coordination of plant organs development was similar during Summer and Spring.

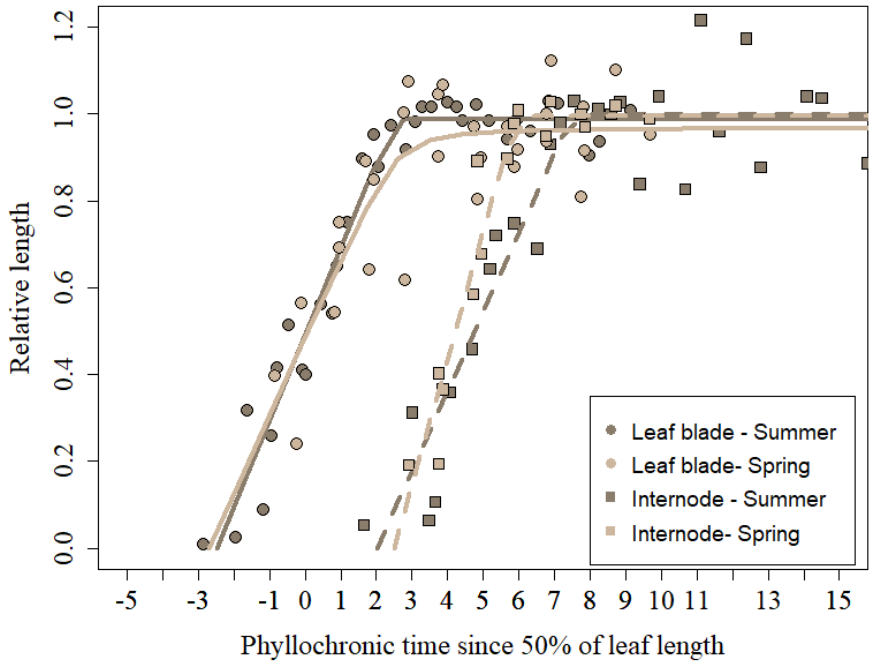

Figure 5.2.8. Dynamics of the relative leaf blade and internode length expressed in phyllochronic units on the main axis of *Pennisetum purpureum* cv. Napier in Summer and Spring.

The dynamics of stem elongation is described for primary axes during Summer, Autumn and Spring on a thermal time basis since node collection (Figures 5.2.9, 5.2.10 and 5.2.11). Maximum values of apical meristem height are reported on the main axes and were successively lower for higher axis ranks. Quadratic curves were fitted for each primary axis. During Autumn, the main axis was not fitted with a regression line, because the maximum value of apical meristem height was observed during the second destructive evaluation.

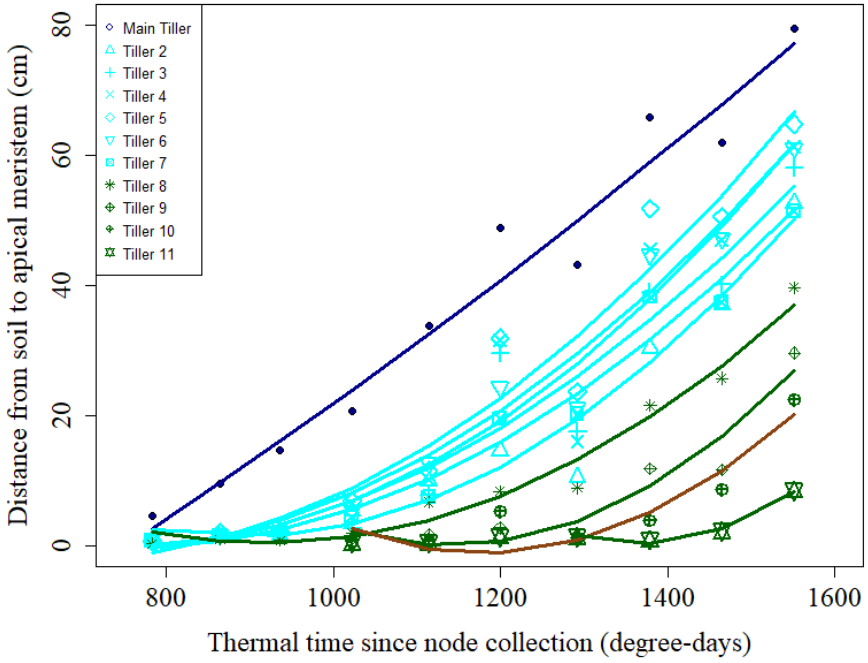

Figure 5.2.9. Apical meristem height (cm) in *Pennisetum purpureum* cv. Napier plotted against thermal time (degree-days (°C)) since node collection for main and primary axes, in Summer. Dark blue - represents main axis; Light blue – represents primary axes, from rank 2 to 7; Dark green – represent topmost primary axes, from rank 8 to 11.

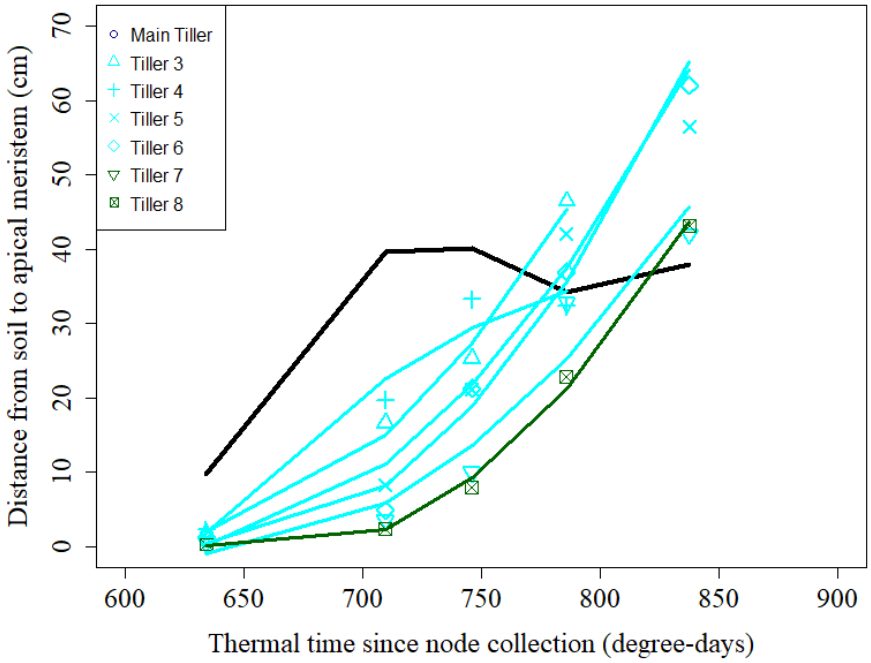

Figure 5.2.10. Apical meristem height (cm) in *Pennisetum purpureum* cv. Napier plotted against thermal time (degree-days (°C)) since node collection for main and primary axes, in Autumn. Dark blue - represents main axis; Light blue – represents primary axes, from rank 2 to 7; Dark green – represent topmost primary axis, leaf rank 8.

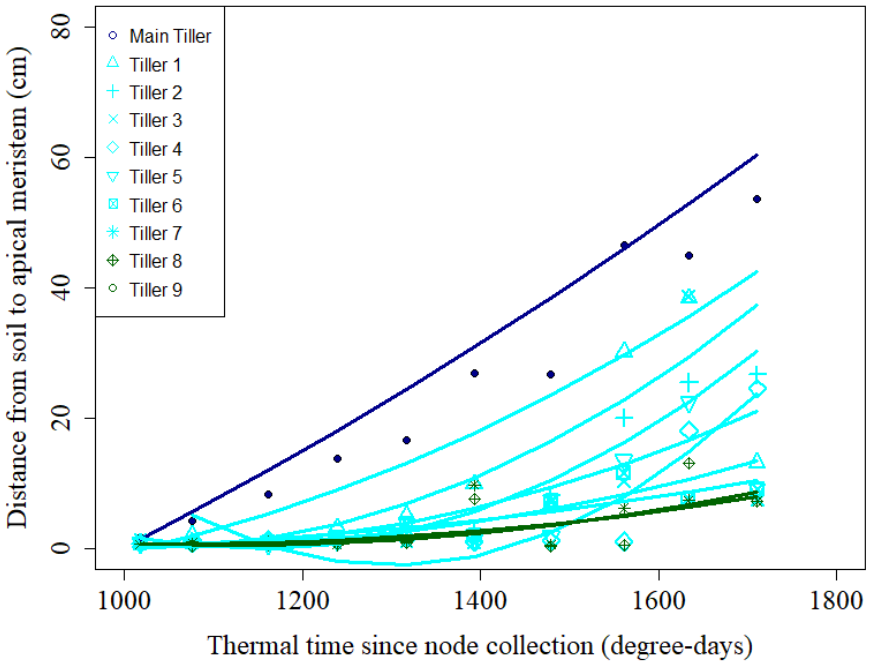

Figure 5.2.11. Apical meristem height (cm) in *Pennisetum purpureum* cv. Napier plotted against thermal time (degree-days (°C)) since node collection for main and primary axes, in Spring. Dark blue - represents main axis; Light blue – represents primary axes, from rank 2 to 7; Dark green – represent topmost primary axes, from rank 9 to 11.

The relationship between stem elongation and shoot development, i.e. number of emerged leaves, was investigated for each primary axis by plotting apical meristem height against last visible leaf during Summer and Autumn (Figures 5.2.12 and 5.2.13). During Autumn, due to the small number of leaves produced and the faster stem elongation relative to the frequency of sampling, it was not possible to obtain this relationship. During Summer and Spring, apical meristem height increased slowly during the initial phase, and then abruptly afterwards, in diferent starting points depending on the primary axis rank. The starting point of shoot development to increase in stem elogation varied from leaf 13 to approximately leaf 5 in both seasons of the year depending on the primary axis rank.

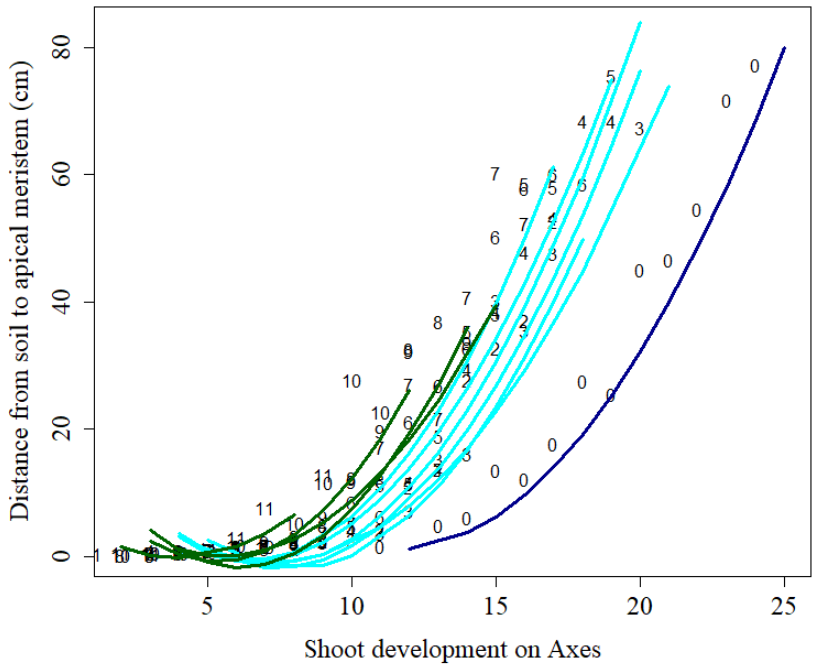

Figure 5.2.12. Apical meristem height (cm) in *Pennisetum purpureum* cv. Napier plotted against shoot development, i.e. number of emerged leaves, since node collection for main axis primary axes, in Summer. Dark blue - represents main axis; Light blue – represents primary axes, from rank 2 to 7; Dark green – represent topmost primary axes, from rank 9 to 11.

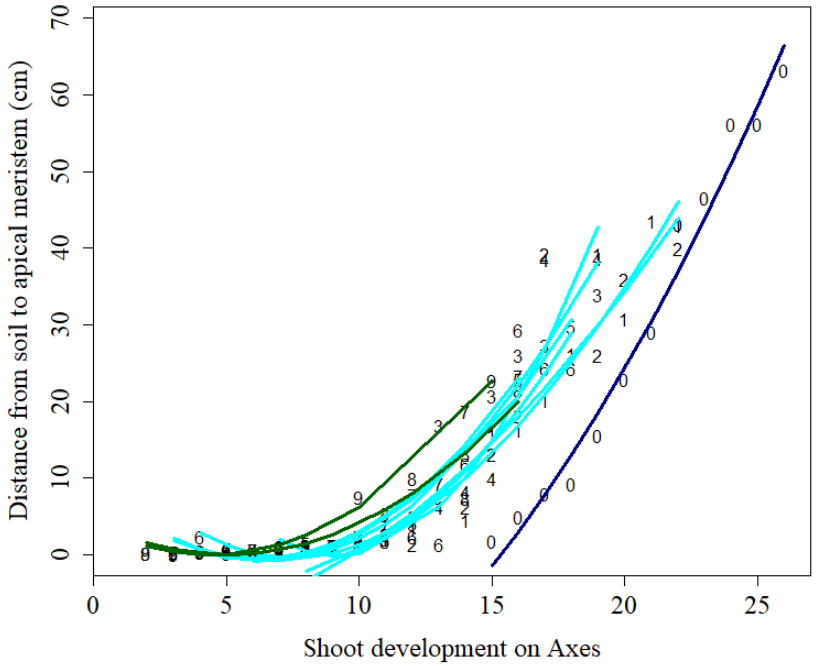

Figure 5.2.13. Apical meristem height (cm) in *Pennisetum purpureum* cv. Napier plotted against shoot development, represented by leaf number, for main axis and primary axes in Spring. Dark blue - represents main axis; Light blue – represents primary axes, from rank 2 to 7; Dark green – represent topmost primary axes, rank 8 and 9.

As reported above (Figure 5.2.8), the coordination between relative leaf blade and internode length presented a strong synchronism across seasons of the year. During Summer and Spring, internode initiation started approximately 5 phyllochronic units after leaf appearance. In this sense, based on shoot development at the beggining of stem elongation it is possible to indicate the corresponded internode that is elongating. In this sense, for each curve presented above, it was possible to identify the shoot development stage at the begning of apical meristem displacement and subtract the difference in phyllochronic units, allowing to plot the first node to elongate for each axis rank (Figure 5.2.13). Primary axes presented a hierarchical starting point of the internode that elongates, both during Summer and Spring. For the main axis, the first node to elongate was from phytomer 8-9, and successively lower on increasing primary axes rank. A linear regression curve was fitted and represents the relationship between first node to elongate and axes rank (Figure 5.2.13).

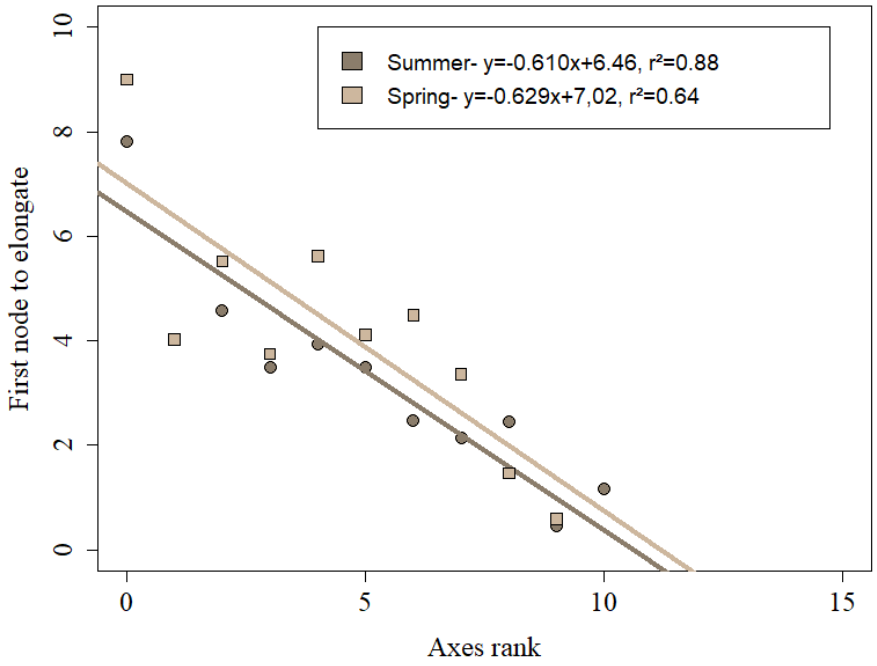

Figure 5.2.15. Number of the first node to elongate in *Pennisetum purpureum* cv. Napier plotted against axes rank. Axes rank 0 refers to the main axis. Circles: Summer (2016); Squares: Spring (2015).

5.2.1.1. Relationship between sheath tube length and shoot development

At the time of the longitudinal dissection of the axes during the destructive analyses, the distance from the apical meristem to the collar of the last expanded leaf was measured and

it was described as sheath tube length. These analyses were performed solely during Summer and Spring, since during Autumn a limited number of leaves was produced. Independently of the season of the year, all primary axes reached the same value of maximum sheath tube length. However, successive primary axes reached their maximum size at different shoot development stages, but coincident to the beginning of stem elongation, as presented in Figures 5.2.12 and 5.2.13. During Summer, maximum values of sheath tube length were around 13 cm and shoot development varied from leaf 13-14 to leaf 6 for main and primary axis number 11, respectively (Figure 5.2.16). During Spring, maximum values of sheath tube length were slightly smaller than those during Summer, and corresponded to around 11 cm with shoot development varying from leaf 14 to leaf 8 for main and primary axis number 9, respectively (Figure 5.2.17).

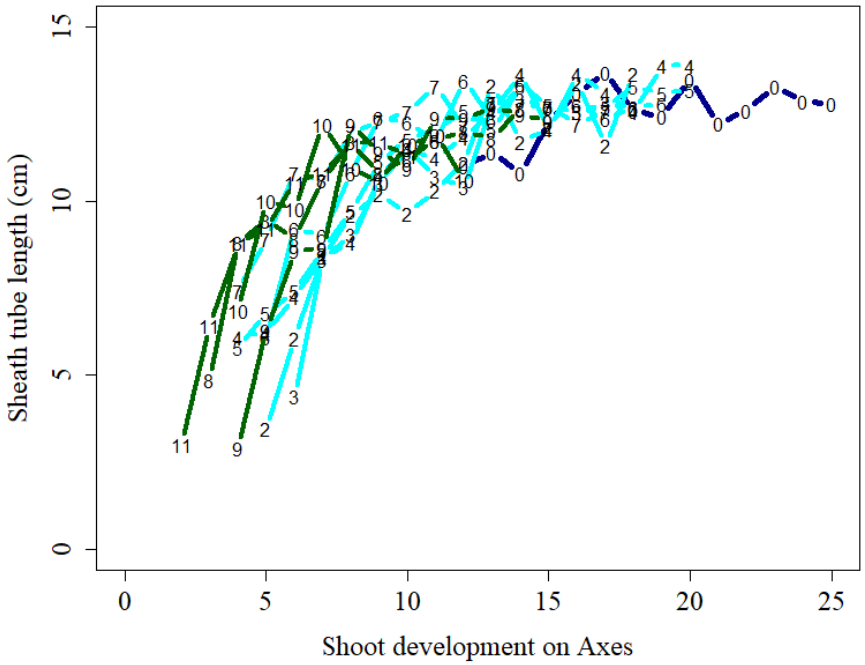

Figure 5.2.16. Sheath tube length (cm) in *Pennisetum purpureum* cv. Napier plotted against shoot development on axes, for main and primary axes, in Summer. Dark blue - represents main axis; Light blue – represents primary axes, from rank 2 to 7; Dark green – represent topmost primary axes, from rank 9 to 11.

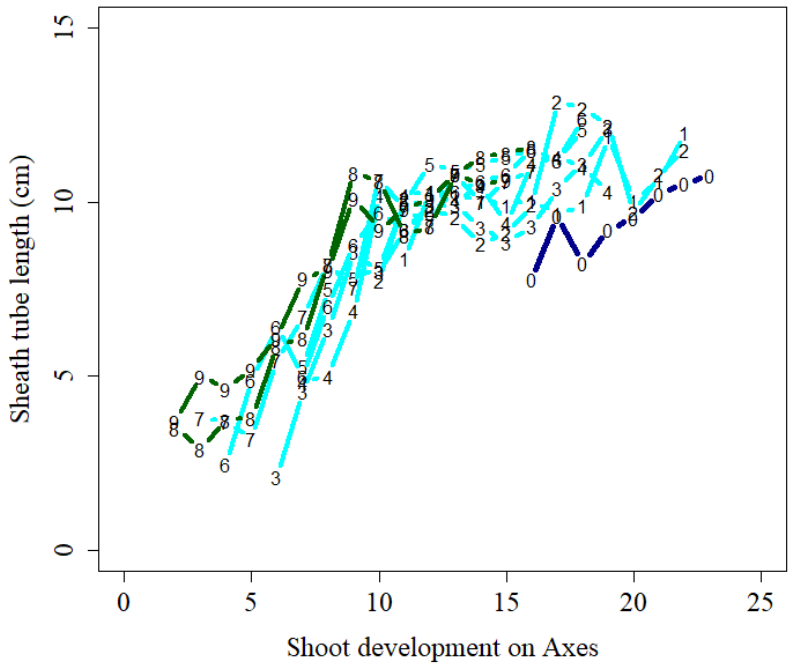

Figure 5.2.17. Sheath tube length (cm) in *Pennisetum purpureum* cv. Napier plotted against shoot development on axes, for main and primary axes in Spring. Dark blue - represents main axis; Light blue – represents primary axes, from rank 2 to 7; Dark green – represent topmost primary axes, from rank 8 to 9.

5.2.2. DISCUSSION II

The morphological changes involved in growth and development of grasses derive from their ontogenetic program and environmental conditions. The environmental conditions affect the sink-to-source relations by changing assimilates partitioning priority to different plant organs, especially leaves and stems. In this sense, stem elongation is a key process regarding the development of grass species. Stem elongation affects the vertical distribution of leaf area and light interception, and ultimately the production and distribution of assimilates among vegetative and reproductive cycles, influencing herbage yield and quality (Birch et al., 2008). In general, tillers initial development occurs through mobilization of photoassimilates to produce leaves (Richards, 1993), consequently, favoring light interception and increasing the photosynthetic capacity of axes. Especially for tropical perennial grasses, stem elongation depends on environment, mainly light-related relations (Ballare et al., 1991), and also on plants' ontogenetic development. In this study, internode elongation began at different thermal time (degree-days (°C)) for each season. This difference suggests that thermal time does not explain the onset of stem elongation solely. Initially, the process of stem elongation starts at lower rates and increases continuously, following a quadratic curve

between apical meristem height and growing degree-days. However, during the vegetative phase, stem elongation follows a similar pattern of development for all seasons when expressed on a shoot development basis (number of emerged leaves on the axis). The displacement of the apical meristem initiates at a predictable leaf number (i.e. shoot development), approximately at leaf 13 in Summer and Spring (Figure 5.2.2). The consistency between stem elongation and shoot development was also described for genotypes of maize (Robertson, 1994). At the simplest level, plant height could be modelled based on the relationship between plant height and final leaf number, assuming an average rate of stem elongation per phyllochron. For different genotypes of maize, a model was based on the elongation rate of 2.5 cm per phyllochron until emergence of leaf 7, and then 15.2 cm per phyllochron from leaf 7 until flag leaf appearance. In sweet sorghum, plant age expressed by number of appeared leaves on the main axis could be used as an indicator for growth and to describe events such as internode elongation (Nakamura et al., 2011; Goto et al., 1994).

Stem elongation elevates the apical meristem through the elongation of succesive internodes. The stable relationship between shoot development, expressed by number of emerged leaves, was used to describe the number of internodes produced at a given development stage. During the vegetative phase, a similar linear relationship was obtained for Summer and Spring which shows consistency between increasing number of internodes produced and leaves produced. The coefficients of the linear regressions close to 1.0 indicate that internodes production is synchronized with leaf appearance on the main axis. The synchronization between successive events could be usefull to follow plant development and monitor stem elongation. Studies with maize suggest that the number of phytomers produced largely determines the schedule of internode extension, and thus competition between these organs for assimilates and growth substances (Birch et al., 2002). Therefore, total number of phytomers may be a useful parameter to describe the meristem apex height and internode length.

In *Pennisetum purpureum* cv. Napier, a consistent increase in internode length from the same phytomer rank was observed regardeless of season of the year and axes stage of development, i.e. vegetative or reproductive. Final internode length increased after phytomer 8 and reached a maximum size at approximately phytomer 13, for all seasons (Figure 5.2.4). Successive internode extension was similar during the vegetative phase in both Summer and Spring, with shorter internodes on phytomers 8 and 9, approximately 2-4 cm, and a maximum value on phytomer 13, approximately 7-9 cm. In three cultivars of maize cultivated in Australia and France, internode length increased progressively starting from node 6-7, with

median lengths of 0.7 and 0.4 cm, until phytomers 10 and 13 depending on the cultivar, reaching maximum values of internode of approximately 22 cm (Birch et al., 2002). Therefore, even during the reproductive phase (i.e. Autumn), internodes started to elongate, showing a strong descriptor related to the ontognetic development of the plant. During Autumn, when elephant grass plants were at the reproductive phase, internode length was much greater relative to the vegetative phase, and reached a maximum value for phytomer 13 around 20 cm. This result suggests that internodes younger than phytomer 8 on the main axis seem to be "vegetative" internodes and are not able to elongate, even during transition to flowering. In fact, some internodes do not elongate, some remain short but elongate very little, and others elongate further (Fournier and Andrieu, 2000a). In maize, during the vegetative growth, the meristem initiates a predictable number of leaves, and once all vegetative nodes have been produced, the meristem initiates the primordia of florets, i.e. the meristem does not become committed to form a tassel until the initiation of all vegetative nodes is finished (Irish and Nelson, 1991). In the C4 grasses Switchgrass and Kleingrass, internode elongation started when four to five live leaf blades had been produced on an axis (Sanderson, 1992).

Understanding of the stem elongation process during the vegetative development of grasses requires detailed analysis of successive internodes elongation dynamics (development of individual phytomers), since they are synchronized events from phytomer to phytomer. During all seasons of the year, the first internodes that elongate, i.e internode 8, are smaller, and progressively increase in size as phytomer rank increases until reaching a maximum in phytomer rank 13. Internode elongation began slowly, then accelerated progressively, and finally decelerated. In maize, internodes 8 through 12 elongated quickest and internodes 13 and 14 had slower growth rates and shorter final lengths due to assimilate partitioning between internodes and associated ears. Finally, internode 15 (and 16 through 18) resumed vegetative development to elevate the tassel (Morrison et al., 1994). Successive internodes develop according to stepwise process, in which one internode approaches maturity before adjacent ones enter their periods of fastest growth, while deceleration of elongation occurrs in an internode before elongation activity intensifies in the successive internodes above.

The dynamics of relative extension of leaves and internodes showed a strong timing coordination and duration of elongation (Figure 5.2.8). This coordination supports marked phase transitions in organ extension being coordinated with leaf emergence events. During the vegetative phase, Summer and Spring, the same coordination was reported, the internode elongation occured systematically at approximately 5 phyllochronic units after leaf

appearance and started to elongate concomitantly with the cessation of leaf elongation. This consistent relationship allows the prediction of the onset of internode elongation and of the internode that will elongate at a given time. Synchrony between cessation of leaf elongation and the onset of internode elongation are in line with the results of previous studies with the C4 perennial tropical grass *C. squarrosa*, that reported sheath elongation ending with ligule emergence (Yang et al., 2016). In maize, Fournier and Andrieu (2000a) also described that collar emergence of the ligule *n* was coordinated with the decline in elongation rate of the sheath *n* and rapid increase in elongation rate of internode *n*. This coordination was corrobored later in sweet sorghum (Nakamura et al., 2011) and in maize (Zhu et al., 2014) by using functional-structural plant modelling.

Fournier and Andrieu (2000a) suggested that the rates of leaf and internode initiation are quite stable and the synchrony of sheath emergence with the end of the exponential phase of internode growth for phytomers 11 to 15 suggests that sheath emergence might act as a trigger. The authors identifiyed four phases of internode elongation kinetics and related them with the phases previously described by Sachs (1965). Initially, internode growth (exponential growth) corresponds to cellular multiplication; followed by establishment of the elongation region at the internode base (phase II). The third phase comprises the stationary production of mature cells, and phase IV the progressive regression of meristem. In this study, the transition from sheath length to internode length was a striking event, coordinated with the beginning of the linear growth phase, suggesting that sheath tube length indirectly controls internode length. In elephant-grass, during the vegetative development, similar maximum sheath tube length was obtained for all primary axes and seemed to be related to the transition to the internode elongation stage. The beginning of internode elongation on axes occurred in different shoot development stages according to axes rank. Regardless of season of the year, higher rank axes began to elongate earlier. The reasons for such a pattern are not clear yet, and might be related either to genetic expressions at the apical meristem level or morphological changes.

5.2.3. CONCLUSION II

The process of stem elongation was integrated with the ontogenetic development of elephant grass and could be adequately described by the number of leaves produced on the axis. Independently of season of the year, the first internode to elongate in main axis belongs to phytomer 8. Internode length started to increase progressively as leaf rank increased until

reaching a maximum length in phytomer 13. However, internodes were greater in Autumn relative to Summer and Spring due to flowering at that time of the year. There is a strong coordination between timing of leaf elongation and internode elongation, with a common pattern of coordination during the vegetative phase (Summer and Spring). Internode elongation was initiated aproximatelly 5 phyllochronic units after the beginning of leaf elongation and was synchronized with the cessation of leaf elongation. A hierarchical organization of the first internode to elongate was decribed for primary axes ranks, common to all seasons of the year. This study brings new information on the ontogenetic program of stem elongation in elephant grass. The results provide key elements towards a better understanding of plant plasticity and useful information to identify the beginning of stem elongation in the field. Further, these results potentially could be used to functional–structural plant modelling.

6. GENERAL CONSIDERATIONS

Morphological changes in plant development might result from the integrated responses of genetic and physiological aspects or might be driven by environmental cues. Environmental effects result from variations in light, water and nutrient availability and relations. These effects can also be modified by plant growth in interaction with neighbouring plants. In contrast, intrinsic changes to plant development, i.e. ontogenetic development, are a result of variation arising from gradient changes in gene expression in plant meristems related to a specific phase of development (Poethig 1990; Wiltshire et al., 1994). Morphophysiological changes on a same individual may vary considerably throughout its development and could be considered an intrinsic dynamic feature of plant growth (Gifford and Foster, 1996). Thus, to analyze the effects of environmental changes on patterns of plant growth and development, it is necessary to start from the ontogenic patterns of plant development. Such dynamic patterns occur predictably during ontogeny, resulting in allometric relationships among plant structures, spatial positioning of organs, and patterns of biomass allocation within and among plant modules (Hutchings and Kroon 1994; Huber and Stuefer 1997; Kroon and Hutchings 1995). How plants respond to environmental cues in order to adapt its structure and functioning, i.e. plant plasticity (Evers et al., 2011), is a central issue in plant ecology. In this sense, the understanding of the ontogenetic organization of plants and the hierarchical synchronism of its interconnected modules, i.e. phytomers, have implications on mechanisms and magnitude of plant plasticity, adaptation to competition with neighboring plants within a dense canopy, survival strategies, and the extent to which certain species adapt to a particular environment and to different strategies of defoliation.

In perennial tropical forage grasses, morphogenetic adaptation to diverse conditions is often associated with analogous developmental patterns described for temperate forage grasses. However, to date, especially in the case of elephant grass cv. Napier, there was no studies characterizing the ontogenic program of development using an isolated plant protocol like the one used in this study. Determination of the ontogenetic development is essential for analysing plant morphogenetic adaptation to both sward structure (competition for light) and defoliation pattern (plant-animal interactions). This work aimed at elucidating ontogenetic development of elephant grass and emphasize differences in growth patterns between temperate and perennial tropical forage grasses. Topics such as dynamic changes in morphogenic traits according to ontogenetic development of elephant grass, coordination and synchrony of internode and leaf development, and importance of internode elongation in

determining leaf dimensions and axillary branches development have never been reported before in the literature.

The results revealed the apparent importance of sheath tube length and internode length in determining processes at the axis development level. Environmental conditions influence apical meristem functioning by altering mechanisms of cell production and extension, directly affecting LAR. As the elephant grass axis development progressed, the number of accumulated leaves (NLL) increased following a linear relationship as a function of temperature. Axis development began with production of successive leaves and increment in sheath tube and leaf blade length. The length of the sheath tube directly affects LER by defining the size of the elongation zone through the number of cells produced, since the appearance of leaf tip over the worhl determined the onset of ligule formation. In addition, the length of the sheath tube also determines LED by affecting the duration of lamina extension. The successive increase in LER and LED with the appearance of successive leaves led to increased final leaf length (FLL), consequence of the product between LER × LED. At the axis level, leaves production progressed until the sheath tube length reached a maximum value, after which sheath tube and sheath length remained constant during the vegetative phase (Spring and Summer). Concomitantly with maximum sheath length, sheath tube length was reached, and the internode elongation process started. Stem elongation rate (SER) was also influenced by the environment, likely through the production of cells at the intercalary meristem region and by affecting the expansion of the produced cells. At this point, LER also reached its maximum value and remained constant, while LED continued to increase. Such results strongly suggest an impact of internode elongation dynamics on plant ontogenetic program by favouring an increase in LED and, consequently, in FLL. Although there was a distinct shoot development for each axis rank at which such changes occured, i.e. NLL was dependent of the axes, these relationships were explained for all axes and could be expressed by the following diagram (Figure 6.1).

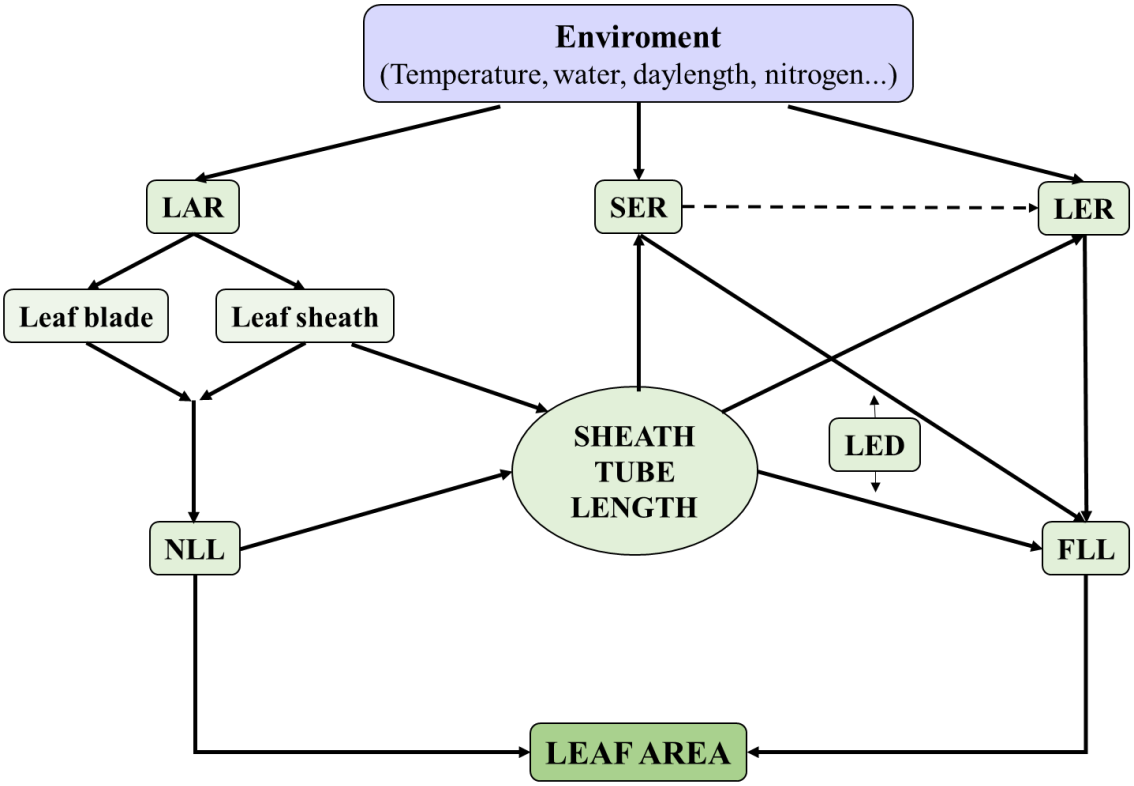

Figure 6.1. Conceptual model of axis development of *Pennisetum purpureum* cv Napier during vegetative phase, under free growth conditions using isolated plant protocol.

Information about the importance of internode elongation to leaf growth is scarce and needs to be investigated mainly in aspects related to the mechanisms involved in the increase of FLL by the presence of elongating internodes presented for the main axis in the first hipothesis. These findings open a series of questions that could be answered in future research, such as: i) Is sheath tube length a determinant of stem elongation? How is it operated? ii) Considering that phyllochron is constantly independent of the developmental stage under isolated growth conditions, how could defoliation affect leaf dimension? Would it be just through a mechanical reduction of sheath tube length or would it be through other effects?

Contrary to temperate forage grasses, LED expressed in phyllochronic units was not constant and increased during plant ontogeny. Therefore, LED was determinant of the progressive increase in final leaf length. Additionally, still opposite to what is described for temperate forage grasses, phyllochron (or LAR) was constant during the vegetative development of elephant grass. The FLL increased without changes in maximum sheath and sheath tube length. This disproportionality of sheath:blade ratio has never been reported in the

literature and strongly suggests that internode should be integrated as a component of phytomer development. As reported in chapter 2 and corroborated by Yang et al. (2016) and Zhu et al. (2014), the onset of internode elongation occured concomitantly with the cessation of lamina elongation, at the moment of collar emergence over the worhl. This information makes possible to follow internode elongation of a phytomer by measuring collar displacement after its emergence without the need to cut the axis (observation in the field). Consequently, it is possible to easily identify the position of the apical meristem without dissecting the axis. This could be useful for identification of defoliation severity under grazing. However, further studies are needed to verify this pattern under grazing and within plant comunity.

Results clearly show that the presence of elongating internodes occurs without light limitations at a predictable moment regardless of season of the year and axes stage of development. In tropical grasslands, the stem component is a key feature driving grazing management because of its considerable effect on forage quality and on herbage intake. Several authors have plausibly showed the use of leaf area index, leaf stage, sward height and light interception as relevant parameters for controlling and executing grazing management. However, scientists frequently are challenged and questioned about the constancy of such methods under different enviroments, seasons, soils etc... Some authors frequently present inconsistency of methods, but unfortunately do not deeply investigate such inconsistencies to clarify the real aspects involved. In terms of grazing management, this thesis provoques new insights about the process of control of stem production in pastoral systems. Stem production is knownly influenced by defoliation regimes, light and environmental conditions, but it is also related to plants' ontogenetic development and occurs at a predictable moment independently of environment. Further, the coordination between leaf and internode development allows the direct prediction of the onset of internode elongation in field conditions. This coordination also identifies which internodes are elongating, since it is possible to know in which phytomer the internode starts to elongate and the phyllocronic lag from leaf appearance to the beginning of internode elongation. In this sense, the question that rises is: Is it worth to integrate the ontogenetic program for stem elongation to manage grasslands? Further research is needed to investigate the applicability of this knowledge under grazing and to which extend it drives grazing strategies.

Additionally, these data can be integrated into functional-structural plant models (FSPM) to describe the architectural development based on the stability of coordination between developmental events. Over the past 10 years, architectural modelling grasses

program has made significant progress both in terms of concepts and for the development of tools for research and tecnichal aplications. However, there are no models for perennial tropical grasses integrating the internode elongation during the ontogenic pattern of plant development.

REFERENCES

ABIEC (2016) Perfil da Pecuária no Brasil. Anu report. http://www.newsprime.com.br/img/upload2/2016_FolderPerfil_PT.pdf. Accessed 11 September 2017

Aguilar-Martinez JA, Poza-Carrion C, Cubas P (2007) Arabidopsis BRANCHED1 Acts as an Integrator of Branching Signals within Axillary Buds. Plant Cell Online 19:458–472. doi: 10.1105/tpc.106.048934

Andrieu B, Hillier J, Birch C (2006) Onset of sheath extension and duration of lamina extension are major determinants of the response of maize lamina length to plant density. Ann Bot 98:1005–1016. doi: 10.1093/aob/mcl177

Bahmani I, Hazard L, Varlet-Grancher C et al (2000) Differences in tillering of long- and short-leaved perennial ryegrass genetic lines under full light and shade treatments. Crop Sci 40:1095–1102. doi: 10.2135/cropsci2000.4041095x

Baldissera TC, Frak E, Carvalho PCDF, Louarn G (2014) Plant development controls leaf area expansion in alfalfa plants competing for light. Ann Bot 113:145–157. doi: 10.1093/aob/mct251

Ballare CL, Scopel AL, Sánchez RA (1991) Photo control of stem elongation in plant neighbourhoods: Effect of photon fluence rate under natural conditions of radiation. Plant Cell Environ 14:57–65

Barillot R, Chambon C, Andrieu B (2016) CN-Wheat, a functional-structural model of carbon and nitrogen metabolism in wheat culms after anthesis. I. Model description. Ann Bot 1–17. doi: 10.1093/aob/mcw143

Begg JE, Wright MJ (1962) Growth and Development of leaves from intercalary meristems in *Phalaris arundinacea* L. Nature 194:1097–1098

Bell AD (1991) Plant form. Oxford University Press, Oxford

Bennett T, Leyser O (2006) Something on the side: Axillary meristems and plant development. Plant Mol Biol 60:843–854. doi: 10.1007/s11103-005-2763-4

Birch CJ, Andrieu B, Fournier C (2002) Dynamics of internode and stem elongation in three cultivars of maize. Agronomie 511–524. doi: 10.1051/agro:2002030

Birch CJ, Andrieu B, Fournier C, Kroesen C (2007) Kinetics of leaf extension in maize: Parameterization for two tropically adapted cultivars planted on two dates at Gatton. Eur J Agron 27:215–224. doi: 10.1016/j.eja.2007.04.003

Birch CJ, Thornby D, Adkins S, et al (2008) Architectural modelling of maize under water stress. Aust J Exp Agric 48:335–341. doi: 10.1071/EA06105

Bohlool BB, Ladha JK, Garrity DP, George T (1992) Biological nitrogen fixation for sustainable agriculture: A perspective. Plant Soil 141:1–11 . doi: 10.1007/BF00011307

Bonhomme R (2000) Bases and limits to using “degree day” units. Eur J Agron 13:1–10. doi: 10.1016/S1161-0301(00)00058-7

Brougham RW (1955) A study in rate of pasture growth. Aust J Agric Res 6:804–812. doi: 10.1071/AR9550804

Burson BL, Young BA (2001) Breeding and improvement of tropical grasses. In: Sotomayor-Ríos A, Pitman WD (eds) Tropical forage tropical forage plants : development and use, 1st edn. CRC Press, Florida, pp 63–83

Carareto R (2007) Uso de uréia de liberação lenta para vacas alimentadas com silagem de milho ou pastagens de capim-elefante manejadas com intervalos fixos ou variáveis de desfolhas. Dissertation, University of São Paulo - Luiz de Queiroz “College of Agriculture”

Carvalho MM, Alvim MJ, Xavier DF, Carvalho LL (1994) Capim-elefante: produção e utilização. EMBRAPA-CNPGL, Coronel Pacheco

Carvalho MM, Alvim MJ, Xavier DF, Carvalho LL (1997) Capim-elefante: produção e utilização. EMBRAPA- CNPGL, Juiz de Fora

Carvalho PCF, Bremm C, Bonnet OJF, et al (2016) Como a estrutura do pasto influencia o animal em pastejo? Exemplificando as interações planta-animal sob as bases e fundamentos do Pastoreio “Rotatínuo” In: VIII Simpósio sobre manejo estratégico da pastagem, 8th edn. UFV, Viçosa, MG, p 21

Casey IA, Brereton AJ, Laidlaw AS, McGilloway DA (1999) Effects of sheath tube length on leaf development in perennial ryegrass (*Lolium perenne* L.). Ann Appl Biol 134:251–257. doi: 10.1111/j.1744-7348.1999.tb05261.x

CEPAGRI (2017) Centro de Pesquisas Metereológicas e Climáticas Aplicadas a Agricultura. In: Clima dos Municípios Paul. http://www.cpa.unicamp.br/outras-informacoes/clima_muni_490.html. Accessed 11 Nov 2017

Chapman D, Lemaire G (1993). Morphogenetic and structural determinants of plant regrowth after defoliation. In: INTERNATIONAL GRASSLAND CONGRESS, 17, 1993, Austrália. Proceedings...., p. 95-104

Chapman D (2016) Using ecophysiology to improve farm efficiency: application in temperate dairy grazing systems. Agriculture 6:1–19. doi: 10.3390/agriculture6020017

Chaves CS, Gomide CAM, Ribeiro KG, et al (2013) Forage production of elephant grass under intermittent stocking. Pesqui Agropecu Bras 48:234–240. doi: 10.1590/S0100-204X2013000200015

Chen Y, Carver BF, Wang S, et al (2009) Genetic loci associated with stem elongation and winter dormancy release in wheat. Theor Appl Genet 118:881–889. doi: 10.1007/s00122-008-0946-5

Cóser AC, Martins CE, Deresz F (2000) Capim-elefante : formas de uso na alimentação animal. EMBRAPA-CNPGL, Coronel Pacheco

Cruz P, Boval M. Effect of nitrogen on some traits of temperate and tropical perennial forage grasses. In: Grassland Ecophysiology and Grazing Ecology, 2000, Curitiba. Proceedings... Curitiba, 2000, p. 134-150

Da Silva SC (2011) O manejo do pastejo e a intensificação da produção animal em pasto. In: Simpósio de Produção Animal a Pasto- SIMPA. Maringá, PR, pp 80–100

Da Silva SC, Carvalho PCF (2005) Foraging behaviour and herbage intake in the favourable tropics / sub- tropics. In: McGilloway DA (ed) XX International Grassland Congress - Grassland a Global Resource. Wageningen Academic Publishers, Dublin, Ireland, pp 81–95

Da Silva S, Sbrissia AF, Pereira LET (2015) Ecophysiology of C4 forage grasses—understanding plant growth for optimising their use and management. Agriculture 5:598–625. doi: 10.3390/agriculture5030598

Deregibus VA, Sanchez RA, Casal JJ (1983) Effects of light quality on tiller production in *Lolium* spp. Plant Physiol 72:900–902. doi: 10.1104/pp.72.3.900

Duru M, Ducrocq H (2000a) Growth and Senescence of the Successive Grass Leaves on a Tiller. Ontogenic Development and Effect of Temperature. Ann Bot 85:635–643. doi: 10.1006/anbo.2000.1116

Duru M, Ducrocq H (2000b) Growth and senescence of the successive leaves on a cocksfoot Tiller . Effect of nitrogen and cutting regime. Ann Bot 85:645–653. doi: 10.1006/anbo.2000.1117

Duru M, Justes E, Langlet A, et al (1993) Comparaison des dynamiques d'apparition et de mortalité des organes de fétuque élevée, dactyle et luzerne (feuilles, talles et tiges). Agronomie 13:237–252

Egle RB, Domingo AJ, Bueno C et al (2015) Variability and synchronism of leaf appearance and leaf elongation rates of eleven contrasting rice genotypes. Agric Sci 6:1207–1219

Embrapa (1997) Manual de métodos de análise de solo. EMBRAPA-CNPS, Brasilia

Evers JB, Van der Krol AR, Vos J, Struik PC (2011) Understanding shoot branching by modelling form and function. Trends Plant Sci 16:464–467. doi: 10.1016/j.tplants.2011.05.004

Faverjon L, Escobar-Gutiérrez AJ, Litrico I, Louarn G (2017) A Conserved potential development framework applies to shoots of legume species with contrasting morphogenetic strategies. Front Plant Sci 8:1–14. doi: 10.3389/fpls.2017.00405

Fournier C, Andrieu B (2000a) Dynamics of the elongation of internodes in maize (*Zea mays* L.). Effects of shade treatment on elongation patterns. Ann Bot 86:1127–1134. doi: 10.1006/anbo.2000.1280

Fournier C, Andrieu B (2000b) Dynamics of the elongation of internodes in maize (*Zea mays* L.): analysis of phases of elongation and their relationships to phytomer development. Ann Bot 86:551–563. doi: 10.1006/anbo.2000.1217

Fournier C, Durand JL, Ljutovac S, et al (2005) A functional-structural model of elongation of the grass leaf and its relationships with the phyllochron. New Phytol 166:881–894. doi: 10.1111/j.1469-8137.2005.01371.x

Fulkerson WJ, Slack K (1995) Leaf number as a criterion for determining defoliation time for Lolium perenne. 2. Effect of defoliation frequency and height. Grass Forage Sci 50:16–20. doi: 10.1111/j.1365-2494.1994.tb02013.x

Gallagher JN (1979) Field Studies of Cereal Leaf Growth. I. Initiation and expanion in relation to temperature and ontogeny. J Exp Bot 30:625–636

Gastal F, Lemaire G (2015) Defoliation, shoot plasticity, sward structure and herbage utilization in pasture: review of the underlying ecophysiological processes. Agriculture 5:1146–1171. doi: 10.3390/agriculture5041146

Geremia EV (2013) Estrutura do dossel e taxa de consumo de forragem de capim-elefante cv . Napier submetido a estratégias de pastejo rotativo. Dissertation, University of São Paulo - Luiz de Queiroz “College of Agriculture”

Gifford EM, Foster AS (1996) Morphology and evolution of vascular plants. W.H. Freeman and Company, New York

Gomide JA, Gomide CAM (1999) Fundamentos e estratégias do manejo de pastagens. In: Ferreira CCB, Marinho D de B, Faria DA de, et al. (eds) I Simpósio de produção de gado de corte, 1st edn. Visconde do Rio Branco: Suprema Gráfica e Editora Ltda., pp 179–200

Gomide CAM, Paciullo DSC, Costa IA, et al (2011) Morphogenesis of dwarf elephant grass clones in response to intensity and frequency of defoliation in dry and rainy seasons. Rev Bras Zootec 40:1445–1451. doi: 10.1590/S1516-35982011000700007

Gomide CAM, Chaves CS, Ribeiro KG, et al (2015) Structural traits of elephant grass (*Pennisetum purpureum* Schum.) genotypes under rotational stocking strategies. African J Range Forage Sci 1–5. doi: 10.2989/10220119.2014.930929

González FG, Slafer GA, Miralles DJ (2005) Floret development and survival in wheat plants exposed to contrasting photoperiod and radiation environments during stem elongation. Funct Plant Biol 32:189–197. doi: 10.1071/FP04104

Goto Y, Nakamura S, Sakai K, Hoshikawa K (1994) Analysis of elongation and thickening of internodes in sweet sorghum (Sorghum bicolor Moench). Japanese J Crop Sci 63:473–479. doi: 10.1248/cpb.37.3229

Hodgson J (1985) The control of herbage intake in the grazing ruminant. Proc Nutr Soc 44:339–346

Hodgson J (1990) Grazing management: Science into practice. John Wiley: Longman Scientific and technical, New York

Hodgson J, Da Silva SC. Options in tropical pasture management. In: Batista AMV, Barbosa SBP, Santos MVF, Ferreira LMC. (Org.). Anais de Palestras da 39 Reunião Anual da Sociedade Brasileira de Zootecnia. Recife, PE: , 2002, 180-202

Huber H, Stuefer JF (1997) Shade-induced changes in the branching pattern of a stoloniferous herb: functional response or allometric effect? Oecologia 110:478–486. doi: 10.1007/s004420050183

Hull RJ (1999) Back to basics. How turfgrasses grow. TurfGrass trends 8:7–12

Hutchings MJ, de Kroon H (1994) Foraging in Plants: The Role of Morphological Plasticity in Resource Acquisition. Adv Ecol Res 25:159–238. doi: 10.1016/S0065-2504(08)60215-9

IBGE (2016) Indicadores IBGE. Estatística da Produção Pecuária. Inst. Bras. Geogr. e Estatística

Irish EE, Nelson TM (1991) Identification of multiple stages in the conversion of maize meristems from vegetative to floral development. Development 112:891–898

Ishii Y, Hamano K, Kang DJ, et al (2013) C4- Napier grass cultivation for cadmium phytoremediation activity and organic livestock farming in kyushu, Japan. J Agric Sci Technol 3:321–330

Jaffuel S, Dauzat J (2005) Synchronism of leaf and tiller emergence relative to position and to main stem development stage in a rice cultivar. Ann Bot 95:401–412. doi: 10.1093/aob/mci043

Kebrom TH, Spielmeyer W, Finnegan EJ (2013) Grasses provide new insights into regulation of shoot branching. Trends Plant Sci 18:41–48. doi: 10.1016/j.tplants.2012.07.001

Kirby EJM (1990) Co-ordination of leaf emergence and leaf and spikelet primordium initiation in wheat. F Crop Res 25:253–264. doi: 10.1016/0378-4290(90)90008-Y

Kirby EJM, Appleyard M, Simpson NA (1994) Co-ordination of stem elongation and Zadoks growth stages with leaf emergence in wheat and barley. J Agric Sci 122:21–29. doi: 10.1017/S0021859600065746

Kronenberg L, Yu K, Walter A, Hund A (2017) Monitoring the dynamics of wheat stem elongation: genotypes differ at critical stages. Euphytica 213:1:13. doi: 10.1007/s10681-017-1940-2

Kroon H, Hutchings MJ (1995) Morphological plasticity in clonal plants : the foraging concept reconsidered. J Ecol 83:143–152

Lafarge T, Tardieu F (2002) A model co-ordinating the elongation of all leaves of a sorghum cultivar was applied to both Mediterranean and Sahelian conditions. J Exp Bot 53:715–725. doi: 10.1093/jexbot/53.369.715

Lafarge TA, Broad IJ, Hammer GL (2002) Tillering in grain sorghum over a wide range of population densities: Identification of a common hierarchy for tiller emergence, leaf area development and fertility. Ann Bot 90:87–98. doi: 10.1093/aob/mcf152

Lafarge T. 1998. Analyse de la mise en place de la surface foliaire du sorghograin (*Sorghum bicolor* L. Moench) au champ. Etablissement d'un modèle de développement valable en conditions sahéliennes et nord méditerraneéennes. Dissertation, Orsay Paris-Sud University

Lambers H, Chapim III FS, Pons TL (2008) Plant Physiological Ecology, Springers, New York

Langer RHM (1979) How grasses grow. Edward Arnold Publishers Ltd, London

Lemaire, G. Ecophysiology of grasslands: dynamics aspects of plant populations in grazed swards. In: INTERNATIONAL GRASSLAND CONGRESS, 19, 2001, São Pedro. Proceedings... p.29-37.

Lemaire, G.; Agnusdei, M. Leaf tissue turn-over and efficiency of herbage utilization. In: Lemaire, G., Hodgson, J., Moraes, A., Nabinger, C., Carvalho, P.C.F. (Ed.) Grassland Ecophysiology and Grazing Ecology. CAB International, 2000. p. 265-288.

Lemaire, G.; Chapman, D. Tissue fluxes in grazing plant communities. In: Hodgson, J.; Illius, A.W. (Ed.). The ecology and management of grazing systems. Wallingford: CAB International, 1996. p. 3-36.

Lemaire G, Gastal F (1997) N uptake and distribution in plant canopies. In: Lemaire G, ed. Diagnosis on the nitrogen status in crops. Heidelberg: Springer-Verlag, 3–43

Lemaire G, Millard P (1999) An ecophysiological approach to modelling resource fluxes in competing plants. J Exp Bot 50:15–28. doi: 10.1093/jxb/50.330.15

Lestienne F, Gastal F, Moulia B, Thornton B (2002) Pattern of leaf and tiller development of perennial ryegrass plants. In: European Grassland Federation EGF (ed) 19th General Meeting on "Multi-function grassland: Quality Forage, Animal Products and Landscapes." France, pp 332–333

Lira MA, Santos MVF, Dubeux Jr JCB, Mello ACL (2010) Capim-elefante: fundamentos e perspectivas. IPA/UFRPE, Recife

Lowe AJ, Thorpe W, Teale A, Hanson J (2003) Characterisation of germplasm accessions of Napier grass (*Pennisetum purpureum* and *P. purpureum* x *P. glaucum* Hybrids) and comparison with farm clones using RAPD. Genet Resour Crop Evol 50:121–132. doi: 10.1023/A:1022915009380

McMaster GS, Wilhelm WW, Palic DB, et al (2003) Spring wheat leaf appearance and temperature: Extending the paradigm? Ann Bot 91:697–705. doi: 10.1093/aob/mcg074

Melo ACL, Veras ASC, Lira MA, Santos MVF, Dubeux Jr JCBD, Freitas EV, Cunha MV (2008) Pastagens de capim-elefante: produção intensive de leite e carne. IAP, Recife

Miglietta F (1991) Simulation of wheat ontogenesis. I. Appearance of main stem leaves in the field. Clim Res 1:145–150. doi: 10.3354/cr001145

Moore KJ, Moser LE (1995) Quantifying developmental morphology of perennial grasses. Crop Sci 35:37–43. doi: 10.2135/cropsci1995.0011183X003500010007x

Morrison TA, Kessler JR, Buxton DR (1994) Maize internodes elongation patterns. Crop Sci 34:1055–1060. doi: 10.2135/cropsci1994.0011183X003400040040x

Moulia B, Loup C, Chartier M, et al (1999) Dynamics of Architectural Development of Isolated Plants of Maize (*Zea mays* L.), in a Non-limiting Environment: The Branching Potential of Modern Maize. Ann Bot 84:645–656. doi: 10.1006/anbo.1999.0960

Nakamura S, Nakajima N, Nitta Y, Goto Y (2011) Analysis of Successive Internode Growth in Sweet Sorghum Using Leaf Number as a Plant Age Indicator. Plant Prod Sci 14:299–306. doi: 10.1626/pps.14.299

Negawo AT, Teshome A, Kumar A, et al (2017) Opportunities for Napier Grass (*Pennisetum purpureum*) Improvement Using Molecular Genetics. Agronomy 7:1–21. doi: 10.3390/agronomy7020028

Nelson, CJ. Shoot morphological plasticity of grasses: leaf growth vs. tillering. In: Lemaire G., Hodgson J., Moraes A., de Cavalho P.C., Nabinger C., eds. Grassland ecophysiology and grazing ecology. 2000. Wallingford, UK: CABI Publishing, p. 101-126.

Oborny B (2004) External and internal control in plant development. Complexity 9:22-28

Ong CK (1983) Response to temperature in a stand of pearl millet (*Pennisetum typhoides* S. & H.). J Exp Bot 34:322–336

Parsons AJ, Johnson IR, Harvey A (1988) Use of a model to optimize the interation between frequency and severity of intermittent desfoliation and to provide a fundamental comparison of the continuous and intermittent desfoliation of grass. Grass Forage Sci 43:49–59

Parsons AJ, Penning PD (1988) The effect of the duration of regrowth on photosynthesis, leaf death and the average rate of growth in a rotationally grazed sward. Grass Forage Sci 43:15–27 . doi: 10.1111/j.1365-2494.1988.tb02137.x

Parsons A, Rowarth J, Thornley J, Newton P (2011) Primary production of grasslands, herbage accumulation and use, and impacts of climate change. In: Lemaire G, Hodgson J, Chabbi A (eds) Grassland productivity and ecosystem services, 1st edn. Cabi, Wallingford, UK, p 436

Patrick JW (1972) Distribution of assimilate during stem elongation in wheat. Aust J Biol Sci 25:455–467. doi: http://www.publish.csiro.au/BI/pdf/BI9720455

Passos LP, Carvalho LA, Martins CE, Bressan M, Pereira AV (1999) Biologia e manejo do capim-elefante. EMBRAPA-CNPGL, Juiz de Fora

Peixoto AM, Moura JC, Faria VP (1994) Manejo do capim-elefante. FEALQ, Piracicaba

Pereira AV, Auad AM, Lédo, FJS, Barbosa S (2010) *Pennisetum purpureum*. In: Fonseca, D.M.; Martuscello, J.A. (Ed.) Plantas forrageiras. UFV, Viçosa, pp 197-219

Pereira LET, Paiva AJ, Geremia EV, Da Silva SC (2013) Regrowth patterns of elephant grass (Pennisetum purpureum Schum) subjected to strategies of intermittent stocking management. Grass Forage Sci 70:195–204 . doi: 10.1111/gfs.12103

Pereira LET (2013) Dinâmica do crescimento e componentes do acúmulo de forragem de capim-elefante cv. Napier submetido a estratégias de pastejo rotativo. Dissertation, University of São Paulo - Luiz de Queiroz “College of Agriculture”

Pereira LET, Paiva AJ, Geremia EV, Da Silva SC (2014a) Components of herbage accumulation in elephant grass cvar Napier subjected to strategies of intermittent stocking management. J Agric Sci 152:954–966. doi: 10.1017/S0021859613000695

Pereira LET, Paiva AJ, Geremia EV, Da Silva SC (2014b) Grazing management and tussock distribution in elephant grass. Grass Forage Sci 70:406–417. doi: 10.1111/gfs.12137

Poethig RS (1990) Phase change and the regulation of shoot morphogenesis in plants. Science 250:923–930

R Development Core Team (2014). R: A Language and Environment for Statistical Computing. R Foundation for Statistical Computing, Vienna.

Richards, J.H. 1993. Physiology of plants recovering from defoliation. p. 85-94. In Proc. Int. Grassl. Cong., 17th Rockhampton, Australia. 8-12 Feb. 1993. Proceedings.... Dunmore Press Ltd., Palmerston North, New Zealand.

Robertson MJ (1994) Relationships between internode elongation, plant height and leaf appearance in maize. F Crop Res 38:135–145. doi: 10.1016/0378-4290(94)90085-X

Robin AHKR (2011) Segmental Morphology of Perennial Ryegrass (*Lolium perenne* L.): A Study of Functional Implications of Plant Architecture. Massey University

Rodrigues CS, Nascimento Jr D, Da Silva SC, et al (2011) Characterization of tropical forage grass development pattern through the morphogenetic and structural characteristics. Rev Bras Zootec 40:527–534

Rusdy M (2016) Elephant grass as forage for ruminant animals. Livest Res Rural Dev 28:1–5

Sachs RM (1965) Stem elongation. Annu Rev Plant Physiol 16:73–96

Sachs T (1999) “Node counting”: an internal control of balanced vegetative and reproductive development. Plant, Cell Environ 22:757–766. doi: 10.1046/j.1365-3040.1999.00220.x

Sanderson MA (1992) Morphological Development of Switchgrass and Kleingrass. Agron J 84:415–419

Sartie AM (2006) Phenotypic assessment and quantitative trait locus (QTL) analysis of herbage and seed production traits in perennial ryegrass. Massey University, Institute of natural Resources, College of Sciences

Sbrissia AF, Duchini P, Echeverria JR, et al (2017) Produção animal em pastagens cultivadas em regiões de clima temperado da América Latina. In: XXV Reunión de la Asociación Latinoamericana de Producción Animal. Archivos Latinoamericanos de Producción Animal, Recife, pp 47–60

Sharman BC (1942) Developmental anatomy of the shoot of *Zea mays* L. Ann Bot 6:245–282

Shimizu-Sato S, Mori H (2001) Control of outgrowth and dormancy in axillary buds. Plant Physiol 127:1405–1413. doi: 10.1104/pp.010841

Skinner RH, Moore KJ (2007) Growth and development of forage plants. In: Barnes RF, Nelson CJ, Moore KJ, Collins M (eds) Forages: The Science of Grassland Agriculture, 6th edn. USA: Blackwell Publishing, Ames, IA, pp 53–66

Skinner RH, Nelson C. J (1995) Elongation of the grass leaf and its relationship to the phyllochron. Crop Sci 35:4–10. doi: 10.2135/cropsci1995.0011183X003500010002x

Skinner RH, Nelson CJ. (1994) Role of leaf appearance rate and the coleoptile tiller in regulating tiller production. Crop Sci 34:71–75

Solomon JKQ, Macoon B, Lang DJ (2017) Harvest management based on leaf stage of a tetraploid vs. a diploid cultivar of annual ryegrass. Grass Forage Sci 1–14. doi: 10.1111/gfs.12313

Sousa BML, Nascimento Jr D, Monteiro HC de F, Fonseca DM (2012) Dynamics of production and forage utilization on elephant grass pastures managed with different post-grazing heights. Rev Bras Zootec 41:1840–1847. doi: 10.1590/S1516-35982012000800006

Souza CC, Oliveira FA, Silva I de F, Amorim M da S (2000) Avaliação de Métodos de Determinação de Água Disponível e Manejo da Irrigação em Terra Roxa Sob Cultivo de Algodoeiro Herbáceo. Rev Bras Eng Agrícloa e Ambient 4:338–342. doi: 10.1590/S1415-43662000000300006

Speck T, Burgert I (2011) Plant Stems: functional design and mechanics. Annu Rev Mater Res 41:169–193. doi: 10.1146/annurev-matsci-062910-100425

Taiz L, Zeiger E (2010) Plant Physiology. Sinauer Associates, Sunderland

Thornley JH, Johnson IR (1990) Plant and crop modelling. The Blackburn Press.

Verdenal A, Combes D, Escobar-Gutiérrez AJ (2008) A study of ryegrass architecture as a self-regulated system, using functional-structural plant modelling. Funct Plant Biol 35:911–924. doi: 10.1071/FP08050

Verdenal A. (2009) De la simulation de la morphogénèse de l'appareil aérien du ray-grass anglais (Lolium perenne L.). Exploration d'un schéma cybernétique inspiré du concept d'auto-organisation et applications. PhD Thesis, Universite de Poitiers, Poitiers.

Vicente-Chandler J (2001) Intensive management of forage grasses in the humid tropics. In: Sotomayor-Ríos A, Pitman WD (eds) Tropical forage tropical forage plants : development and use, 1st edn. CRC Press, Florida, pp 166–190

Voltolini TV (2006) Adequação protéica em rações com pastagens ou com cana-de- açúcar e efeito de diferentes intervalos entre desfolhas da pastagem de capim Elefante sobre o desempenho lactacionald. PhD thesis, University of São Paulo - Luiz de Queiroz "College of Agriculture"

Voltolini TV, Santos FAP, Martinez JC, et al (2010) Características produtivas e qualitativas do capim-elefante pastejado em intervalo fixo ou variável de acordo com a interceptação da radiação fotossinteticamente ativa. Rev Bras Zootec 39:1002–1010. doi: 10.1590/S1516-35982010000500009

Yang F, Gong XY, Liu HT, et al (2016) Effects of nitrogen and vapour pressure deficit on phytomer growth and development in a C4 grass. AoB Plants 8:plw075. doi: 10.1093/aobpla/plw075

Warrington IJ, Kanemasu ET (1983) Corn growth response to temperature and photoperiod. II. Leaf-initiation and leaf-appearance rates. Agronomy Journal 75: 755–761

West SH, Pitman WD (2001) Seed production technology forages, of tropical forages. In: Sotomayor-Ríos A, Pitman WD (eds) Tropical forage tropical forage plants : development and use, 1st edn. CRC Press, Florida, pp 143–165

Wilhelm WW, McMaster GS (1995) Importance of the Phyllochron in Studying Development and Growth in Grasses Importance of the Phyllochron in Studying Development and Growth in Grasses. Crop Sci 35:1–3

Williams RF (1960) The physiology of growth in the wheat plant. I. Seedling growth and the pattern of growth at the shoot apex. Aust J Biol Sci 13:401–432. doi: 10.1071/BT9700127

Wilson RE, Laidlaw AS (1985) The role of the sheath tube in the development of expanding leaves in perennial regrass. Ann Appl Biol 106:385–391

Wiltshire RJE, Murfet IC, Reid JB (1994) The genetic control of heterochrony: Evidence from developmental mutants of *Pisum sativum* L. J Evol Biol 7:447–465. doi: 10.1046/j.1420-9101.1994.7040447.x

Woodard KR, Sollenberger LE (2011) Production of biofuel crops in florida: elephantgrass. Agron. Dep. UF/IFAS Ext. 1–3

Zhu J, Andrieu B, Vos J, et al (2013) Simulating maize plasticity in leaf appearance and size using regulation rules. In: Sievänen R, Nikinmaa E, Godin C, et al. (eds) Proceedings of the 7th International Conference on Functional-Structural Plant Models, 9-14 June, Saariselkä, Finland. Saariselkä, Finland, pp 273–275

Zhu J, Vos J, Van Der Werf W et al (2014) Early competition shapes maize whole-plant development in mixed stands. J Exp Bot 65:641–653. doi: 10.1093/jxb/ert408

Zhu Y, Tang L, Tan Z-H et al (2009) Modeling leaf sheath and internode growth dynamics in wheat. Crop Model Decis Support 86–91